AN INVESTIGATION INTO CONSEQUENCES OF CLASSIFYING ORTHOGONAL ABERRATIONS BY DEGREE

by

Steve Clarence Johnston

A Dissertation Submitted to the Faculty of the

COMMITTEE ON OPTICAL SCIENCES (GRADUATE)

In Partial Fulfillment of the Requirements
For the Degree of

DOCTOR OF PHILOSOPHY

In the Graduate College

THE UNIVERSITY OF ARIZONA

1988

Order Number 8814246

An investigation into consequences of classifying orthogonal aberrations by degree

Johnston, Steve Clarence, Ph.D.

The University of Arizona, 1988

U·M·I
300 N. Zeeb Rd.
Ann Arbor, MI 48106

AN INVESTIGATION INTO CONSEQUENCES OF CLASSIFYING ORTHOGONAL ABERRATIONS BY DEGREE

by

Steve Clarence Johnston

A Dissertation Submitted to the Faculty of the

COMMITTEE ON OPTICAL SCIENCES (GRADUATE)

In Partial Fulfillment of the Requirements
For the Degree of

DOCTOR OF PHILOSOPHY

In the Graduate College

THE UNIVERSITY OF ARIZONA

1988

THE UNIVERSITY OF ARIZONA
GRADUATE COLLEGE

As members of the Final Examination Committee, we certify that we have read the dissertation prepared by Steve Clarence Johnston

entitled An Investigation into Consequences of Classifying Orthogonal Aberrations by Degree

and recommend that it be accepted as fulfilling the dissertation requirement for the Degree of Doctor of Philosophy.

R N Shack	4/18/88 Date
Roland V. Shack	4/18/88 Date
Kenneth P. Thompson	4/18/88 Date
	Date
	Date

Final approval and acceptance of this dissertation is contingent upon the candidate's submission of the final copy of the dissertation to the Graduate College.

I hereby certify that I have read this dissertation prepared under my direction and recommend that it be accepted as fulfilling the dissertation requirement.

Roland V. Shack — Dissertation Director

4/18/88 — Date

STATEMENT BY AUTHOR

This dissertation has been submitted in partial fulfillment of requirements for an advanced degree at The University of Arizona and is deposited in the University Library to be made available to borrowers under rules of the Library.

Brief quotations from this dissertation are allowable without special permission, provided that accurate acknowledgment of source is made. Requests for permission for extended quotation from or reproduction of this manuscript in whole or in part may be granted by the head of the major department or the Dean of the Graduate College when in his or her judgment the proposed use of the material is in the interests of scholarship. In all other instances, however, permission must be obtained from the author.

SIGNED: Steve Johnston

ACKNOWLEDGEMENTS

I am indebted to my dissertation advisor, Dr. Roland Shack, for suggesting the research topic, and am grateful for his suggestions and comments during the course of the work. I am also relieved at his tremendous patience and kind responses to my stupid questions and occasional erroneous assumptions about one or another aspect of optics -- I suspect this is the lot of most research advisors.

I also wish to convey my sincerest thanks to Dr. Stephen Jacobs, who encouraged me to play in the real world of science, the laboratory. His kindness in allowing me to work with a long list of items such as Helium-Neon lasers, Fabry-Perot interferometers, cryogenic systems, vacuum systems, piezoelectric materials, lock-in amplifiers, and high frequency electronics is greatly appreciated and resulted in a rich learning experience.

And finally I would like to express my love to Mary Ochotorena ("When are you ever going to finish? . . . I don't believe you!"), who sustained me during times that would try the patience of the Pope. May we all persevere.

TABLE OF CONTENTS

TABLE OF CONTENTS--Continued

TABLE OF CONTENTS--Continued

LIST OF ILLUSTRATIONS

LIST OF ILLUSTRATIONS--Continued

ABSTRACT

The motivation for this research stems from the optical design problem. From a mathematical perspective the problem can be stated as follows: given a starting optical configuration and a set of variable parameters, determine the specific configuration which yields the global minimum of the merit function which represents the imaging quality of the system. Currently, no satisfactory solution to this problem has been found, although a process called "simulated annealing" has shown some potential. The idea behind this research is that perhaps a merit function can be constructed in such a way that information contained in higher order polychromatic aberration coefficients can be used to indicate the region of the global minimum.

In pursuit of this, the construction of two physically significant merit functions (the wavefront variance and the mean square ray aberration) is formulated in such a way as to allow the segregation of aberration coefficients by order within the merit function. This suggests a sequence of merit "subfunctions" can be constructed in such a way that each member of the sequence is associated with a particular order of aberration, and that the sequence itself converges to the complete merit function.

In order to compute the polychromatic aberration coefficients needed to construct the merit functions, an algorithmic approach to proximate ray tracing is developed. This is shown to be an extension of the original form of proximate ray tracing and has proved highly successful in the computation of polychromatic aberration coefficients.

The behavior of three optical systems with respect to their effective design

parameters is then investigated. The investigation takes the form of topographic maps of the merit subfunctions. A study of the maps reveals that the global topography of the subfunctions remains relatively invariant with respect to order. Also, any minima present tend to remain relatively stationary with respect to order, although any particular one can slowly migrate within some small region of parameter space.

CHAPTER 1

INTRODUCTION

On October 2, 1608, the Dutch spectacle maker Hans Lippershey applied for a patent on his newly invented refracting telescope[1]. Soon after, Johannes Kepler replaced its concave eyepiece with a convex lens. At about the same time, the compound microscope was invented, probably by the Dutchman Zacharias Janssen. It too was soon followed by a new design in which Francisco Fontana replaced the concave eyepiece with a convex lens. Then in 1611 Kepler published "Dioptrice", in which he presents the small angle approximation to the law of refraction. This allowed him to derive a first order treatment of thin lens systems which he used to explain the operation of both the Keplerian and Galilean telescopes.

However, first order optics was not sufficient to describe accurately the behavior of optical systems. A giant step forward in addressing this problem occurred around 1621 when Willebrord Snell empirically discovered the exact form of the law of refraction. At about the same time Rene Descartes independently derived the same law using a propagation model in which light transmission occured as a pressure wave. Snell's law allowed the exact path of any light ray to be determined. Thus, deviations from first order optics could be determined exactly.

Aberration Coefficients

The jump from first to third order calculation occured in the late 1850's[2]. Seidel and his contemporary Petzval both expanded ray trace equations which allowed them to derive simple formulas for the third order aberration coefficients of the power series expansions of ray properties. In addition, Schwartzschild in 1905 determined the third order coefficients of the Seidel Eikonal. Due to the success of these developments, an optical system could be designed to third order before it was actually built.

Aberration coefficients of order past the third were first calculated by Wachendorf[3] in 1949 when he developed a method to calculate fifth order coefficients (this was later extended by Hopkins[4] in 1976 to the seventh order using a concept he termed proximate ray tracing). Then about 1951, Buchdahl began development of his treatment of aberration coefficients that in principal could be extended to arbitrary order. Unfortunately, its utility past the fifth order has not been demonstrated.

In order to allow the convenient calculation of coefficients to arbitrary order, Andersen[5] in 1980 published a method using power series manipulations which efficiently utilized the computational power of the digital computer. Forbes[6] subsequently developed powerful extensions to Andersen's methods which greatly improved their utility.

Merit Functions

The focus of this chapter will now shift from the development of methods used to calculate aberration coefficients to the development of the merit function in optical design. With the advent of the computer in the late 1950's, the process of optical design became much more computationally intensive due to the convenience with which optical quantities could be accurately calculated. This produced a shift in

optical design technique.

Prior to the introduction of the digital computer, optical design was commonly carried out through the elimination of appropriate third order aberration coefficients, and then using real ray data from a few laboriously traced rays to complete the design. After the computer was introduced, real ray data could be calculated so easily that a new method was needed in order to utilize efficiently the resulting mountain of data. This led to the concept of minimizing the defined aberrations in a least squares sense. The mountain of data was reduced to a single number by squaring and then summing the aberrations in a quadratic form. This form became known as the figure of merit, or merit function (because of its functional behavior with respect to the system design variables).

Unfortunately, the merit function was (and is) usually constructed in an ad hoc manner using real ray data with selected first, third (and occasionally fifth) order aberration coefficients sometimes included. The success of this technique depends largely on the skill and experience of the optical designer.

An improvement over the ad hoc technique was published by Unvala[8] in 1967 when he showed how to use the wavefront aberration coefficients to construct a merit function in the usual quadratic form with the useful property of being of physical significance, namely the wavefront variance. He computed the square of the wavefront aberration function and then averaged over an unvignetted pupil. This yielded a quadratic form in the coefficients. By triangularizing the resulting matrix (the triangularized matrix will be termed the transformation matrix for the purposes of the present research), a new quadratic form resulted which was a sum of squared linear combinations of the coefficients. The linear combinations were termed orthonormal aberrations. They describe a natural balance among the wavefront aberration

coefficients which reduces the merit function.

Using the methods of Unvala, Wiese[9] in 1974 showed how to construct the mean square spot size merit function and included first order chromatic effects. The associated orthonormal aberrations could be classified by aberration type. The merit function was then applied to the design of the landscape and triplet lenses. Unfortunately, due to the inability to calculate monochromatic wavefront aberration coefficients past the fifth order and polychromatic coefficients past the first, his design technique was necessarily limited. The use of real ray data was considered a mandatory aid in the final stages of the design process.

The Present Research

The original motivation for this investigation was based on the possibility that the properties of aberration coefficients could be used in some way to reveal the global minimum of a merit function constructed from them. In other words, the motivation arose from the optical design problem. Some thoughts on the problem are presented below as a vehicle to introduce the reader to that motivation.

The mathematical aspect of the optical design problem can be stated as follows: given a starting optical configuration and a set of variable parameters, determine the specific configuration which yields the smallest possible value for (the global minimum of) the error function of the system. The error function is some relevant measure of system performance — in the optical community, the error function is traditionally termed the merit function.

The problem is generally extremely difficult to solve because of the usually large nonlinear behavior of the merit function with respect to the parameters. Most methods attack the problem by using "local" information about the merit function to

predict a new configuration that should reduce its value. The process is repeated until the merit function can be reduced no further. While this is practical and is the most widely used technique, the end result is usually a system that "lies" in a local, rather than global, minimum because only local information about the merit function is utilized.

A method currently under investigation[15] that has shown some potential to locate the global minimum is called "simulated annealing" after some its properties which resemble the annealing process of physical materials upon cooling, and is essentially probabilistic in nature. It is not clear that this approach will prove generally useful.

This brings one to the fundamental idea behind the current research. Instead of relying on probability to locate the global minimum, could information of a global nature be extracted from the merit function itself? Perhaps the information contained in higher degree aberration coefficients might indicate the region of the global minimum. In pursuit of this, Chapter Two will present the formulation of the mean wavefront variance and mean square ray aberration merit functions (in a manner similar to that of Unvala and Wiese) from the coefficients of the polychromatic Taylor series expansion of wavefront aberration and squared ray aberration respectively. The resulting transformation matrix will be partitioned and the orthonormal aberrations classified by aberration order. This will be shown to have several advantages over partitioning and classifying by aberration type: the invariant extension of the transformation matrix to higher orders, the convenient identification of those partitions which have less significance in their contribution to the merit function, and less computational burden if the least significant partitions of the orthogonalization matrix are removed.

The classification according to aberration order allows the merit function to be written as the limit of a sequence of merit "subfunctions", each of which can be associated with a particular aberration order. In Chapter Five it will be demonstrated that measuring the merit function relative to the aberrated image centroid, not the Gaussian image point, will have decreasing effect with increasing order of subfunction. The behavior of the subfunctions (to ninth order in the aberration coefficients) with respect to the design parameters of three optical systems will be investigated to provide for the possible identification of a new optical design strategy. Finally, as a consequence of the investigation into the behavior of the merit subfunctions, Chapter Six will present suggestions for the direction of future research in this area.

The preceding investigation is predicated upon the ability to compute the polychromatic aberration coefficients of wavefront aberration or squared ray aberration. In Chapters Three and Four the proximate ray trace approach of Wachendorf and Hopkins will be extended to include chromatic effects and automated by showing how the operations of addition, multiplication, and square root can be carried out by programming the algorithms which implement these operations. Some advantages and disadvantages of this approach over the methods of Andersen and Forbes will be discussed as well as its relationship to real ray tracing and power series methods.

The algorithmic approach to proximate ray tracing developed here is significant, since previous to this work, proximate ray tracing has been carried out through explicit equations laboriously derived by expanding ray trace equations. In the present work, application of the algorithms will be rendered more convenient through the development of ray trace equations appropriate to rotationally symmetric systems which allow the calculation of wavefront aberration or squared ray aberration.

CHAPTER 2

PHYSICALLY SIGNIFICANT MERIT FUNCTIONS

In this chapter the construction of two physically significant merit functions is formulated. The merit functions are the mean wavefront variance at the exit pupil and mean square ray aberration at the image. The expressions for these two merit functions are transformed from an inconvenient quadratic form to a convenient sum of squares form. The terms of the sum are then associated with polychromatic aberration coefficients and segregated by degree. The consequences of this segregation will be examined in Chapter Five.

Wavefront Variance

For perfect optical systems, all wavefronts exiting the system are coincident with spherical surfaces centered on the Gaussian image point. Real systems always possess aberrations, however, and for this reason the wavefronts are deformed from the spherical ideal. This deformation is referred to as the wavefront aberration.

Wavefront Aberration Function

The wavefront aberration of an axially symmetric system can be defined as the optical path between the aberrated wavefront and the ideal wavefront at the exit pupil. This aberration may be visualized with the aid of Figure 1. It is a function of three variables: the wavelength λ, a field point $\vec{h}$, and the axial component $\vec{p}$ of a point

$\vec{\rho}^*$ on the ideal reference sphere. It will be assumed for the remainder of this dissertation that $\vec{h}$ is normalized with respect to the maximum field height and that $\vec{\rho}$ is normalized with respect to the exit pupil semi-diameter. The $\vec{h}$ and $\vec{\rho}$ coordinates are illustrated in Figure 2.

From simple symmetry considerations of axially symmetric systems, the monochromatic wavefront aberration function can be expanded as a Taylor series of the following form:

$$W = \sum_{j=0}^{\infty}\sum_{k=0}^{\infty}\sum_{l=0}^{\infty}\left[W_{jkl} (\vec{h}\cdot\vec{h})^j \ (\vec{h}\cdot\vec{\rho})^k \ (\vec{\rho}\cdot\vec{\rho})^l \right], \tag{2.1}$$

where the coefficients W_{jkl} are the coefficients of the Taylor series, $\vec{\rho}$ is the fractional pupil variable, and $\vec{h}$ is the fractional field variable.

The wavefront aberration is also a function of wavelength, which implies that each coefficient W_{jkl} is a function of wavelength and can thus be expanded as a Taylor series in the wavelength. However for reasons to be explained later, the wavelength λ is not the best variable about which to expand since this will lead to slow convergence of the series. A better variable is a so-called chromatic variable ν, which is itself a function of wavelength. Forbes[10] has considered several forms for the chromatic variable and has suggested the following useful form:

$$\nu(\lambda) = \nu^* \ \frac{\lambda - \lambda_0}{\lambda - \lambda^*}, \tag{2.2}$$

where $\nu^* = 2.48664$, $\lambda_0 = .489678$, $\lambda^* = .177003$, and the wavelength is measured in

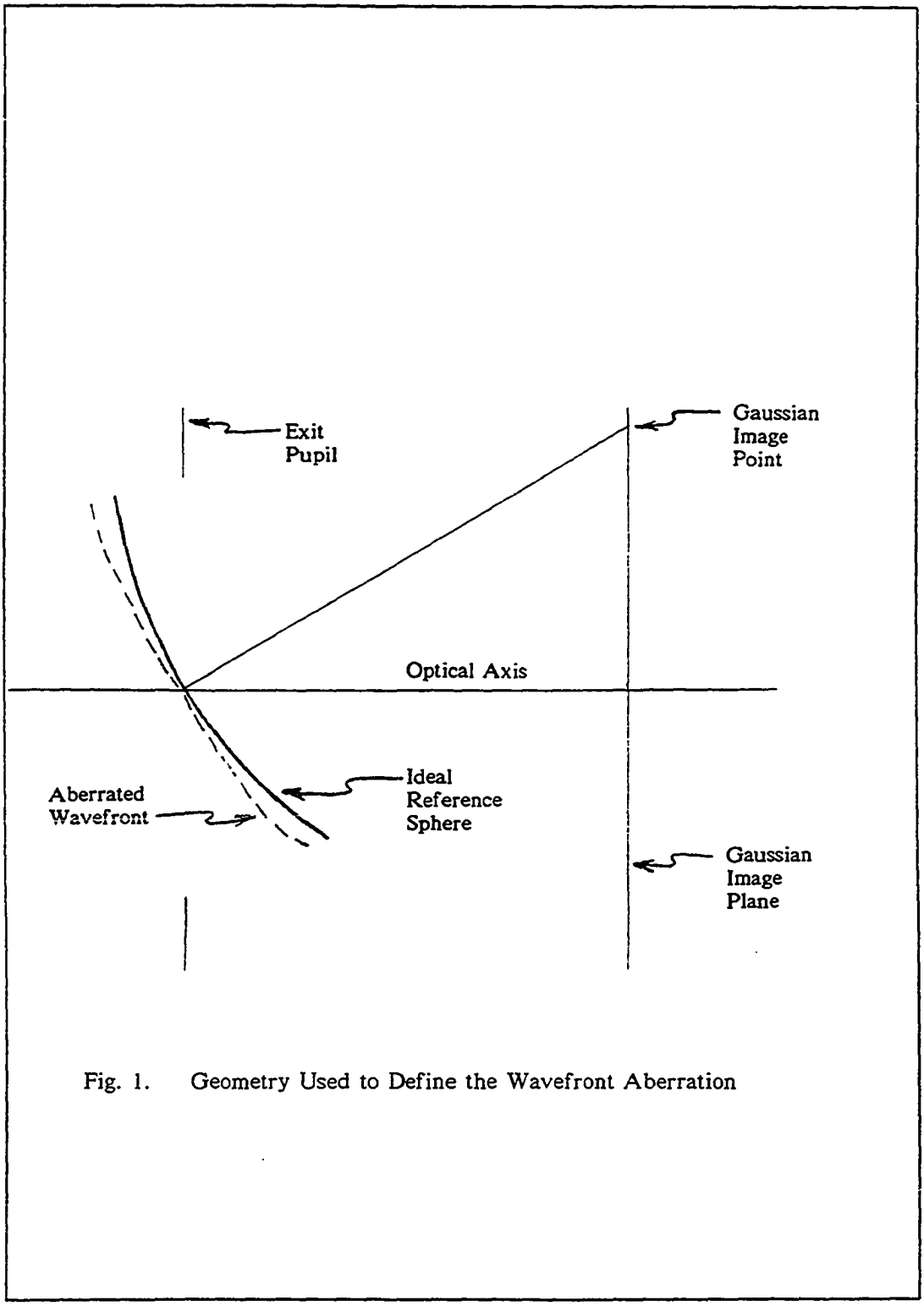

Fig. 1. Geometry Used to Define the Wavefront Aberration

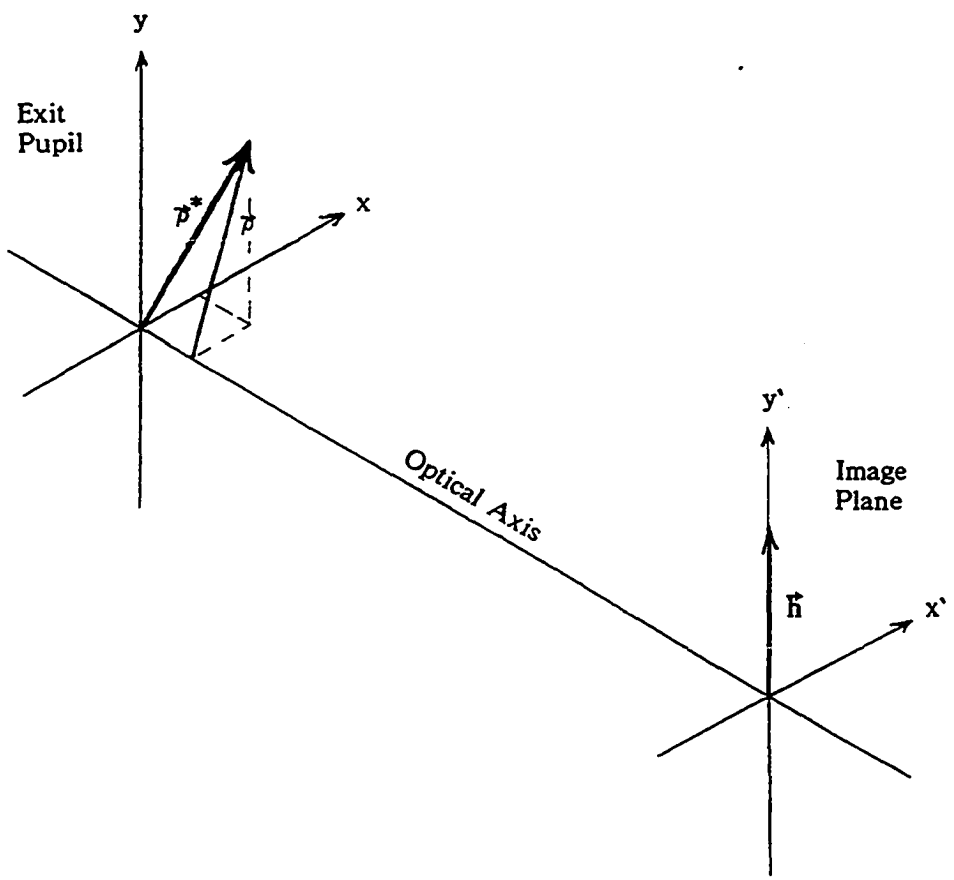

Fig. 2. Diagram of the Pupil and Field Coordinates

$\vec{p}^*$ locates a point on the reference sphere. $\vec{p}$ is the radial component of $\vec{p}^*$. $\vec{h}$ locates a point on the image plane.

micrometers. In addition, the chromatic variable is normalized so that $\nu(.4) = -1$ and $\nu(.7) = 1$.

With the chromatic variable defined, one writes each coefficient W_{jkl} as

$$W_{jkl} = \sum_{i=0}^{\infty} \left[W_{ijkl} \ \nu^i \ \right]. \tag{2.3}$$

Substitute Equation 2.3 into Equation 2.1 and rearrange the order of summations to obtain the following polychromatic aberration series:

$$W = \sum_{i=0}^{\infty}\sum_{j=0}^{\infty}\sum_{k=0}^{\infty}\sum_{l=0}^{\infty} \left[W_{ijkl} \ \nu^i \ (\vec{h}\cdot\vec{h})^j \ (\vec{h}\cdot\vec{\rho})^k \ (\vec{\rho}\cdot\vec{\rho})^l \ \right]. \tag{2.4}$$

The degree m of any term in the series is given by $m = i + j + k + l$. Note that aberrations of like degree are not grouped together in the above summation. This will be shown later to be inconvenient for an investigation based on classifying aberrations by degree. A modification of the series form which groups aberrations of like degree together is

$$W = \sum_{m=0}^{\infty}\sum_{n=0}^{m}\sum_{p=0}^{n}\sum_{q=0}^{p} \left[W_{mnpq} \ \nu^{(m-n)} \ (\vec{h}\cdot\vec{h})^{(n-p)} \ (\vec{h}\cdot\vec{\rho})^{(p-q)} \ (\vec{\rho}\cdot\vec{\rho})^{(q)} \right]. \tag{2.5}$$

This series contains precisely the same terms as the previous series except that they are labeled differently and are summed in a different order. A list the terms in the series up to degree five appears in Appendix B.

Definition of Wavefront Variance

The definition of the wavefront variance for a given wavelength and field point is

$$\sigma^2 = < W^2 >_{\vec{\rho}} - < W >^2_{\vec{\rho}} , \tag{2.6}$$

where the angle brackets denote averaging over the unvignetted area of the pupil. To obtain a merit function which describes the average image quality over the entire field and wavelength ranges, the variance is averaged over the field and chromatic variables as follows:

$$\Phi = < < \sigma^2 >_{\lambda} >_{\vec{h}} , \tag{2.7}$$

where the inner angle brackets denote averaging over the wavelength, and the outer brackets denote averaging over the field variable.

To derive a single equation which expresses the mean wavefront variance merit function, one substitutes Equation 2.7 into Equation 2.6. The resulting equation is written in its explicit integral form as

$$\Phi = \int_0^1 \int_0^{2\pi} \int_{\lambda^-}^{\lambda^+} \int_0^1 \int_0^{2\pi} \left[W^2 \, \Omega(\rho,\lambda,h) \, \frac{d\theta}{2\pi} \, \rho d\rho \;\; d\lambda \, \frac{d\phi}{2\pi} \;\; h dh \right] -$$

$$\int_0^1 \int_0^{2\pi} \int_{\lambda^-}^{\lambda^+} \left[\int_{\rho_0}^1 \int_0^{2\pi} W \;\; \Omega(\rho,\lambda,h) \; \frac{d\theta}{2\pi} \; \rho d\rho \right]^2 \; d\lambda \; \frac{d\phi}{2\pi} \; h dh \; . \qquad (2.8)$$

The weighting function $\Omega(\rho,\lambda,h)$ is defined as ($w_\rho(\rho)$ $w_\lambda(\lambda)$ $w_h(h)$) where the three weighting functions $w_\rho(\rho)$, $w_\lambda(\lambda)$, and $w_h(h)$ have been included to increase the utility of the merit function. λ^- and λ^+ define the range of the chromatic integration.

It is important to note that the functions in the above equation are separable so that each integral may be evaluated independently. One should also note that the pupil integration assumes a circular pupil.

The weighting function $w_\rho(\rho)$ is a radially symmetric function which allows portions of the pupil to be weighted differently than normal. For example, one might wish to design an optical system which images with high contrast. This can be achieved by increasing the weight of the inner portion of the pupil. $w_h(h)$ is a radially symmetric field weighting function that allows portions of the field to be weighted differently. This might be of use in the design of an optical tracking system in which the center of the field may require much higher image quality than the outer portions of the field. Finally, $w_\lambda(\lambda)$ is a chromatic weighting function that allows different portions of the wavelength range to be weighted differently. $w_\lambda(\lambda)$ can be used to tailor the image quality of the system with respect to wavelength in order to match the spectral response of a detector. A functional form for each of the weighting functions will be given during the evaluation of the averaging integrals.

It will prove convenient to carry out the dot products in the aberration terms of Equation 2.5 before proceeding with the development of Equation 2.8. This yields

$$W = \sum_{m=0}^{\infty} \sum_{n=0}^{m} \sum_{p=0}^{n} \sum_{q=0}^{p} \left[W_{mnpq} \; \nu^{(m-n)} \; |h|^{(2n-p-q)} \; \mathrm{Cos}(\theta)^{(p-q)} \; \rho^{(p+q)} \right] . \qquad (2.9)$$

The obvious next step in the development of the merit function is to substitute the aberration series Equation 2.9 into Equation 2.8 and perform the integrations. Because the length of the resulting equation would be excessive if written down in its entirety, only the first term of Equation 2.8 will be written explicitly. After proceeding with the development of this term, the second term can then be written conveniently.

Substitution of Equation 2.9 into the first term of Equation 2.8 yields after separation of the integrals

$$T_1 = \sum_{m_1}^{\infty} \sum_{m_2}^{\infty} \sum_{n_1}^{m_1} \sum_{n_2}^{m_2} \sum_{p_1}^{n_1} \sum_{p_2}^{n_2} \sum_{q_1}^{p_1} \sum_{q_2}^{p_2} (\; W_{m_1 n_1 p_1 q_1} \; W_{m_2 n_2 p_2 q_2}$$

$$\int_0^{2\pi} \frac{d\phi}{2\pi} \int_0^1 h^{(2n_1-p_1-q_1+2n_2-p_2-q_2)} \; w_h(h) \; h dh \int_{\lambda^-}^{\lambda^+} \nu(\lambda)^{(m_1-n_1+m_2-n_2)} \; w_\lambda(\lambda) \; d\lambda$$

$$\int_{\rho_0}^1 \rho^{(p_1+q_1+p_2+q_2)} \; w_\rho(\rho) \; \rho d\rho \int_0^{2\pi} \mathrm{Cos}(\theta)^{(p_1-q_1+p_2-q_2)} \; \frac{d\theta}{2\pi}) \; . \qquad (2.10)$$

These integrals can be evaluated with the explicit forms for the weighting functions $w_\rho(\rho)$, $w_h(h)$, and $w_\lambda(\lambda)$ given below.

Pupil Averaging

Pupil averaging occurs as two integrations, one involving the pupil radial coordinate (ρ) only, and one involving the pupil angle coordinate (θ) only.

Pupil Angle Integration. This integral is

$$S(M) = \int_0^{2\pi} \mathrm{Cos}(\theta)^{(M)} \frac{d\theta}{2\pi} \tag{2.11}$$

$$= \begin{cases} \dfrac{M!}{2^M \left[\frac{M}{2}!\right]^2} & \text{if } M = 0,2,4,\ldots \\ 0 & \text{if } M = 1,3,5,\ldots \end{cases}, \tag{2.12}$$

and can also be evaluated according to the recursion relation

$$S(M+2) = \frac{M+1}{M+2} S(M), \qquad S(0) = 1, \quad S(1) = 0 . \tag{2.13}$$

This allows one to observe two useful properties of the function $S(M)$:

$$S(\mathrm{odd}) = 0 , \text{ and} \tag{2.14}$$

$$1 = S(0) > S(M) > S(M+2) > 0, \qquad M=2,4,6,\ldots . \tag{2.15}$$

Pupil Radial Integration. A convenient normalized weighting function for this integral is

$$w_\rho(\rho) = \frac{\alpha + 2}{1 - \rho_0^{(\alpha+2)}} \rho^\alpha , \qquad \alpha = -1,0,1,\ldots . \tag{2.16}$$

Normalization with respect to the weighting function means that the integral evaluates to unity when the integrand of Equation 2.17 below is a constant.

The weighting function above provides for a centrally obscured pupil of radius ρ_0 and allows the outer portion of the pupil to be weighted differently than the inner portion. Setting $\alpha = -1$ yields uniform radial weighting over the pupil while setting $\alpha = 0$ yields linear radial weighting. Setting $\alpha > 1$ assigns heavier weighting to the outer portion of the pupil.

With the above weighting function defined, the integral can be evaluated as

$$R(a) = \int_{\rho_0}^{1} \rho^{(a)} \rho d\rho , \qquad a = 0,1,2,\ldots \tag{2.17}$$

$$= \frac{\alpha + 2}{a + \alpha + 2} \frac{1 - \rho_0^{(a+\alpha+2)}}{1 - \rho_0^{(\alpha+2)}} . \tag{2.18}$$

From the above expression for the radial pupil, one can derive the following useful property of $R(a)$:

$$1 = R(0) > R(a) > R(a+1) > 0 , \qquad a = 1,2,3,\ldots . \tag{2.19}$$

Field Averaging

The integration over the field is accomplished with the following normalized field weighting function:

$$w_h(h) = (\beta + 2)\, h^{\beta}, \qquad \beta = -1,0,1,\ldots \quad . \tag{2.20}$$

where $w_h(h)$ can be used to increase the weight of the outer portions of the field by adjusting the power β of the fractional radial field variable h. Setting $\beta = -1$ is used for uniform radial field weighting while setting $\beta = 0$ is used for linear radial field weighting. An emphasis on the outer portions of the field can be achieved by setting $\beta > 0$.

The complete field integral is

$$T(c) = \int_0^{2\pi} \frac{d\phi}{2\pi} \int_0^1 h^{(c)}\, w_h(h)\, h\, dh, \qquad c = 0,1,2\ldots \tag{2.21}$$

$$= \frac{\beta + 2}{c + \beta + 2}. \tag{2.22}$$

A useful property of the field integral which is similar to that of the pupil integrals is

$$1 = T(0) > T(c) > T(c+1) > 0, \qquad c = 1,2,3,\ldots \quad . \tag{2.23}$$

Chromatic averaging

Uniform weighting is a common form of chromatic averaging, but often it is desirable to match the chromatic weighting to the response of a detector. In this case a weighting function that is approximately Gaussian in shape is a common choice. But the functional form of Equation 2.2 makes evaluation of the chromatic integral with Gaussian weighting difficult. The "Witch of Agnesi" function (which resembles the Gaussian function) is a weighting function which enables evaluation of the integral. Its

form is

$$w_\lambda(\lambda) = \frac{K}{1 + \sigma^2(\lambda - \bar{\lambda})^2}, \tag{2.24}$$

where K is a normalizing constant which need not be explicitly determined. $\bar{\lambda}$ is the wavelength at which the peak value of the weighting function occurs and σ is the reciprocal of the width of the weighting function. The introduction of σ as the reciprocal of the weighting function width allows the function to be used for uniform spectral weighting by setting $\sigma = 0$.

With the weighting function defined, the chromatic integral is

$$U(d) = \int_{\lambda^-}^{\lambda^+} \nu(\lambda)^{(d)}\, w_\lambda(\lambda)\, d\lambda, \qquad d = 0,1,2,\ldots . \tag{2.25}$$

An explicit analytic solution of the integral is difficult for arbitrary values of the chromatic coordinate power d, but a recursion relation between the intregrals for various values of d can be worked out. The recursion relation can then be used to numerically compute the integrals.

The development of the recursion relation is easier if a transformation of variables from λ to ν is performed. One inverts the chromatic variable function (Equation 2.2) to give

$$\lambda(\nu) = \lambda^* \frac{\nu - \nu_0}{\nu - \nu^*}, \tag{2.26}$$

where $\nu_0 = \nu^* \lambda_0 / \lambda^* = 6.87928$. The differential of the above function is

$$d\lambda = \lambda^* \frac{(\nu_0 - \nu^*)}{(\nu - \nu^*)^2} d\nu \ . \tag{2.27}$$

The inversion of the weighting function $w_\lambda(\lambda)$ is

$$w_\nu(\nu) = \frac{K_2 (\nu - \nu^*)^2}{c \nu^2 + b \nu + a} \ . \tag{2.28}$$

where

$$K_2^2 = \sigma^2 (\lambda^* - \bar{\lambda})^2 \ ,$$

$$\nu_1 = \frac{\lambda^* \nu_0 - \bar{\lambda} \nu^*}{\lambda^* - \bar{\lambda}} \ ,$$

$$c = 1 - K_2^2 \ ,$$

$$b = 2 (K_2^2 \nu_1 - \nu^*) \ ,$$

$$a = \nu^{*2} - K_2^2 \nu_1^2 \ , \text{ and}$$

$$q = 4 a c - b^2 \ . \tag{2.29}$$

The quantity q will appear in later equations.

With the above definitions, the chromatic integral transformed from λ-space to ν-space is thus found to be

$$U(d) = K\, k_0 \int_{\nu^-}^{\nu^+} \frac{\nu(d)}{c\,\nu^2 + b\,\nu + a}\, d\nu \,. \tag{2.30}$$

Finally, define

$$I(d) = \frac{U(d)}{K\, k_0} \,. \tag{2.31}$$

The preliminaries are now complete and the recursion relation for the integral $I(d)$ can be determined. In doing so one is forced to deal with two distinct situations: $q < 0$ (nonuniform spectral weighting, $\sigma^2 > 0$), and $q = 0$ (uniform spectral weighting, $\sigma^2 = 0$).

Nonuniform Spectral Weighting. A perusal of a table of integrals will reveal the following recursion relation for $I(d)$

$$I(d) = \frac{(\nu^+)^{(d-1)} - (\nu^-)^{(d-1)}}{c\,(d-1)} - \frac{b}{c}\, I(d-1) - \frac{a}{c}\, I(d-2) \,, \qquad d = 2,3,4\ldots \,. \tag{2.32}$$

The recursion is initiated with

$$I(0) = \frac{1}{\sqrt{-q}} \ln\left[\frac{1+A}{1-A}\right], \qquad A = \frac{4\,c\,\sqrt{-q}}{b^2 - 4\,c^2 + q} \,, \text{ and} \tag{2.33}$$

$$I(1) = \frac{1}{2\,c} \ln\left[\frac{1+B}{1-B}\right] - \frac{b}{2\,c}\, I(0) \,, \qquad B = \frac{b}{a+c} \,. \tag{2.34}$$

Finally, the desired chromatic averaging function is simply

$$U(d) = \frac{I(d)}{I(0)} . \tag{2.35}$$

Uniform Spectral weighting. In this case Equation 2.30 degenerates to

$$I'(d) = \int_{\nu^-}^{\nu^+} \frac{\nu(d)}{(\nu - \nu^*)^2} \, d\nu , \tag{2.36}$$

and an integral table lookup gives

$$I'(d) = \frac{1}{(d-1)} \left[\frac{\nu^+(d)}{\nu^+ - \nu^*} - \frac{\nu^-(d)}{\nu^- - \nu^*} \right] + \frac{d\,\nu^*}{d-1} I'(d-1) , \quad d = 2,3,4,\ldots . \tag{2.37}$$

The recursion is initiated with

$$I'(0) = \frac{1}{(\nu^- - \nu^*)} - \frac{1}{(\nu^+ - \nu^*)} , \text{ and} \tag{2.38}$$

$$I'(1) = \ln\left[\frac{\nu^+ - \nu^*}{\nu^- - \nu^*} \right] + \nu^* I'(0) . \tag{2.39}$$

Finally as before, one concludes with

$$U(d) = \frac{I'(d)}{I'(0)} . \tag{2.40}$$

A useful property of $U(d)$ is similar to that for $R(a)$ and $T(c)$ and is given by

$$1 = U(0) > U(d) > U(d+2) > 0 , \qquad d = 2,4,6,\ldots \text{ , and} \tag{2.41}$$

$$\bar{1} > \bar{U}(\bar{1}) > \bar{U}(d) > \bar{U}(d+2) > 0 , \qquad d = 3,5,7,\ldots . \tag{2.42}$$

The Complete Wavefront Variance Equation

With the integral functions $S(M)$, $R(a)$, $T(c)$, and $U(a)$ defined above, one can write the first term of the wavefront variance (Equation 2.10) in terms of these functions as follows:

$$T_1 = \sum_{m_1}^{\infty}\sum_{m_2}^{\infty}\sum_{n_1}^{m_1}\sum_{n_2}^{m_2}\sum_{p_1}^{n_1}\sum_{p_2}^{n_2}\sum_{q_1}^{p_1}\sum_{q_2}^{p_2} (W_{m_1n_1p_1q_1} W_{m_2n_2p_2q_2}$$

$$U(m_1-n_1+m_2-n_2)\, T(2n_1-p_1-q_1+2n_2-p_2-q_2)\, R(p_1+q_1+p_2+q_2)\, S(p_1-q_1+p_2-q_2)) . \tag{2.43}$$

The second term of Equation 2.8 can be written in the same way through substitution of the wavefront aberration series and the functions

$$T_2 = \sum_{m_1}^{\infty}\sum_{m_2}^{\infty}\sum_{n_1}^{m_1}\sum_{n_2}^{m_2}\sum_{p_1}^{n_1}\sum_{p_2}^{n_2}\sum_{q_1}^{p_1}\sum_{q_2}^{p_2} (W_{m_1n_1p_1q_1} W_{m_2n_2p_2q_2}$$

$$U(m_1-n_1+m_2-n_2)\, T(2n_1-p_1-q_1+2n_2-p_2-q_2)\, R(p_1+q_1)\, R(p_2+q_2)\, S(p_1-q_1)\, S(p_2-q_2)) . \tag{2.44}$$

The complete wavefront variance merit function is then found by subtracting the T_2 term from the T_1 term. When this is done the merit function can be written (after some simplification by combining the summations in the two terms)

$$\Phi = \sum_{m_1}^{\infty}\sum_{m_2}^{\infty}\sum_{n_1}^{m_1}\sum_{n_2}^{m_2}\sum_{p_1}^{n_1}\sum_{p_2}^{n_2}\sum_{q_1}^{p_1}\sum_{q_2}^{p_2}\left\{W_{m_1n_1p_1q_1}\ W_{m_2n_2p_2q_2}\ a_{12}\ \right\}. \qquad (2.45)$$

where the factors a_{12} are termed coupling constants because they couple $W_{m1n1p1q1}$ to $W_{m2n2p2q2}$ in the merit function. From Equations 2.43, 2.44, and 2.45 one notices that they are given in terms of the averaging functions as

$$a_{12} = U(m_1-n_1+m_2-n_2)\ T(2n_1-p_1-q_1+2n_2-p_2-q_2)$$

$$\left[R(p_1+q_1+p_2+q_2)\ S(p_1-q_1+p_2-q_2) - R(p_1+q_1)\ S(p_1-q_1)\ R(p_2+q_2)\ S(p_2-q_2)\right]. \qquad (2.46)$$

Mean Square Ray Aberration

In real optical systems a ray usually does not pass through the ideal Gaussian image point because of aberrations in the system. The departure of the rays from the Gaussian image point is called the ray aberration.

Squared Ray Aberration

The ray aberration $\vec{\epsilon}$ is depicted in Figure 3. To obtain the squared ray aberration, one forms the dot product of the ray aberration with itself:

$$E^2 = \vec{\epsilon}\cdot\vec{\epsilon}\ . \qquad (2.47)$$

The squared ray aberration is a function of wavelength and the fractional pupil and field coordinates of the ray. In fact, its symmetry properties are the same as those for

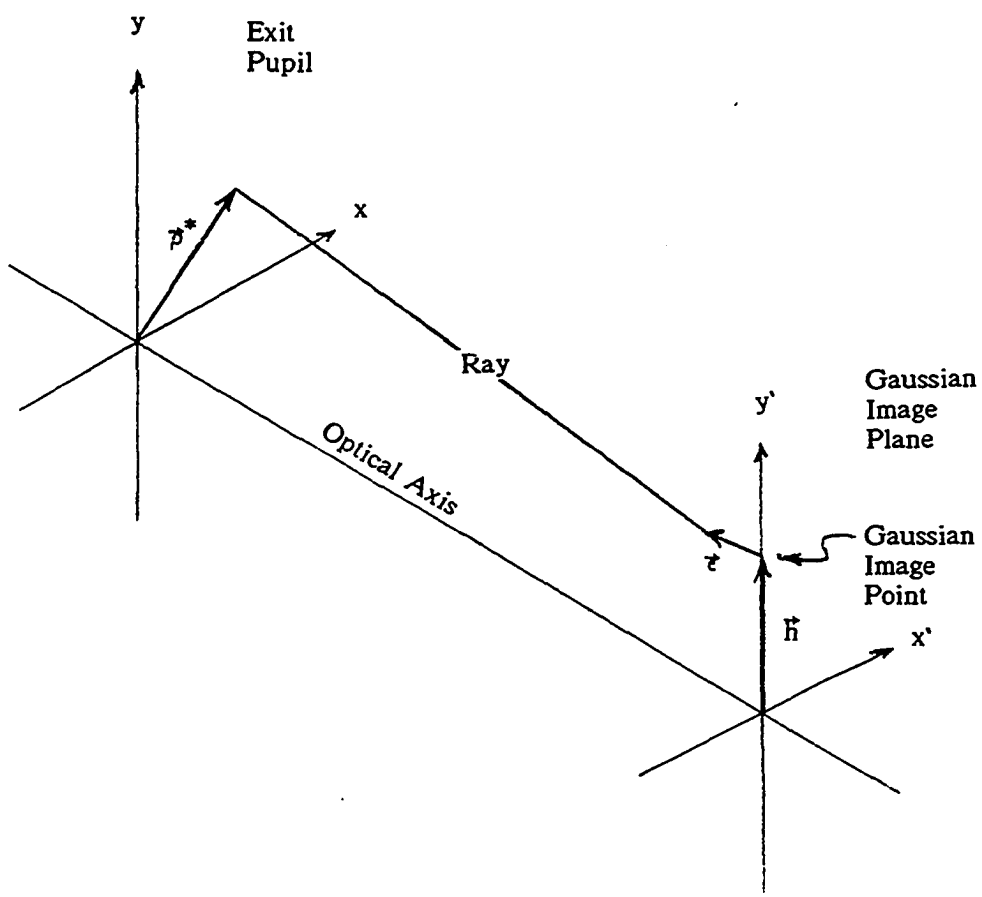

Fig. 3. Geometry Used to Define the Ray Aberration

the wavefront aberration function. For this reason the squared ray aberration can be expanded as

$$E^2 = \sum_{m=0}^{\infty} \sum_{n=0}^{m} \sum_{p=0}^{n} \sum_{q=0}^{p} \left[E_{mnpq} \; \nu^{(m-n)} \; (\vec{h}\cdot\vec{h})^{(n-p)} \; (\vec{h}\cdot\vec{\rho})^{(p-q)} \; (\vec{\rho}\cdot\vec{\rho})^{(q)} \right], \tag{2.48}$$

which upon expanding the dot products in each term becomes

$$E^2 = \sum_{m=0}^{\infty} \sum_{n=0}^{m} \sum_{p=0}^{n} \sum_{q=0}^{p} \left[E_{mnpq} \; \nu^{(m-n)} \; |h|^{(2n-p-q)} \; \mathrm{Cos}(\theta)^{(p-q)} \; \rho^{(p+q)} \right], \tag{2.49}$$

which is identical in form to the expansion for the wavefront aberration function.

Definition of Mean Square Ray Aberration

Averaging E^2 over the pupil yields the ray aberration for a single wavelength and field point. To obtain the aberration averaged over both wavelength and field, one writes

$$\Phi = \int_0^1 \int_0^{2\pi} \int_{\lambda^-}^{\lambda^+} \int_{\rho_0}^1 \int_0^{2\pi} E^2 \; w_\rho(\rho) \; w_\lambda(\lambda) \; w_h(h) \; \frac{d\theta}{2\pi} \; \rho d\rho \; d\lambda \; \frac{d\phi}{2\pi} \; h dh \; . \tag{2.50}$$

The form of this equation is very similar to that of the equation for the wavefront variance. In fact, after substituting the squared ray aberration series into the above equation, the form of the integrals are identical to those in the first term of

Equation 2.8. For this reason the following details of the formulation of the mean square aberration are abbreviated since similar details have been presented in the derivation of the wavefront variance merit function.

After substituting the squared ray aberration series into Equation 2.50 one has

$$\Phi = \sum_{m_1}^{\infty}\sum_{m_2}^{\infty}\sum_{n_1}^{m_1}\sum_{n_2}^{m_2}\sum_{p_1}^{n_1}\sum_{p_2}^{n_2}\sum_{q_1}^{p_1}\sum_{q_2}^{p_2}\left[E_{m_1n_1p_1q_1}\, E_{m_2n_2p_2q_2}\, a_{12} \right], \tag{2.51}$$

where the coupling constants a_{12} are given by

$$a_{12} = U(m_1-n_1+m_2-N_2)\, T(2n_1-p_1-q_1+2n_2-p_2-q_2)\, R(p_1+q_1+p_2+q_2)\, S(p_1-q_1+p_2-q_2)\,. \tag{2.52}$$

It is interesting to note that if the wavefront variance merit function were instead defined as the mean square wavefront aberration merit function, the coupling constants of the two merit functions would be identical. That is, Equation 2.52 would be identical to Equation 2.46. This would mean that any differences in the behaviors of the two merit functions would be independent of the coupling constants, and would depend solely on differences in the two sets of aberration coefficients.

The Quadratic Form

A comparison of Equation 2.45 to Equation 2.51 reveals that both merit functions are of the identical quadratic form in the aberration coefficients. This quadratic form can be written in matrix notation as follows:

$$\Phi = \vec{x}^t A \vec{x} , \tag{2.53}$$

where A is the matrix of coupling constants a_{12}, and x is the aberration vector formed from the aberration coefficients X_{mnpq} . The first few elements of $\vec{x}^t$ are $<X_{0000}, X_{1000}, X_{1100}, X_{1110}, X_{1111}, X_{2000}, ...>$. Note that the components of $\vec{x}$ occur in the same order as their occurance in the aberration series.

The matrix A couples the aberration vector to its transpose and for this reason will be termed the coupling matrix. Each matrix element couples together two aberration coefficients through a term of the form

$$X_{m_1n_1p_1q_1} \; a_{12} \; X_{m_2n_2p_2q_2} . \tag{2.54}$$

This can be seen in Equations 2.45 and 2.51.

Properties of the Coupling Matrix

The coupling matrix defines the physical meaning of the merit function and is not determined by the specific optical system. That is, its elements are independent of any characteristic of the optical system -- they depend only on the definition of the merit function. But on the other hand, many of the properties of the merit function are determined by the properties of the coupling matrix. For this reason several properties

are briefly discussed below.

Matrix Elements. Each element of the coupling matrix for the wavefront variance is given by Equation 2.46. Each element of the coupling matrix for the mean square ray aberration are given by Equation 2.52.

Matrix Symmetry. The coupling matrix is symmetric. That is

$$\mathbf{A} = \mathbf{A}^{t} . \tag{2.55}$$

Matrix symmetry follows from Equations 2.46 and 2.52 and the fact that $R(a+b) = R(b+a)$, $S(a+b) = S(b+a)$, $T(a+b) = T(b+a)$, and $U(a+b) = U(b+a)$.

Odd/Even Aberration Decoupling. One can classify an aberration as either even or odd in the pupil variables according to whether p-q is an even or odd integer. Even and odd aberrations do not interact in the merit function because the coupling matrix element that couples an even aberration coefficient to an odd aberration coefficient is zero. This follows from the property of the pupil angular integral that $S(\text{odd}) = 0$.

The decoupling defines two vector spaces composed of the aberration coefficients of the even and odd aberrations respectively. These two vector spaces possess a null intersection and for this reason the coupling matrix can be written as the sum of an even and an odd coupling matrix $A_e + A_o$. Although this fact will not be exploited here, the merit function can thus be written as a sum of even and odd merit functions:

$$\Phi = \vec{x}_e^{\,t} A_e \vec{x}_e + \vec{x}_o^{\,t} A_o \vec{x}_o$$
$$= \Phi_e + \Phi_o \,. \qquad (2.56)$$

Elements of the coupling matrix are non-negative. The elements of the coupling matrix satisfy

$$1 >= a_{ij} >= 0 \,. \qquad (2.57)$$

This follows from the properties of the averaging functions -- Equations 2.14, 2.15, 2.19, 2.23, 2.41, and 2.42.

For the mean square ray aberration merit function, Equation 2.57 is trivially true since the averaging functions are all non-negative and each matrix element is formed as the product of averaging functions. For the wavefront variance merit function, Equation 2.46 indicates that one need only show that

$$R(a_1+a_2)\, S(b_1+b_2) - R(a_1)\, R(a_2)\, S(b_1)\, S(b_2) >= 0 \,. \qquad (2.58)$$

This is easily accomplished since

$$R(a_1+a_2) >= R(a_1)\, R(a_2) \quad \text{, and} \qquad (2.59)$$

$$S(b_1+b_2) >= S(b_1)\, S(b_2) \,. \qquad (2.60)$$

Coupling Matrix Element Magnitudes. Generally the magnitude of the elements of A decrease with increasing distance down the diagonal and with increasing distance horizontally away from the diagonal. That is

$$a_{ij} > a_{kl} . \qquad \text{for } k,l >> i,j . \tag{2.61}$$

which follows from the defining equation for the coupling matrix and the properties (Equations 2.14, 2.15, 2.19, 2.23, 2.41 and 2.42) of the averaging integrals. This would lead one to expect that the coupling between aberration coefficients of high degree contribute less to the merit function than coupling between lower degree coefficients.

An interesting aspect of the wavefront variance coupling matrix is that any row or column that couples to a pupil independent aberration is identically zero. One can understand this from the fact that the variance of a constant is zero. It is mathmatically demonstrated by the defining equation for the wavefront variance matrix (Equation 2.46) and the fact that $p = q = 0$ for pupil independent aberrations. In this case one has

$$R(0+a)\,S(0+b) - R(0)\,R(a)\,S(0)\,S(b) = R(a)\,S(b) - R(a)\,S(b) = 0 . \tag{2.62}$$

Another interesting property of the wavefront variance coupling matrix is that the value of the matrix elements for very high order coupling become almost equal to the value of the corresponding matrix elements for the mean square ray aberration. By comparing Equations 2.46 and 2.52, one sees this is true if

$$\lim_{a,b \to \infty} \left| R(a+b)\, S(c+d) - R(a)\, R(b)\, S(c)\, S(d) \right| \quad \to \quad R(a+b)\, S(c+d) \,. \tag{2.63}$$

The following demonstrates this (an unobscured pupil is assumed for simplicity)

$$\lim_{a,b \to \infty} \left[\frac{R(a)\, R(b)}{R(a+b)} \right] = \lim_{a,b \to \infty} \left[\frac{\frac{(\alpha+2)}{(a+\alpha+2)} \frac{(\alpha+2)}{(b+\alpha+2)}}{\frac{(\alpha+2)}{(a+b+\alpha+2)}} \right] = 0 \,. \tag{2.64}$$

Thus differences in the behavior of the high order components of the two merit functions are independent of the coupling matrix and must depend only on differences in the behavior of the aberration vectors $\vec{x}$.

Orthogonalization of the Aberrations

The quadratic form associated with the merit function is inconvenient because aberration coefficients of differing degree are coupled together -- that is, off diagonal elements of the coupling matrix can be nonzero. This makes classification of terms based on degree difficult to implement. By transforming the quadratic form into a sum of squared terms, one can classify each of the resulting terms according to the degree of that term. To accomplish this, one determines a transformation matrix R that transforms the aberration vector $\vec{x}$ according to

$$\vec{f} = R\, \vec{x} \,, \tag{2.65}$$

so that the merit function is transformed to

$$\Phi = \vec{f}^t \vec{f} \tag{2.66}$$

$$= \Sigma f_i^2 \, . \tag{2.67}$$

The elements f_i of the vector $\vec{f}$ will be termed orthogonal aberrations because they occur in the merit function only in squared form. There is no cross coupling between orthogonal aberrations -- hence the term "orthogonal". The absence of cross coupling means that the coupling matrix has been transformed by the matrix factorization to a diagonal matrix (in fact, the identity matrix -- which makes it useless).

The matrix R will be termed the transformation matrix because it transforms the classical aberration vector to the orthogonal aberration vector. The following shows how the transformation matrix R is determined from the coupling matrix A .

The Cholesky Matrix Factorization

The coupling matrix satisfies

$$\Phi = \vec{x}^t \; A \; \vec{x} \; >= \; 0 \tag{2.68}$$

for all possible values of the classical aberration vector $\vec{x}$ because the merit function represents a physical quantity that must be non-negative. That physical quantity is either the wavefront variance or the mean square ray aberration. The coupling matrix is thus said to be positive definite and can be factored into the product of a right triangular matrix times its transpose

$$A = R^t R . \tag{2.69}$$

One sees that the matrix R is the transformation matrix of Equation 2.65 through the following:

$$\begin{aligned} \Phi &= \vec{x}^t A \vec{x} \\ &= \vec{x}^t (R^t R) \vec{x} \\ &= (\vec{x}^t R^t)(R \vec{x}) \\ &= (R \vec{x})^t (R \vec{x}) \\ &= \vec{f}^t \vec{f} . \end{aligned} \tag{2.70}$$

The factorization of A is called the Cholesky matrix factorization. If the elements of R are denoted by r_{ij} , and the symbol := denotes the replacement operation, then an algorithm which implements the Cholesky factorization is

```
for k = 0, 1, 2, ..., n-1
    for j = k, k+1, k+2, ..., n-1
        r_kj = a_kj / sqrt(a_kk)

    for i = k+1, k+2, k+3, ..., n-1
        for j = k+1, k+2, k+3, ..., n-1
            a_ij := a_ij - a_kj a_ki / a_kk .
```
(2.71)

Properties of the Transformation Matrix

Orthogonal Aberrations. Each orthogonal aberration is a linear combination of classical aberration coefficients where the linear combination is determined from the rows of the transformation matrix. This follows from Equation 2.65 which can be explicitly written as

$$f_i = \sum_{j=i}^{\infty} r_{ij} x_j , \qquad \text{for } i = 0,1,2,\ldots \quad . \tag{2.72}$$

The summation index starts at $j = i$ because the transformation matrix is right triangular.

The above equation indicates how to classify the orthogonal aberrations. Any particular orthogonal aberration f_i is classified as belonging to the same degree as its corresponding classical aberration coefficient x_i. x_i appears in the first term of Equation 2.72, and all coefficients x_j that follow in the summation must have the same or higher degree. For example, f_6 is classified as a second degree orthogonal aberration because the classical aberration coefficients that appear in the summation for f_6 are of second degree and higher.

Elements of the Transformation Matrix are Non-negative. The elements of the transformation matrix satisfy

$$1 > r_{ij} > 0 . \tag{2.73}$$

This follows from the similar property of the coupling matrix (Equation 2.57) and the Cholesky matrix factorization algorithm 2.71. The generation of the transformation matrix can be viewed as a sequence of row operations on the coupling matrix. Each row operation preserves Equation 2.73. This is easily understood by examining the equations inside the j loops of the factorization algorithm.

Transformation Matrix Element Magnitudes. The elements of the transformation matrix satisfy

$$r_{ij} > r_{kl} \qquad \text{for } k,l >> i,j\,. \tag{2.74}$$

This follows from a similar property of the coupling matrix (Equation 2.61) and the Cholesky matrix factorization algorithm 2.71 with the same explanation as in the previous paragraph.

First Degree Adjustments on the Merit Functions

Mean Square Ray Aberration. The current definition of the mean square ray aberration merit function references the squared ray aberration to the Gaussian image point. If the optical system suffers from distortion, the centroid of the image spot is displaced from the Gaussian image point, which results in a large value for the merit function even though the image spot may be very small. For this reason a more appropriate reference point location is the centroid of the aberrated image spot. With this reference point the merit function is a measure of the aberrated spot size, which is usually the physical quantity of interest.

Because of aberrations, the plane of best average image quality is usually not coincident with the Gaussian plane. For this reason it is appropriate to allow a defocus of the reference plane from the Gaussian plane to the plane which yields the smallest average spot size over the field.

Wavefront Variance. The current definition of the wavefront variance merit function requires that the wavefront aberration be measured from a reference sphere centered on the Gaussian image point. A more appropriate reference sphere is the one which achieves a "best fit" to the aberrated wavefront (which in the presence of a small amount of aberration is centered on the peak of the diffraction image). This reference is achieved by adding the appropriate amount of tilt and defocus to the

reference sphere at each image point.

The Method of Adjustment

Locating the Image Centroid. The wavefront aberration is defined with respect to a reference sphere centered on the Gaussian image point. The mathematical description of tilting the reference sphere a small amount is achieved by adding a tilt term of the form

$$\Delta W_{1110}\,(\vec{h}\cdot\vec{\rho}) \;=\; \Delta W_{1110}\,|h|\;\mathrm{Cos}(\theta)\,\rho \qquad (2.75)$$

to the aberration function. The amount of the tilt is determined by the magnitude of the coefficient ΔW_{1110} .

If the aberration function is written as a Taylor series, then the effect of a tilted reference sphere can be simply incorporated into the aberration expansion of Equation 2.5 by replacing the tilt aberration coefficient W_{1110} by the sum W_{1110} + ΔW_{1110}. The resultant term is then:

$$(\,W_{1110} \;+\; \Delta W_{1110}\,)\,|h|\;\mathrm{Cos}(\theta)\,\rho\;. \qquad (2.76)$$

It is important to note that the addition of ΔW_{1110} to the tilt aberration does not change the physical wavefront in any way -- it merely results in a description of the wavefront aberration function that is measured from a reference sphere that is tilted with respect to the ideal reference sphere.

The above discussion associates the addition of a tilt term to the wavefront aberration expansion with the addition of tilt to the ideal reference sphere. In the same

way, the addition of a tilt term of the form

$$\Delta E_{1110} \, |h| \, \mathrm{Cos}(\theta) \, \rho \tag{2.77}$$

to the squared ray aberration expansion associates the term with a shift of the reference location. That is, the squared ray aberration is measured from a reference point that is shifted from the Gaussian image point.

The problem is to determine the amount of tilt term that must be added to either of the aberration expansions in order to measure the aberrations from the desired reference. Fortunately, the procedure which accomplishes this is relatively simple and is the same for both aberrations.

Let one average the aberration over the pupil and chromatic coordinates, but not the field coordinate. This defines a merit function which is a measure of the image quality as a function of field. Following the same procedures as those outlined earlier in the chapter, the merit function can be written in the same quadratic form as in Equation 2.45:

$$\Phi(h) = \sum_{m_1}^{\infty} \sum_{m_2}^{\infty} \sum_{p_1}^{m_1} \sum_{p_2}^{m_2} \sum_{q_1}^{p_1} \sum_{q_2}^{p_2} \left[X_{m_1 p_1 q_1} \, X_{m_2 p_2 q_2} \, a''_{12} \right], \tag{2.78}$$

were each coefficient X_{mpq} of the reduced set of aberrations is a function of field and can be written

$$X_{mpq} = \sum_{n=0}^{\infty} \left[X_{mnpq} \left| h \right|^{(n)} \right] . \tag{2.79}$$

A new coupling matrix A'' is generated which will be termed the reduced coupling matrix because it is determined by a reduced set of aberrations. Its elements, a''_{12} , are given by

$$a''_{12} = U(m_1-p_1+m_2-p_2)\, R(p_1+q_1+p_2+q_2)\, S(p_1-q_1+p_2-q_2) \tag{2.80}$$

for the mean square ray aberration, and by

$$a''_{12} = U(m_1-p_1+m_2-p_2) \left(R(p_1+q_1+p_2+q_2)\, S(p_1-q_1+p_2-q_2) - R(p_1+q_1)\, R(p_2+q_2)\, S(p_1-q_1)\, S(p_2-q_2) \right) \tag{2.81}$$

for the wavefront variance.

The specific value for ΔX_{1110} which locates the desired aberration reference is determined by the following procedure: Factoring the reduced coupling matrix generates a reduced transformation matrix R'' and a set of orthogonal aberrations f''_i which are functions of field height. However, only one of the orthogonal aberrations will contain the tilt aberration. The best that can be done to reduce the merit function by adjusting ΔX_{1110} (since only one orthogonal aberration contains ΔX_{1110}) is to adjust it to zero (or balance) the linear combination of reduced aberration coefficients that make up the orthogonal aberration. The balance is automatically accomplished by simply zeroing out that row of R'' associated with the tilt orthogonal aberration.

For the squared ray aberration, the physical interpretation of balancing out

the orthogonal aberration is moving the ray aberration reference point to the image centroid. For the wavefront aberration, the interpretation (for small aberrations) is tilting the reference sphere so that its center coincides with the peak of the diffraction image. For large aberrations, the balancing determines a best fit to the aberrated wavefront.

Suppose, however, that distortion is important in the particular application under study. In this case one would not want to completely ignore its effects. If this is the case then the relative importance of distortion can be simply incorporated into the merit function. One would not simply zero the appropriate row of the transformation matrix R'' as suggested above, but would multiply it by a factor which is between zero and unity, and is proportional to the importance attached to the effects of distortion.

The final form of the merit function is achieved by averaging over the field. The first step to accomplish this is to multiply the modified transformation matrix by its transpose to generate a modified reduced coupling matrix A' whose elements are denoted by a_{12}'. Next one multiplies out the resulting quadratic form after expanding each of the aberration coefficients according to Equation 2.79. The final averaging over the field variable can then be performed. Operationally, this can be carried out in an easy way by simply forming each element of the complete coupling matrix from

$$a_{12} = T(m_1-n_1+m_2-n_2)\, a_{12}' \,. \tag{2.82}$$

This coupling matrix manifests the merit function with the desired aberration reference. It is then factored to obtain the transformation matrix which in turn defines the orthogonal aberrations. This completes the process.

Locating the Best Average Image plane. The procedure that locates the best average image plane is similar to the procedure which locates the image centroid as an aberration reference. For the wavefront aberration one adds a focus shift to the ideal reference sphere -- while for the squared ray aberration one adds a focus shift to the imaging plane. In either case the focus shift is manifested by adding a defocus term of the form:

$$\Delta X_{1111}\,(\vec{\rho}\cdot\vec{\rho}) \;=\; \Delta X_{1111}\,\rho^2 \tag{2.83}$$

to the aberration function. The defocus term is incorporated into the original aberration series expansion by replacing the coefficient X_{1111} by the sum $X_{1111} + \Delta X_{1111}$.

As with the tilt term, the addition of the defocus term to the aberration function does not alter the intrinsic aberration in any way. It simply represents the effect of measuring the aberration relative to an image plane defocused from the Gaussian image plane.

The procedure which determines the amount of defocus needed to locate the plane of best averaging is similar to the procedure above which determines the appropriate amount of tilt. This procedure is simpler, however, because we wish to find the plane of best average imaging over the entire field. For this reason we average over all the variables (chromatic, pupil, and field) just as explained early in the chapter, and then factor the coupling matrix before doing any adjustments. The plane of best average imaging is then obtained by adjusting the defocus coefficient ΔX_{1111} to zero out (balance) the single orthogonal aberration in which it is contained. This is easily accomplished by simply zeroing out that row of the transformation matrix associated with the defocus aberration. The procedure is now complete.

As an aside, if one wishes the merit function to be a measure of the aberration over the surface of best imaging (not necessarily a plane surface), one would follow a procedure exactly analagous to the precedure which determined the amount of tilt for the desired aberration reference.

It is interesting to note that the tilt and defocus adjustments are orthogonal in the sense that the tilt adjustment does not effect the defocus adjustment, with the reverse also being true. This is because the tilt and defocus terms do not couple in the merit function -- tilt is an odd aberration while defocus is an even aberration. Because of this, the two first degree adjustment procedures can be carried out concurrently and independently, which is a great convenience.

Merit Subfunctions

As explained earlier in the chapter, each orthogonal aberration can be associated with an aberration coefficient of a particular degree, say degree j. It is a linear combination of aberration coefficients of degree j and greater, but no degree less than j. For example, any third degree orthogonal aberration is a linear combination of third and higher degree classical aberration coefficients, but no zero, first, or second degree coefficients appear in the linear combination. This suggests how the merit function defined in Equation 2.67 may be classified into a sequence of merit "subfunctions" which isolate the aberration degrees.

One starts with

$$\Phi = \vec{f}^{t}\,\vec{f}$$

$$= \sum_{i=0}^{\infty} f_i^2 \, . \tag{2.84}$$

where the elements of $\vec{f}$ are the orthogonal aberrations f_i . Collect all orthogonal aberration terms of degree j and denote this partial sum T_j^2 . Note that T_j^2 contains aberration coefficients of degree j and greater, but no coefficients of degree less than j. Thus one would expect the characteristics of T_j^2 to be dominated by the characteristics of j^{th} degree aberration coefficients. Equation 2.84 is written

$$\Phi = T_0^2 + T_1^2 + T_2^2 + T_3^2 + \ldots \, , \tag{2.85}$$

where

$$T_j^2 = \sum_i f_i^2 \, . \tag{2.86}$$

The number of terms in the summation is different for each j, and the summation is carried out over all orthogonal aberrations, f_i , of degree j. The above two equations manifest in a fundamental way the classification scheme based on degree.

Consider, however, the above equations in the context of optical design. Normally one would construct Φ (mean square ray error or wavefront variance) using real ray data and then attempt to minimize it with respect to the design variables of the system. One could also attempt to minimze Equation 2.85 with respect to the design variables, but this would be no more useful than attempting to minimize the merit function which was constructed from real rays. Any additional insight to be gained

lies in the study of the T_j terms. In this regard it makes some sense to study each term independently. But notice that, taken independently, none of the terms to be studied can be directly related to the full merit function. It makes more sense to study a sequence of functions that converges to the full merit function. With this in mind, a logical sequence of functions can be constructed in the following way:

$$\phi_0 = T_0^2 + T_1^2 + T_1^2 + T_3^2 + T_4^2 + \ldots, \tag{2.87}$$

$$\phi_1 = T_1^2 + T_2^2 + T_3^2 + T_4^2 + \ldots,$$

$$\phi_2 = T_2^2 + T_3^2 + T_4^2 + \ldots,$$

$$\phi_3 = T_3^2 + T_4^2 + \ldots,$$

$$\phi_4 = T_4^2 + \ldots,$$

and so on.

Each function of the above sequence is termed a merit "subfunction".

Note that $\Phi = \phi_0$, and that the ϕ_j define a sequence of functions that converges to Φ. Also note that ϕ_j contains no aberration coefficients of degree less than j. Thus the characteristics of ϕ_j with respect to the construction variables of an optical system should depend on the characteristics of the aberration coefficients of degree j.

One can think of the subfunctions as manifesting a classification of the merit function by aberration degree -- a classification that many optical designers have contemplated but not attempted because of the lack of a logical approach. Some consequences of this classification scheme will be examined in Chapters Five and Six, and will constitute a preliminary investigation into possible uses of these novel merit subfunctions in optical design. It is also hoped that further explorations of this type

will yield new insight into the behavior of optical systems.

CHAPTER 3

RAYTRACING APPROPRIATE TO POWER SERIES EXPANSIONS

It was shown in the previous chapter how two physically significant merit functions could be expressed as the dot product of an orthogonal aberration vector with itself. The orthogonal aberration vector was expressed as the matrix product of the transformation matrix with the vector of classical aberration coefficients. Equations for computing the elements of the transformation matrix were developed entirely from considerations of the first order geometry of the optical system and the physical meaning of the merit function. In this Chapter, attention is directed to the development of a method to compute the aberration coefficients to arbitrary degree.

There currently exist four methods used to compute aberration coefficients. The first is simply a brute force least squares fit of real ray data. Coefficients determined in this way are only an approximation to the desired Taylor series coefficients. The approximation improves as the degree of the fitting polynomial increases, but if the Taylor series of the aberration function converges slowly, then a great many terms must be included in the fitting polynomial to insure that acceptably accurate values are computed for the coefficients.

The second method uses equations derived by algebraically expanding ray trace equations in the manner of Wachendorf and Hopkins, or by expanding Eikonal functions in the manner of Buchdahl. The equations are algebraically expanded only once, and the resulting equations can then be used repeatedly to trace any number of

rays. The difficulty with this method is that expanding to orders past the fifth is extremely cumbersome and subject to errors during the derivation.

The third method is loosely related to the second method with the difference being that the equations are expanded numerically instead of algebraically. Each quantity in an equation is represented by its power series expansion, and then the coefficients of the expansions are computed numerically -- without explicitly expanding the equations (see Andersen[5]). The expansion is implicit each time a ray is traced. This method is well suited to implementation on digital computers.

The fourth method (which is developed and used by the author specifically for the present research) is closely related to the third method except that quantities are expanded in partially summed series form. As will be shown in the next chapter, the partially summed series are the proximate quantities of Hopkins.

The purpose of this and the next chapter is to show how the polychromatic Taylor series coefficients (aberration coefficients) of either the wavefront aberration at the exit pupil or the squared ray aberration at the image plane can be calculated to arbitrary degree using an algorithmic approach to proximate ray tracing. It should be pointed out that the aberration coefficients of the two aberrations are calculated independently, one is not derived from the other.

Specifically, in this chapter the formulation of an unconventional set of ray trace equations consistent with the partially summed power series associated with proximate quantities is carried out. Because of the symmetry properties of the aberration series (see Equation 2.5), some modifications to the familiar ray trace equations are necessary. To illustrate this point, consider the conventional equation which relates points $\vec{P}$ and $\vec{P}'$ on the ray in Figure 4. These two points are related through the equation,

$$\vec{P}' = \vec{P} + Q\vec{S}, \tag{3.1}$$

where $\vec{S}$ points in the direction of the ray and Q is a scalar related to the distance along the ray from $\vec{P}$ to $\vec{P}'$. The x component of the above equation is

$$P'_X = P_X + Q S_X . \tag{3.2}$$

Now, as will be shown later, P_x and S_x are odd functions of the pupil and field variables and can not be represented by a power series of the form of Equation 2.5. However, Q is an even function of the variables and can be represented by an equation of that form. To implement the above equation, one must implement power series algorithms which can operate on the two different power series forms.

An alternative approach, which is used here, is to retain a single power series form and modify the above equation so that only operations on quantities which are even functions of the variables occur. For example, by incorporating the y component of Equation 3.1, one can form a new equation,

$$(P'_X{}^2 + P'_y{}^2) = (P_X{}^2 + P_y{}^2) + 2Q(P_X S_X + P_y S_y) + Q^2(S_X{}^2 + S_y{}^2), \tag{3.3}$$

in which the quantities in parenthesis are even functions of the variables. This equation can be implemented by utilizing power series operations which involve a unique series form, thus avoiding operations on differing power series forms.

With the above motivation, one can develop a consistent set of ray trace equations which involve only quantities which are even functions of the pupil and field variables. This is essentially equivalent to developing ray trace equations in a

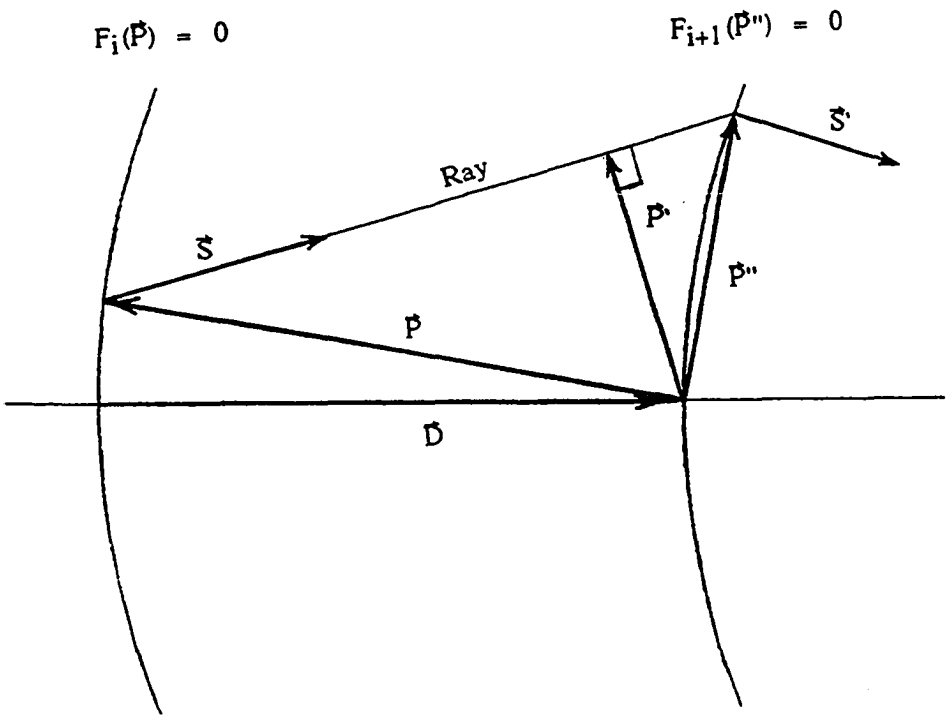

Fig. 4. Illustration of the Vectors Involved in Tracing a Ray Specified by $\vec{P}$ and $\vec{S}$

$\vec{P}'$ identifies the perpendicular point.

cylindrical coordinate system.

Ray Tracing

Ray tracing is a process of repeated ray transfer followed by ray refraction operations. The propagation of a ray from a surface to the succeeding surface is illustrated in Figure 4. The ray is uniquely specified by a position $\vec{P}$ on the ray and the optical direction $\vec{S}$ at point $\vec{P}$. The optical direction vector $\vec{S}$ is the vector which points in the direction of ray propagation and whose length is given by the refractive index of the medium in which the ray lies. The vectors $\vec{P}$ and $\vec{S}$ can be written for convenience in several forms

$$\vec{P} = < P_X, P_y, P_Z > = < \vec{p}, P_Z > \qquad \text{where } \vec{p} = < P_X, P_y, 0 > \text{, and}$$
$$\vec{S} = < S_X, S_y, S_Z > = < \vec{s}, S_Z > \qquad \text{where } \vec{s} = < S_X, S_y, 0 > . \tag{3.4}$$

Note that $\vec{P}$ is the three dimensional position vector and $\vec{p}$ is the component of $\vec{P}$ perpendicular to the optical axis (the z axis).

Maintaining axial symmetry, one can restrict oneself to rotationally symmetric conic surfaces of the form:

$$F(\vec{P}) = P_Z - \frac{1}{2} C ((\vec{p}\cdot\vec{p}) + (1+\kappa) P_Z^2) = 0 , \tag{3.5}$$

where C is the vertex curvature and κ is the conic constant.

Refering to Figure 4, the ray trace problem is stated in the following way: given the vectors $\vec{P}$ and $\vec{S}$ for a ray, propagate the ray to find the corresponding vectors $\vec{P}''$ and $\vec{S}'$. This is accomplished by first determining the intersection $\vec{P}''$ of the ray

with the surface (the transfer operation), and then determining the refracted ray direction $\vec{S}'$ (the refraction operation).

At the start of every transfer however, the position vector is given relative to the vertex of the current surface. To express the position vector relative to the next surface, one simply subtracts the axial thickness D from the z component of the position vector. This yields the desired position vector $\vec{P}$ of Figure 4.

Transfer

The transfer of a ray from point $\vec{P}$ on the ray to an arbitrary point $\vec{P}^*$ on the ray is given by the vector equations

$$\vec{P}^* = \vec{P} + Q\vec{S} \text{ , and} \tag{3.6}$$

$$\vec{S}^* = \vec{S} \tag{3.7}$$

which when expressed in terms of their axial and radial components is equivalent to the following set of equations:

$$\vec{p}^* = \vec{p} + Q\vec{s} \text{ ,} \tag{3.8}$$

$$P_z^* = P_z + Q S_z \text{ ,} \tag{3.9}$$

$$\vec{s}^* = \vec{s} \text{ , and} \tag{3.10}$$

$$S_z^* = S_z \text{ ,} \tag{3.11}$$

where Q is the reduced distance (the physical distance divided by the index of refraction) along the ray and will be termed the transfer parameter. A new set of transfer equations is derived from Equations 3.8 - 3.11 whose transfer is governed by

the transfer parameter as follows:

$$
\begin{aligned}
(\vec{p}\cdot\vec{p})^* &= (\vec{p}\cdot\vec{p}) + 2Q(\vec{p}\cdot\vec{s}) + Q^2(\vec{s}\cdot\vec{s}), \\
(\vec{p}\cdot\vec{s})^* &= (\vec{p}\cdot\vec{s}) + Q(\vec{s}\cdot\vec{s}), \\
(\vec{s}\cdot\vec{s})^* &= (\vec{s}\cdot\vec{s}),
\end{aligned} \tag{3.12}
$$

and

$$
\begin{aligned}
P_z^* &= P_z + Q S_z, \text{ and} \\
S_z^* &= S_z .
\end{aligned} \tag{3.13}
$$

Note that in accordance with the philosphy of this chapter, all the quantities in parentheses are even functions of the field and pupil variables. The optical path length along the ray from point $\vec{P}$ to $\vec{P}^*$ is

$$
\mathrm{OPL} = N^2 Q , \tag{3.14}
$$

where the refractive index N is represented by a power series in the chromatic variable.

These are the general transfer equations for the proximate ray trace. All that remains is to determine that particular value for the transfer parameter Q which transfers the ray to the succeeding surface. Computationally it is convenient to carry out the transfer in two steps: from the surface to a point on the ray nearest the vertex of the next surface, and then from that point to the point of intersection with the next surface. This is illustrated by $\vec{P}'$ and $\vec{P}''$ in Figure 4.

The "Perpendicular Point". The point on the ray nearest the vertex of the surface will be termed the "perpendicular point". It satisfies $\vec{P}'\cdot\vec{S} = 0$ from which is

derived

$$Q = \frac{-(P_z S_z + (\vec{p}\cdot\vec{s}))}{N^2} . \tag{3.15}$$

Note that all operations in the above equation involve only even quantities in the pupil and field variables.

The Surface Intersection Point. The transfer parameter which transfers the ray from the perpendicular point to the surface intersection is determined by simultaneously solving $F(\vec{P}'') = 0$ and $\vec{P}'' = \vec{P}' + Q\,\vec{S}$. Substituting Equation 3.6 into Equation 3.5 and solving for Q gives

$$Q = \frac{-B_t - \sqrt{B_t^2 - A_t D_t}}{A_t} = \frac{D_t}{-B_t + \sqrt{B_t^2 - A_t D_t}} , \tag{3.16}$$

where

$$A_t = C [N^2 + \kappa S_z'^2] ,$$
$$B_t = [1 - C \kappa P_z'] S_z' , \text{ and}$$
$$D_t = C [(\vec{p}\cdot\vec{p})' + (\kappa+1) P_z'^2] - 2 P_z' . \tag{3.17}$$

The above two sets of equations complete the proximate ray transfer.

Refraction

Figure 4 also illustrates the refraction operation. Given $\vec{S}$ and the point of intersection $\vec{P}''$ of the ray with the surface, one wishes to determine $\vec{S}'$. For convenience the double prime notation for $\vec{P}''$ in favor of single prime notation to represent quantities after refraction. One starts with Snell's Law in vector form:

$$\vec{S}' \times \vec{n} = \vec{S} \times \vec{n} \tag{3.18}$$

which implies that the refraction operation obeys the vector equations

$$\vec{P}' = \vec{P} \text{ , and} \tag{3.19}$$

$$\vec{S}' = \vec{S} + \Gamma \vec{n} \text{ ,} \tag{3.20}$$

where $\vec{n}$ is the surface normal vector at point $\vec{P}$ on the surface and Γ is termed the refraction parameter. The surface normal is found by taking the gradient of the surface function. For a conic surface the normal is easily determined to be

$$\vec{n} = < -C\,\vec{p}\,,\ 1 - (1+\kappa)\,C\,P_Z > . \tag{3.21}$$

Since $\vec{s}$ and $\vec{p}$ are odd functions of the pupil and field variables, one must express the refraction operation of Equations 3.19 and 3.20 in the following appropriate form

$$(\vec{p}\cdot\vec{p})' = (\vec{p}\cdot\vec{p}) \text{ ,}$$

$$(\vec{p}\cdot\vec{s})' = (-C\,\Gamma)\,(\vec{p}\cdot\vec{p}) + (\vec{p}\cdot\vec{s}) \text{ ,}$$

$$(\vec{s}\cdot\vec{s})' = (-C\Gamma)^2(\vec{p}\cdot\vec{p}) + 2(-C\Gamma)(\vec{p}\cdot\vec{s}) + (\vec{s}\cdot\vec{s}), \tag{3.22}$$

and

$$P_Z' = P_Z, \text{ and}$$

$$S_Z' = S_Z + \Gamma[1 - (1+\kappa) C P_Z], \tag{3.23}$$

where the quantities in parentheses are even functions of the variables. All that remains is to determine the refraction parameter.

The first step in the determination of the refraction parameter Γ is to square Equation 3.20 by taking the dot product with itself:

$$(\vec{S}'\cdot\vec{S}') = (\vec{S}\cdot\vec{S}) + 2(\vec{S}\cdot\vec{n})\Gamma + (\vec{n}\cdot\vec{n})\Gamma^2. \tag{3.24}$$

Recalling that $(\vec{S}'\cdot\vec{S}') = N'^2$ and $(\vec{S}\cdot\vec{S}) = N^2$, solving for Γ gives

$$\Gamma = \frac{\left[-B_\Gamma \pm \sqrt{B_\Gamma^2 - A_\Gamma D_\Gamma}\right]}{A_\Gamma}, \tag{3.25}$$

where for reflection the sign of the radical is chosen to be opposite in sign to B_Γ. For refraction the same sign is chosen. The quantities A_Γ, B_Γ, and D_Γ are given by

$$A_\Gamma = C^2(\vec{p}\cdot\vec{p}) + [1 - (1+\kappa) C P_Z]^2,$$

$$B_\Gamma = -C(\vec{p}\cdot\vec{s}) + [1 - (1+\kappa) C P_Z] S_Z, \text{ and}$$

$$D_\Gamma = N^2 - N'^2. \tag{3.26}$$

This completes the equations needed for refracting a proximate ray.

Note that in both the transfer and refraction operations, the basic ray quantities have been changed from P_x, P_y, P_z, S_x, S_y, and S_z to $(\vec{p}\cdot\vec{p})$, $(\vec{p}\cdot\vec{s})$, $(\vec{s}\cdot\vec{s})$, P_z, and S_z . The quantities $(\vec{p}\cdot\vec{p})$, $(\vec{p}\cdot\vec{s})$, and $(\vec{s}\cdot\vec{s})$ are often called rotation invariants and occur in a natural way when considering the ray trace problem in a cylindrical coordinate system.

Tilted Reference Spheres

The calculation of wavefront aberration requires that a ray be traced from an object point (or equivalently from the ray's intersection with an object space reference sphere) to its intersection with the reference sphere in image space. The reference spheres are usually chosen to lie in the pupils of the system and to be centered on the Gaussian conjugate points. Because a reference sphere is not a system constant, but is a function of the object or image coordinate, the proximate ray trace must properly account for its behavior. Figure 5 illustrates the entrance and exit pupil reference spheres of a general optical system. Note that they are not constant, but vary with the object and image heights.

The equation which represents a reference sphere can be written in the form:

$$\hat{C}\cdot\vec{P} - .5\, c_V\, \vec{P}\cdot\vec{P} = 0\,, \tag{3.27}$$

where

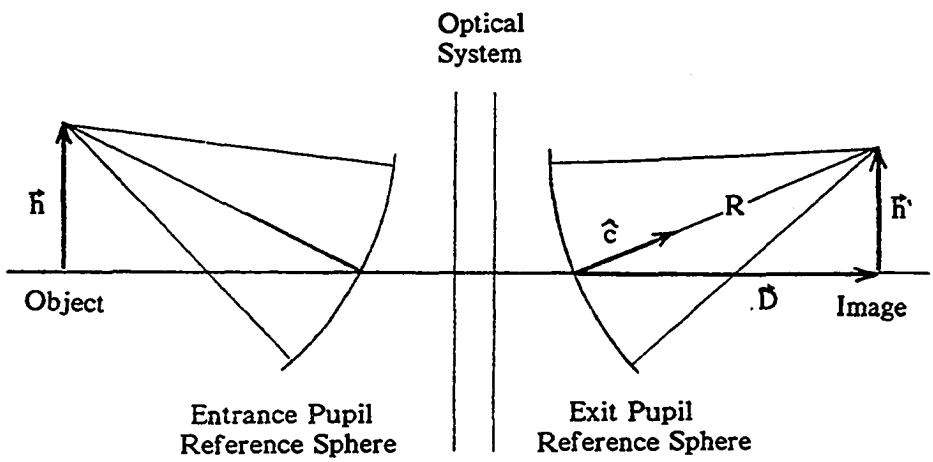

Fig. 5. The Ideal Reference Spheres of an Optical System

The Gaussian object and image points are $\vec{h}$ and $\vec{h}'$ respectively.

$$c_V = \frac{1}{\sqrt{(\vec{D}\cdot\vec{D}) + (\vec{h}'\cdot\vec{h}')}}, \text{ and}$$

$$\hat{C} = c_V (\vec{D} + \vec{h}') = < C_X, C_Y, C_Z > = < \vec{c}, C_Z > . \tag{3.28}$$

The quantity $\hat{C}$ is the unit vector normal to the surface vertex and $\vec{c}$ is the radial component of $\hat{C}$. The quantity c_V is the curvature of the sphere. If the image plane is at infinity then $c_V = 0$.

Note that for Gaussian imaging:

$$\vec{h}' = m \vec{h} , \tag{3.29}$$

where m is the system magnification.

In determining the wavefront aberration for a ray one must determine the intersection of the ray with the tilted exit pupil reference sphere. As with a conic surface, one must first trace the ray to the perpendicular point, then proceed to the surface intersection. But because the reference sphere may be tilted, the transfer parameter Q which gives the ray's intersection with the reference sphere is given by a slightly different version of Equation 3.17. In this case one replaces Equation 3.17 with

$$A_t = c_V N^2 ,$$
$$B_t = (\vec{c}\cdot\vec{s}) + C_Z S_Z , \text{ and}$$

$$D_t = c_V [(\vec{p}\cdot\vec{p}) + P_Z^2] - 2 [(\vec{c}\cdot\vec{p}) + C_Z P_Z] . \tag{3.30}$$

It is important to note that the new quantities $(\vec{c}\cdot\vec{s})$, $(\vec{c}\cdot\vec{p})$ and c_V are even

functions of the pupil variable as required. Unfortunately, they cannot be expressed in terms of the known values for $(\vec{p}\cdot\vec{p})$, $(\vec{p}\cdot\vec{s})$, $(\vec{s}\cdot\vec{s})$, P_z, and S_z at the exit pupil reference sphere. One must resort to transfering the new quantities from surface to surface starting from their known values at the start of the ray trace. This adds the following to the proximate transfer Equations 3.12 and 3.13:

$$\begin{aligned}(\vec{c}\cdot\vec{p})' &= (\vec{c}\cdot\vec{p}) + Q\,(\vec{c}\cdot\vec{s})\ , \text{ and}\\ (\vec{c}\cdot\vec{s})' &= (\vec{c}\cdot\vec{s})\ ,\end{aligned} \tag{3.31}$$

and the following to the proximate refraction Equations 3.22 and 3.23:

$$\begin{aligned}(\vec{c}\cdot\vec{p})' &= (\vec{c}\cdot\vec{p})\ , \text{ and}\\ (\vec{c}\cdot\vec{s})' &= (-c_V\,\Gamma)\,(\vec{c}\cdot\vec{p}) + (\vec{c}\cdot\vec{s})\ .\end{aligned} \tag{3.32}$$

Opening Equations

The transfer and refraction equations developed above are used to trace a ray sequentially from surface to surface. The process is continued until the ray intersection with the ideal reference sphere is reached to determine the wavefront aberration, or until the ray intersection with the ideal image plane is reached to determine the squared ray aberration. But it still remains to develop an appropriate method to start the ray trace, that is, a method for determining the quantities $(\vec{p}\cdot\vec{p})$, $(\vec{p}\cdot\vec{s})$, $(\vec{s}\cdot\vec{s})$, P_z, S_z, $(\vec{c}\cdot\vec{p})$, and $(\vec{c}\cdot\vec{s})$ at the first surface.

The equations for these opening quantities depend on the first order properties of the object space. There are three distinct situations: finite object and entrance pupil locations, infinite object location, and telecentric entrance pupil. The

development of the opening equations for these three situations is somewhat tedious but necessary. It is presented below.

Finite Object and Entrance Pupil Distances

The case of a finite object and entrance pupil locations is shown in Figure 6 and the ray trace is started at the entrance pupil reference sphere. Since these equations are to be evaluated utilizing power series methods, the association between the ray variables ($\vec{P}$ and $\vec{S}$) and the series variables (ν, $\vec{h}$, and $\vec{p}$) must be identified. For this case the association is trivial. The relationship between the ray variables $\vec{P}_0$, $\vec{P}_1$ and the series variables $\vec{h}$, $\vec{p}$ is

$$\vec{h} = \vec{p}_0 \text{ , and}$$
$$\vec{p} = \vec{p}_1 \text{ .} \qquad (3.33)$$

The chromatic variable ν is independent of the geometry of the object space and is always specified by equation 2.2.

The objective is to represent the quantities $(\vec{p}\cdot\vec{p})$, $(\vec{p}\cdot\vec{s})$, $(\vec{s}\cdot\vec{s})$, P_z, S_z, $(\vec{c}\cdot\vec{p})$, and $(\vec{c}\cdot\vec{s})$ at the first surface in terms of the power series quantities ν, $(\vec{h}\cdot\vec{h})$, $(\vec{h}\cdot\vec{p})$, and $(\vec{p}\cdot\vec{p})$.

One starts with expressions for P_{0z} and P_{1z} . Since the object is a plane surface, one has trivially

$$P_{0Z} = 0 \text{ .} \qquad (3.34)$$

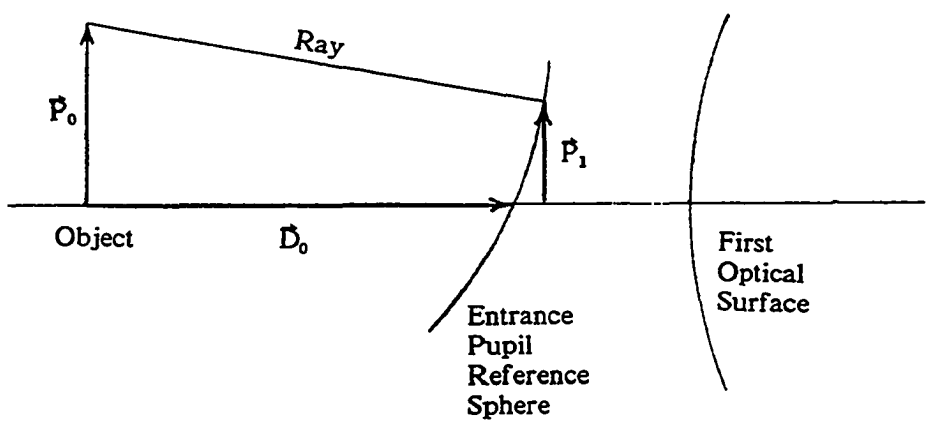

Fig. 6. Finite Object and Reference Pupils

A ray is uniquely specified by $\vec{P}_0$ and $\vec{P}_1$.

The expression for P_{1z} is determined by utilizing Figure 6 and Equation 3.27. This yields the following set of equations:

$$c_{v1} = \frac{1}{\sqrt{D_0^2 + (\vec{h}\cdot\vec{h})}},$$

$$(\vec{c}\cdot\vec{p})_1 = (\vec{h}\cdot\vec{p})\, c_{v1},$$

$$c_z = -D_0\, c_{v1},$$

$$x = c_{v1}\,(\vec{p}\cdot\vec{p}) - 2\,(\vec{c}\cdot\vec{p})_1, \text{ and}$$

$$P_{1z} = \frac{x}{c_z + \sqrt{c_z^2 - c_{v1}\, x}}. \tag{3.35}$$

The optical direction vector $\vec{S}_1$ can be written as

$$\vec{S}_1 = \frac{N_1\left[\vec{D}_0 + \vec{P}_1 - \vec{h}\right]}{\sqrt{(\vec{p}\cdot\vec{p})_1 - 2(\vec{h}\cdot\vec{p})_1 + (\vec{h}\cdot\vec{h}) + (D_0 + P_{1z})^2}}. \tag{3.36}$$

from which is derived the following set of proximate opening equations

$$(\vec{p}\cdot\vec{p})_1 = (\vec{p}\cdot\vec{p}),$$

$$(\vec{p}\cdot\vec{s})_1 = \frac{N_1\left[(\vec{p}\cdot\vec{p}) - (\vec{h}\cdot\vec{p})\right]}{\sqrt{(\vec{p}\cdot\vec{p}) - 2(\vec{h}\cdot\vec{p}) + (\vec{h}\cdot\vec{h}) + (D_0 + P_{1z})^2}},$$

$$(\vec{s}\cdot\vec{s})_1 = \frac{N_1^2\left[(\vec{p}\cdot\vec{p}) - 2(\vec{h}\cdot\vec{p}) + (\vec{h}\cdot\vec{h})\right]}{\sqrt{(\vec{p}\cdot\vec{p}) - 2(\vec{h}\cdot\vec{p}) + (\vec{h}\cdot\vec{h}) + (D_0 + P_{1Z})^2}}, \text{ and}$$

$$S_{1Z} = \frac{N_1 P_{1Z}}{\sqrt{(\vec{p}\cdot\vec{p}) - 2(\vec{h}\cdot\vec{p}) + (\vec{h}\cdot\vec{h}) + (D_0 + P_{1Z})^2}}. \qquad (3.37)$$

Note that N_1 is a power series in v only.

Finally, expressions for $(\vec{c}\cdot\vec{p})$ and $(\vec{c}\cdot\vec{s})$ are needed. At the exit pupil the vector expression for $\vec{c}$ is

$$\vec{c} = \frac{\vec{h}'}{\sqrt{(\vec{D}\cdot\vec{D}) + (\vec{h}'\cdot\vec{h}')}}, \qquad (3.38)$$

where $\vec{h}' = m\,\vec{h}$ and D is the distance from the exit pupil to the image plane. Thus

$$(\vec{c}\cdot\vec{p})_1 = \frac{m\,(\vec{c}\cdot\vec{h})}{\sqrt{(\vec{D}\cdot\vec{D}) + m^2\,(\vec{h}\cdot\vec{h})}}, \text{ and}$$

$$(\vec{c}\cdot\vec{s})_1 = \frac{m\,N_1\left[(\vec{h}\cdot\vec{p}) - (\vec{h}\cdot\vec{h})\right]}{\sqrt{(\vec{D}\cdot\vec{D}) + m^2\,(\vec{h}\cdot\vec{h})}\sqrt{(\vec{p}\cdot\vec{p}) - 2(\vec{h}\cdot\vec{p}) + (\vec{h}\cdot\vec{h}) + (D_0 + P_{1Z})^2}}. \qquad (3.39)$$

Infinite Object

Figure 7 illustrates the case of an infinite object location. The ray trace is started at the entrance pupil reference sphere (which is a tilted plane in this case) and the relationship of the ray variables $\vec{P}_1$ and $\vec{A}_1 = < \vec{a}_1, A_{1Z} >$ to the power series variables $\vec{h}$ and $\vec{p}$ is

$$\vec{h} = \vec{a}_1 ,$$
$$\vec{p} = \vec{p}_1 . \qquad (3.40)$$

The expression for P_{1Z} is

$$P_{1Z} = \frac{(\vec{h}\cdot\vec{p})}{A_{1Z}} . \qquad (3.41)$$

The vector $\vec{S}_1$ is trivially

$$\vec{S}_1 = N_1 \vec{A}_1 = N_1 < \vec{h}, A_{1Z} > , \qquad (3.42)$$

from which is derived the following set of proximate opening equations

$$(\vec{p}\cdot\vec{p})_1 = (\vec{p}\cdot\vec{p}) ,$$
$$(\vec{p}\cdot\vec{s})_1 = N_1 (\vec{h}\cdot\vec{p}) ,$$
$$(\vec{s}\cdot\vec{s})_1 = N_1^2 (\vec{h}\cdot\vec{h}) , \text{ and}$$
$$S_{1Z} = N_0 \sqrt{1 - (\vec{h}\cdot\vec{h})} . \qquad (3.43)$$

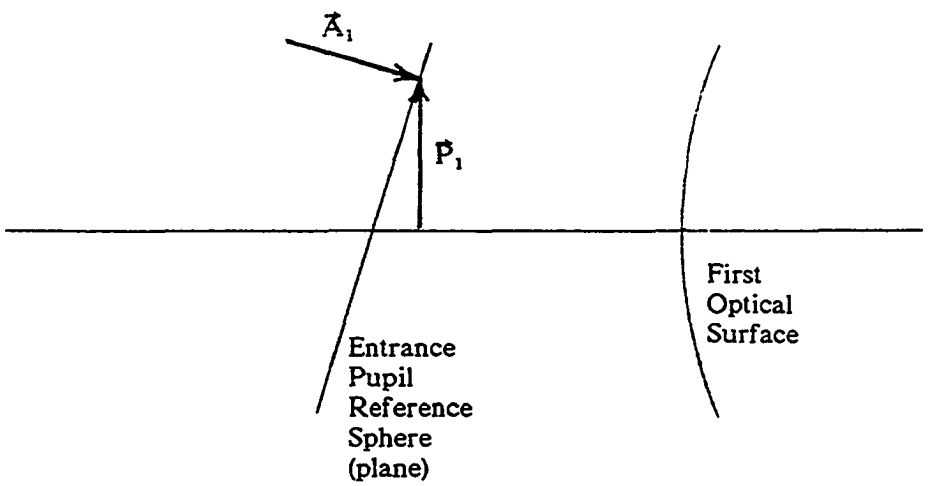

Fig. 7. Infinite Object Location

A ray is uniquely specified by its direction $\vec{A}_1$ and location $\vec{P}_1$ at the entrance pupil reference plane.

The expressions for $(\vec{c}\cdot\vec{p})$ and $(\vec{c}\cdot\vec{s})$ are derived using the following vector expression:

$$\vec{c} = \frac{\vec{h}'}{\sqrt{(\vec{D}\cdot\vec{D}) + (\vec{h}'\cdot\vec{h}')}}, \tag{3.44}$$

where in this case $\vec{h}' = m\,\vec{h} = m\,\vec{a}_1$. Thus

$$(\vec{c}\cdot\vec{p})_1 = \frac{m\,(\vec{h}\cdot\vec{p})}{\sqrt{(\vec{D}\cdot\vec{D}) + m^2(\vec{h}\cdot\vec{h})}}, \text{ and}$$

$$(\vec{c}\cdot\vec{s})_1 = \frac{m\,N_1(\vec{h}\cdot\vec{h})}{\sqrt{(\vec{D}\cdot\vec{D}) + m^2(\vec{h}\cdot\vec{h})}}. \tag{3.45}$$

Telecentric Entrance Pupil

Figure 8 illustrates the telecentric entrance pupil. In this case the ray trace is started at the object point. The relationship of the ray variables $\vec{P}_0$ and $\vec{A}_0 = < \vec{a}_0, A_{0z} >$ to the series variables $\vec{h}$ and $\vec{p}$ is

$$\vec{h} = \vec{p}_0, \text{ and}$$

$$\vec{p} = \vec{a}_0. \tag{3.46}$$

P_{0z} and $\vec{S}_0$ are trivially found to be

$$P_{0z} = 0, \text{ and} \tag{3.47}$$

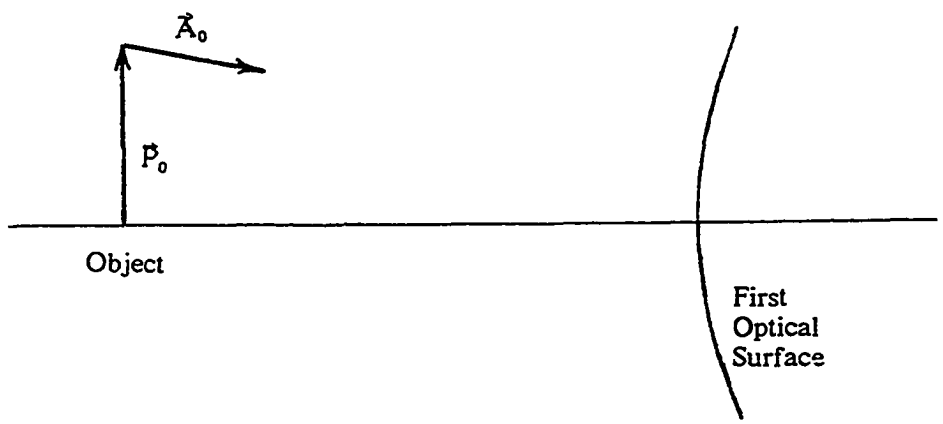

Fig. 8. Telecentric Entrance Pupil

A ray is uniquely specified by its direction $\vec{A}_0$ and location $\vec{P}_0$ in the object plane.

$$\vec{S}_0 = N_0 \vec{A}_0 = N_0 < \vec{p}, A_{0Z} > , \tag{3.48}$$

from which is derived the following set of proximate opening equations:

$$\begin{aligned}
(\vec{p}\cdot\vec{p})_0 &= (\vec{h}\cdot\vec{h}) , \\
(\vec{p}\cdot\vec{s})_0 &= N_0 (\vec{h}\cdot\vec{p}) , \\
(\vec{s}\cdot\vec{s})_0 &= N_0^2 (\vec{p}\cdot\vec{p}) , \text{ and} \\
S_{0Z} &= N_0 \sqrt{1 - (\vec{p}\cdot\vec{p})} .
\end{aligned} \tag{3.49}$$

The expressions for $(\vec{c}\cdot\vec{p})_0$ and $(\vec{c}\cdot\vec{s}_0$ are derived using

$$\vec{c} = \frac{\vec{h}'}{\sqrt{(\vec{D}\cdot\vec{D}) + (\vec{h}'\cdot\vec{h}')}} , \tag{3.50}$$

where $\vec{h}' = m \vec{h} = m \vec{p}_0$. Thus

$$\begin{aligned}
(\vec{c}\cdot\vec{p})_0 &= \frac{m (\vec{h}\cdot\vec{h})}{\sqrt{(\vec{D}\cdot\vec{D}) + m^2 (\vec{h}\cdot\vec{h})}} , \text{ and} \\
(\vec{c}\cdot\vec{s})_0 &= \frac{m N_0 (\vec{h}\cdot\vec{p})}{\sqrt{(\vec{D}\cdot\vec{D}) + m^2 (\vec{h}\cdot\vec{h})}} .
\end{aligned} \tag{3.51}$$

Closing Equations

Closing equations are needed to generate the information needed to compute the wavefront aberration and the squared ray aberrations.

Wavefront Aberration

The wavefront aberration at the exit pupil reference sphere is the difference in optical paths of rays from a single object point. The value for a particular point on the wavefront can be calculated by subtracting the optical path length of a real ray from the optical path of an ideal reference ray.

The ideal wavefront at the exit pupil is simply a sphere centered on the ideal image point and was referred to earlier in the chapter as a reference sphere. Since for ideal imaging the optical path length to the ideal wavefront is a constant, one can determine the ideal path length by tracing a single reference ray. For a real system this ray is the ray along the axis traced in the reference wavelength.

In tracing an arbitrary real ray to the reference sphere one must consider two cases: non-telecentric and telecentric systems. In the non-telecentric system the ray must be traced to a tilted reference sphere. In the telecentric system the wavefront aberration can be determined by tracing the ray to a specific point (to be discussed later) near the ideal image point.

The Non-telecentric Case. This situation is depicted in Figure 9. The ray must be traced to its intersection with the tilted reference sphere. The procedure is to trace the ray to the perpencidular point of the exit pupil reference sphere and then use Equation 3.30 instead of Equation 3.17 to find the surface intersection. The wavefront aberration is then calculated by subtracting the reference ray optical path length from the optical path length of the real ray.

It is important to note that for this transfer the reference sphere surface curvature c_v and the unit vertex normal $< \vec{c}, C_z >$ are not constants of the system (as they are for physically existing surfaces), but are functions of the ray object variable $\vec{h}'$.

The Telecentric Case. In the telecentric case the ideal reference sphere is located at infinity. By considering what happens to the reference sphere in the limit as it approaches an infinite distance from the optical system, one discovers that the wavefront aberration can be exactly calculated by tracing the real ray to its point of closest approach to the ideal image point. This is illustrated in Figure 10. Subtracting the resulting optical path length from the path length of the reference ray yields the wavefront aberration for the ray. As in the non-telecentric case, the reference ray is the axial ray traced to the image plane.

To calculate the point of closest approach of the ray to the ideal image point, one first traces the ray to the perpendicular point of the image plane. The transfer equation from this point to the desired point is determined with the help of Figure 10. One starts with

$$\vec{P} + Q\vec{S} = \vec{h}' + \vec{X} , \tag{3.52}$$

where $\vec{h}' = m\,\vec{h}$. Take the dot product of the above equation with $\vec{S}$ and use the fact that $\vec{P}\cdot\vec{S} = \vec{X}\cdot\vec{S} = 0$ and $\vec{S}\cdot\vec{S} = N^2$ to get

$$Q\,N^2 = m\,(\vec{h}\cdot\vec{s}) = OPL . \tag{3.53}$$

In this case one does not need the auxiliary quantities $(\vec{c}\cdot\vec{p})$ and $(\vec{c}\cdot\vec{s})$.

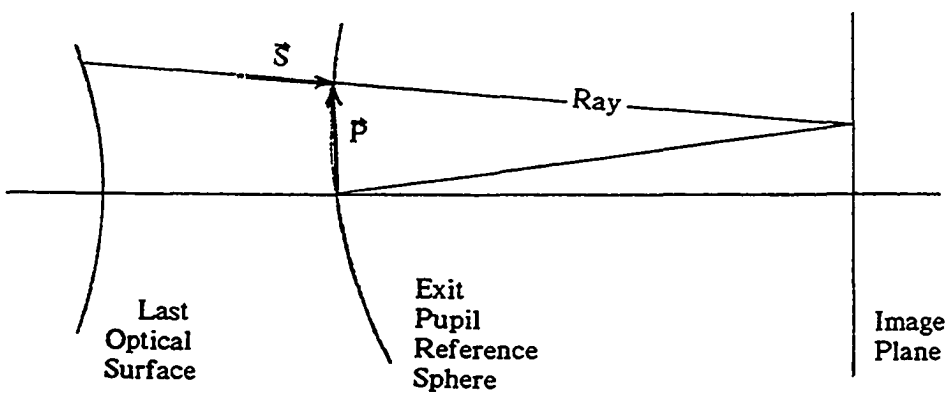

Fig. 9. Non-telecentric Exit Pupil

To compute the wavefront aberration for the ray, determine its intersection with the reference sphere and then subtract the OPL of the reference ray from the OPL of the ray itself.

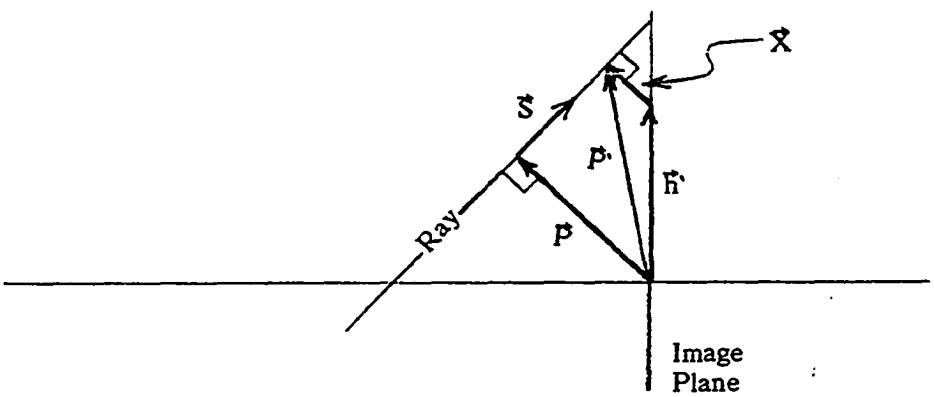

Fig. 10. Telecentric Exit Pupil

To compute the wavefront aberration for the ray, trace the ray to the point $\vec{P}'$ and then subtract the OPL of the reference ray from the OPL of the ray itself.

Instead one carries along the auxiliary quantity $(\vec{h}\cdot\vec{s})$.

Squared Ray Aberration

The squared ray aberration is the square of the distance between the ideal image point and the ray intersection point in the image plane. In tracing a real ray to the image plane one needs to consider two cases: finite and infinite image plane locations. The finite image plane location is the most common situation and will be treated first.

Finite Image Plane Location. This situation is easily treated with the aid of Figure 11. One has trivially from the figure:

$$\vec{\epsilon} = \vec{p} - \vec{h}' . \tag{3.54}$$

Recalling that $\vec{h}' = m\,\vec{h}$ and squaring the above equation by taking the dot product with itself yields

$$(\vec{\epsilon}\cdot\vec{\epsilon}) = (\vec{p}\cdot\vec{p}) - 2m\,(\vec{h}\cdot\vec{p}) + m^2\,(\vec{h}\cdot\vec{h}) . \tag{3.55}$$

The auxiliary quantities $(\vec{c}\cdot\vec{p})$ and $(\vec{c}\cdot\vec{s})$ are not needed to determine the squared ray aberration. Instead one uses the auxiliary quantity $(\vec{h}\cdot\vec{p})$.

Infinite Image Plane Location. This situation is depicted in Figure 12. In this case the image plane is at infinity and one defines the ray aberration as the angular deviation of the ray from the ideal direction. One starts by tracing the ray not to the image plane at infinity, but to the ideal reference sphere (in this case a tilted plane) in the exit pupil. The ray aberration in this case is then given by

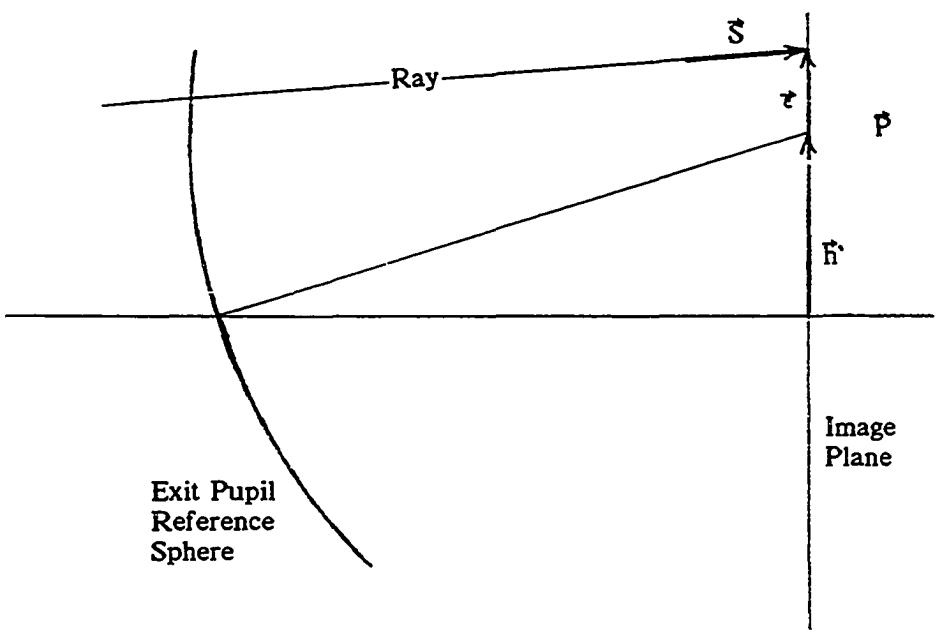

Fig. 11. Finite Image Plane Location

To determine the squared ray aberration, trace the ray to its intersection with the image plane and then compute $\vec{\varepsilon}\cdot\vec{\varepsilon} = (\vec{p}\cdot\vec{p}) - 2m(\vec{h}\cdot\vec{p}) + m^2(\vec{h}\cdot\vec{h})$.

$$\vec{\epsilon} = \vec{s}/N - \vec{\sigma} . \tag{3.56}$$

Here $\vec{\sigma} = \vec{h}' = m\,\vec{h}$ so that

$$(\vec{\epsilon}\cdot\vec{\epsilon}) = (\vec{s}\cdot\vec{s})/N^2 - 2m\,(\vec{h}\cdot\vec{s})/N + m^2\,(\vec{h}\cdot\vec{h}) . \tag{3.57}$$

The necessary auxiliary quantity is $(\vec{h}\cdot\vec{s})$.

One now has at his disposal all the proximate equations necessary to calculate either the wavefront aberration or squared ray aberration of a particular proximate ray in terms of quantities that are even functions of the pupil variable. The next chapter will contain the information needed to apply the proximate operations to the ray trace equations. It will also show how this leads to the computation of the polychromatic aberration coefficients.

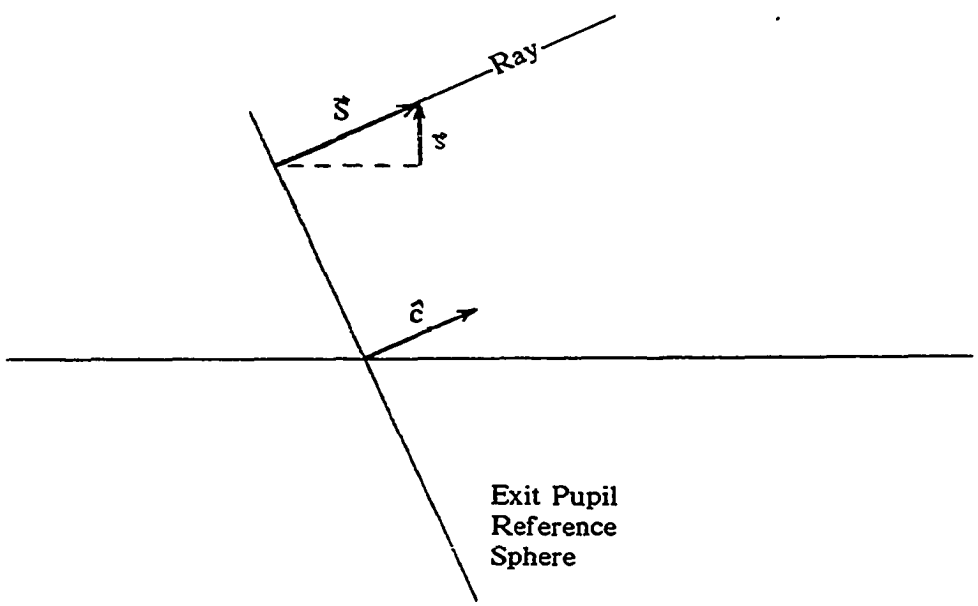

Fig. 12. Infinite Image Plane Location

To determine the squared ray aberration, trace the ray to its intersection with the ideal exit pupil reference sphere and then compute $\vec{e}\cdot\vec{e} = (\vec{s}\cdot\vec{s}) / N^2 - 2m(\vec{h}\cdot\vec{s}) + m^2(\vec{h}\cdot\vec{h})$.

CHAPTER 4

USING PROXIMATE ALGORITHMS TO COMPUTE ABERRATION COEFFICIENTS

The formulation of a unified set of ray tracing equations which allow the calculation of wavefront aberration or mean square ray aberration was presented in the previous chapter. It was developed in a manner consistant with the use of a single power series form for all the quantities involved in the ray trace. This allows a unified set of power series manipulation algorithms to be applied to all of the equations involved in the ray trace.

This chapter will present the relationship between the power series and proximate representations of a quantity. The relationship will then be used to develop numerical algorithms which implement the proximate mathematical operations necessary to carry out the ray trace.

Previous to this work, proximate mathematical operations have been implemented by algebraically expanding ray trace equations. This allows considerable probability for error in the derivation of the expansions and becomes extremely cumbersome when carried past the fifth order. The implementation of algorithms instead of algebraic expansions allows compact expressions for the computation of all ray trace quantities, as well as trivial extension to any desired degree without the need to rederive equations. It will be seen that this is a great advantage.

The Relationship Between the Power Series and Proximate Representation of Quantities

It is assumed that any ray trace quantity X is functionally represented by a power series of the form of Equation 2.5, which is repeated here for convenience:

$$X = \sum_{m=0}^{\infty} \sum_{n=0}^{m} \sum_{p=0}^{n} \sum_{q=0}^{p} \left[X_{mnpq}\, \nu^{(m-n)}\ (\vec{h}\cdot\vec{h})^{(n-p)}\ (\vec{h}\cdot\vec{p})^{(p-q)}\ (\vec{p}\cdot\vec{p})^{(q)} \right]. \qquad (4.1)$$

For the purposes of the present work, the salient property of this particular series form is that the terms are summed according to degree. This is extremely important because it allows an association between the proximate and series representations of quantities in the following way: assume that the power series for the quantity X is evaluated at ν^*, $\vec{h}^*$, and $\vec{p}^*$. The series summation thus becomes a sum of constant terms given by

$$X^* = \sum_{m=0}^{\infty} \sum_{n=0}^{m} \sum_{p=0}^{n} \sum_{q=0}^{p} \left(X_{mnpq}\, \nu^{*(m-n)}\ (\vec{h}^*\cdot\vec{h}^*)^{(n-p)}\ (\vec{h}^*\cdot\vec{p}^*)^{(p-q)}\ (\vec{p}^*\cdot\vec{p}^*)^{(q)} \right). \qquad (4.2)$$

The primary concept behind the proximate representation of a quantity is introduced by writing the partial sum over the three inner summations of the above series as

$$x^{(m)} = \sum_{n=0}^{m} \sum_{p=0}^{n} \sum_{q=0}^{p} \left[X_{mnpq}\, \nu^{*(m-n)}\ (\vec{h}^*\cdot\vec{h}^*)^{(n-p)}\ (\vec{h}^*\cdot\vec{p}^*)^{(p-q)}\ (\vec{p}^*\cdot\vec{p}^*)^{(q)} \right]. \qquad (4.3)$$

The complete summation is then simply

$$X^* = \sum_{m=0}^{\infty} (x^{(m)}) . \qquad (4.4)$$

This is exactly Wachendorf's and Hopkins' proximate representation of an even quantity. A small difference from the present notation is that they label terms $x^{(2m)}$ to indicate that the quantity is an even function of the pupil and field variables. Using this representation (and a representation for odd proximate quantities) they derive a set of proximate ray trace equations by explicitly expanding ray trace equations in terms of proximate quantities.

Here it will be shown how to evaluate the equations presented in the previous chapter using algorithms which operate on even proximate quantities. As mentioned earlier, this offers an advantage over the explicit expansion of equations.

Before giving the algorithms which implement the required mathematical operations, a vector notation for proximate quantities is presented as follows:

$$X = \langle x^{(0)}, x^{(1)}, x^{(2)}, x^{(3)}, \ldots \rangle . \qquad (4.5)$$

This allows simpler presentation of ideas and will prove convenient later in the chapter. The value of a proximate quantity is simply the sum of its vector components.

Proximate Algorithms

The ray trace equations developed in the previous chapter involve only the mathematical operations of addition, subtraction, multiplication, division, and square root. Therefore, these are the only operations that need be implemented as proximate mathematical operations.

The algorithms which implement the operations are given below and are presented for simplicity and ease of understanding. For this reason they may not be the most efficient algorithms possible.

Scalar Multiplication

The multiplication of a proximate quantity X by a scalar constant k is written

$$Y = k X = k \sum_{m=0}^{\infty} (x^{(m)}) = \sum_{m=0}^{\infty} (k x^{(m)}) . \tag{4.6}$$

One wishes to determine the components of the resultant proximate vector Y. The algorithm which accomplishes this is easily seen to be

for $m = 0, 1, 2, \ldots$
$\quad y^{(m)} = k x^{(m)} .$ (4.7)

Addition

The addition of one proximate quantity to another is written

$$Z = X + Y = \sum_{k=0}^{\infty} (x^{(k)}) + \sum_{n=0}^{\infty} (y^{(n)}) , \tag{4.8}$$

where X, Y, and Z are proximate quantities. The m'th component of Z is easily computed by adding the components of X and Y for which $m = k = n$. With this in

mind, the algorithm which adds two proximate quantities is easily seen to be

```
for  m = 0, 1, 2, ...
└──z(m)  =  x(m)  +  y(m) .                                    (4.9)
```

Note that the idea is to determine the algorithm which, given the vector components of the proximate operands, yields the vector components of the proximate result.

Multiplication

The proximate multiplication operation is more complex than the scalar multiplication operation. The equation is written

$$Z = X\,Y = \left[\sum_{m=0}^{\infty} (x^{(m)})\right]\left[\sum_{n=0}^{\infty} (y^{(n)})\right], \tag{4.10}$$

where the resultant proximate quantity is Z and the proximate operands are X and Y. The algorithm which implements proximate multiplication is

```
for  m = 0, 1, 2, ...
┌    z(m)  =  0
│    for  n = 0, 1, 2, ..., m
└──  └──z(m)  :=  z(m)  +  x(n) y(m-n) ,                       (4.11)
```

where the operator := denotes the replacement operation.

Division

The proximate division operation is distinct from the proximate multiplication operation and is slightly more complex. It is written

$$Z = X / Y = \frac{\sum_{m=0}^{\infty} (x^{(m)})}{\sum_{n=0}^{\infty} (y^{(n)})} . \qquad (4.12)$$

The algorithm which implements division can be determined by inverting the above equation and then determining the components of Z which satisfy

$$Y = X Z . \qquad (4.13)$$

In this equation the zero degree component can be computed directly. Then the first degree component can be computed because the zero degree component is known. The second degree component can then be computed, and so on. In this way one continues until the component of the desired degree is computed. The algorithm is

```
for  m = 0, 1, 2, ...
    z(m) = x(m) / y(0)
    for  n = 1, 2, ..., m
        z(m) := z(m) - y(n) z(m-n) / y(0) .
```

(4.14)

Note that the second loop index starts at 1 and that the division operation is

undefined for $y^{(0)} = 0$.

Square Root

The proximate square root algorithm is similar to the division algorithm and in fact is determined in much the same way. The equation is written

$$Z = \sqrt{X} = \sqrt{\sum_{m=0}^{\infty} (x^{(m)})} \; . \tag{4.15}$$

To determine the algorithm, one inverts the above equation and then determines the elements of the proximate quantity Z which satisfy

$$Z Z = \left[\sum_{n=0}^{\infty} (z^{(n)}) \right] \left[\sum_{k=0}^{\infty} (z^{(k)}) \right] = X \; . \tag{4.16}$$

The algorithm which implements the square root operation is

$$\begin{aligned} & z^{(0)} = \sqrt{x^{(0)}} \\ & \text{for } m = 1, 2, \ldots \\ & \quad z^{(m)} = .5\, x^{(m)} / z^{(0)} \\ & \quad \text{for } n = 2, 3, 4, \ldots, m \\ & \quad\quad z^{(m)} := z^{(m)} - .5\, z^{(n-1)}\, z^{(m-n+1)} / z^{(0)} \; . \end{aligned} \tag{4.17}$$

Note that the outer loop index starts at 1 and the inner loop index starts at 2. Note also that the square root operation is undefined for $x^{(0)} < 0$.

The Computation of Power Series Coefficients Using Proximate Data

One must recall that the purpose of using proximate algorithms to trace rays is to allow the computation of the power series coefficients for the wavefront aberration or the mean square ray aberration. Hopkins has shown how this can be accomplished and a similar method is presented here.

Consider the calculation of the wavefront aberration for a particular proximate ray. It is determined by using the opening equations presented in the previous chapter followed by the ray trace equations applied on a surface by surface basis until the intersection of the ray with the exit pupil reference sphere is achieved. Each ray trace equation is implemented through proximate algorithms.

The result of the ray trace is the proximate wavefront aberration vector W for that ray:

$$W = \langle W^{(0)}, W^{(1)}, W^{(2)}, W^{(3)}, \ldots \rangle . \tag{4.18}$$

Because W was computed for a particular ray (for example at $\nu = .1$, $\vec{p} = \langle .5, .5 \rangle$, $\vec{h} = \langle 0, .7 \rangle$), each $W^{(m)}$ is a linear equation (given by Equation 4.3) in the unknown aberration coefficients W_{mnpq} . Thus if one traces the same number of linearly independent rays as the number of unknown coefficients, each coefficient can be determined by simultaneously solving a set of linear equations. It is important to note at this point that the coefficients determined in this way are the true Taylor series coefficients for the aberration function, not an approximation to them.

An example of the procedure which computes the first degree wavefront aberration coefficients is now given to help clarify the above explanation. There are

four first degree terms in the power series for the wavefront aberration. That is, the first degree proximate vector component of the wavefront aberration contains four terms. These terms are given by Equation 4.3 (with m = 1):

$$W^{(1)} = W_{1000}\, \nu + W_{1100}\, (\vec{h}\cdot\vec{h}) + W_{1110}\, (\vec{h}\cdot\vec{p}) + W_{1111}\, (\vec{p}\cdot\vec{p})\,. \tag{4.19}$$

If one traces four independent proximate rays specified by ν_i, $\vec{h}_i$, and $\vec{p}_i$ where i = 1, 2, 3, 4, the result of the four ray traces is four independent values for the first degree proximate value $W^{(1)}$ of the wavefront aberration. These four values are denoted by $W_i^{(1)}$ for i = 1, 2, 3, 4. One can then form a vector of known first degree aberrations $\vec{d}^{(1)} = < W_1^{(1)},\ W_2^{(1)},\ W_3^{(1)},\ W_4^{(1)} >$ and a vector of unknown wavefront aberration coefficients $\vec{w}^{(1)} = <W_{1000},\ W_{1100},\ W_{1110},\ W_{1111}>$ as well as the matrix F_1 of values of the functional forms:

$$F_1 = \begin{bmatrix} \nu_1 & \left[\vec{h}_1\cdot\vec{h}_1\right] & \left[\vec{h}_1\cdot\vec{p}_1\right] & (\vec{p}_1\cdot\vec{p}_1) \\ \nu_2 & \left[\vec{h}_2\cdot\vec{h}_2\right] & \left[\vec{h}_2\cdot\vec{p}_2\right] & (\vec{p}_2\cdot\vec{p}_2) \\ \nu_3 & \left[\vec{h}_3\cdot\vec{h}_3\right] & \left[\vec{h}_3\cdot\vec{p}_3\right] & (\vec{p}_3\cdot\vec{p}_3) \\ \nu_4 & \left[\vec{h}_4\cdot\vec{h}_4\right] & \left[\vec{h}_4\cdot\vec{p}_4\right] & (\vec{p}_4\cdot\vec{p}_4) \end{bmatrix}. \tag{4.20}$$

Thus one sees that there are four equations in the four unknown aberration coefficients. They can be determined by solving the following matrix equation for $\vec{w}^{(1)}$:

$$\vec{d}^{(1)} = F_1 \vec{w}^{(1)} \tag{4.21}$$

The solution can be determined by any of the methods used to solve a set of linear simultaneous equations of the type given by the above equation.

The aberration coefficients of any other degree are determined in the same way as the example above. The only difference is that there are more coefficients at higher orders, and thus, a larger number of independent rays in the ray set. This illuminates a disadvantage of the proximate ray technique: the accuracy of the solution of Equation 4.21 depends on the conditioning of the matrix F. An ill-conditioned matrix can result in values for the aberration coefficients that are not numerically accurate due to computational round off errors.

Fortunately, the matrix is completely determined by the ray set, and one can choose a ray set that yields a well conditioned matrix. Unfortunately, the author has not been able to automate the selection of a ray set which yields a well conditioned matrix for all degrees. However, a ray set that yields well conditioned matrices for degrees up to the fifth has been determined by the author and is presented in Appendix A.

The computation of the series coefficients for the squared ray aberration is accomplished by exactly the same method as for the wavefront aberration. The only difference is that the rays from the ray set are traced to determine the proximate components of the squared ray aberration instead of the wavefront aberration. In fact, the matrices of the functional forms are identical since the same ray set can be used to compute either aberration.

CHAPTER 5

EXAMPLES

This chapter begins with a brief review of some of the developments to this point. It was shown in Chapter Two that two physically significant merit functions could be constructed from polychromatic aberration coefficients in such a way that coefficients of a particular and higher degrees could be isolated from coefficients of lower degrees (see Equation 2.84). This allowed the construction of a sequence of merit subfunctions which converges to the complete merit function (see Equation 2.86). Each subfunction is associated with a particular aberration degree.

In Chapters Three and Four it was shown how the aberration coefficients which make up the merit function are computed using an algorithmic approach to proximate ray tracing. This development allows one to actually compute the merit functions -- ensuring that the current research is not a purely intellectual excercise.

In this chapter, the behavior of the merit subfunctions with respect to appropriate parameters of some simple optical systems are investigated by examining their topography. The obvious vehicle for the investigation takes the form of contour maps of the subfunctions. The graphical presentation of subfunction topography allows convenient qualitative interpretation of behavior, and will be used to investigate three relatively simple optical systems.

In all of the contour maps to follow, each contour line represents a line of constant subfunction value and the contour interval follows logarithmic spacing.

Specifically, each contour line represents a value ten times larger or ten times smaller than its neighboring lines -- and each line is labeled with the power of ten (in units of wavelength squared) associated with that line.

Unfortunately, graphical presentation restricts the useful number of system variable parameters to two because of obvious difficulties in presenting data of more than three dimensions in two dimensional form. This in turn restricts the complexity of optical systems that can be conveniently examined in this way. But because of the preliminary nature of the investigation, it would be inappropriate to attempt an investigation of complex optical systems until the behavior of simple systems has been investigated.

In order of increasing complexity, the simple systems to be studied are the landscape lens, the telescopic doublet, and the symmetric dual dialyte.

Preservation of First Order Properties

Before the investigation is begun, one must note that it is desireable to preserve all first order properties of the system when varying any parameter. Since the parameter to be varied will frequently be the bending parameter of a thick lens, equations are presented which allow the bending of the lens while maintaining all of its first order properties.

The bending parameter X is defined

$$X = \frac{C_1 + C_2}{C_1 - C_2}, \tag{5.1}$$

where C_1 and C_2 are the curvatures of the first and second surfaces of the lens

respectively.

Normally a lens is specified by its index of refraction N, its curvatures C_1 and C_2, and its thickness T. However the same lens can be equally well specified by its power P, bending parameter X, index of refraction N, and reduced thickness $\tau = T/N$.

The appropriate relationships between the two sets of parameters are

$$P_1 = \frac{(1+X)P}{1+\sqrt{1-(1-X)(1+X)\tau P}}, \text{ and}$$

$$P_2 = \frac{(1-X)P}{1+\sqrt{1-(1-X)(1+X)\tau P}}, \tag{5.2}$$

where P_1 and P_2 are the surface powers of the lens. The surface curvatures can then be computed from

$$C_1 = \frac{P_1}{(N' - N)}, \text{ and}$$

$$C_2 = \frac{P_2}{(N - N')}, \tag{5.3}$$

where N' is the index of the medium surrounding the lens.

The above equations indicate how to calculate the curvatures of a thick lens given its power and bending parameter. Note that this form of bending preserves the thickness of the lens.

In order to preserve the first order properties of the system in which the lens is a part, one must preserve the spacing between principal planes of the system components. The location of the principal planes of a thick lens are given by

$$\delta_1 = \frac{\tau P_2}{P} \text{ , and}$$

$$\delta_2 = \frac{-\tau P_1}{P} \text{ .} \qquad (5.4)$$

where δ_1 is the reduced distance from the vertex of surface 1 to the front principal plane and δ_2 is the distance from the vertex of surface 2 to the rear principal plane.

The relationships presented above are used to preserve the first order properties of all three optical sytems to be presented in this chapter.

The Landscape Lens

The landscape lens of Figure 13 is a moderately simple system with two effective design variables. These are the stop position D measured from the principal plane, and the lens bending parameter X. Figure 14 is a map of the design variable space that indicates with cross hatching those system configurations that are not optically realizable because rays miss a surface, are totally internally reflected, etc. The horizontal axis is the stop position and the vertical axis is the bending parameter.

Figure 15 shows the contour map of the wavefront variance merit function accurate to the fifth degree. In this case first degree adjustments on the merit function have been made according to the concepts of Chapter Two. Thus, the merit function represents the variance of the wavefront aberration measured from a reference sphere centered on the peak of the difraction image and defocussed to the best average image plane. Figures 16 through 18 are the contour maps of the third through fifth degree wavefront variance subfunctions respectively.

It is immediately obvious from the higher degree maps of Figures 16 through 18 that the higher degree subfunctions are less linear than the lower degree

Focal length:	9.69147 mm
Thickness:	0.10000 mm
Bending Factor:	0.00000
Glass:	BK7
F/number:	19.383
Half Field of View:	25 degrees
Wavelength Range:	0.4 to 0.7 microns
Primary Wavelength:	0.58756 microns

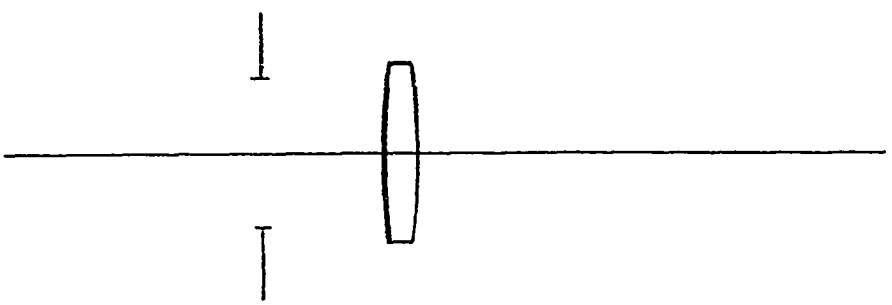

Fig. 13. Sketch of the Landscape Lens

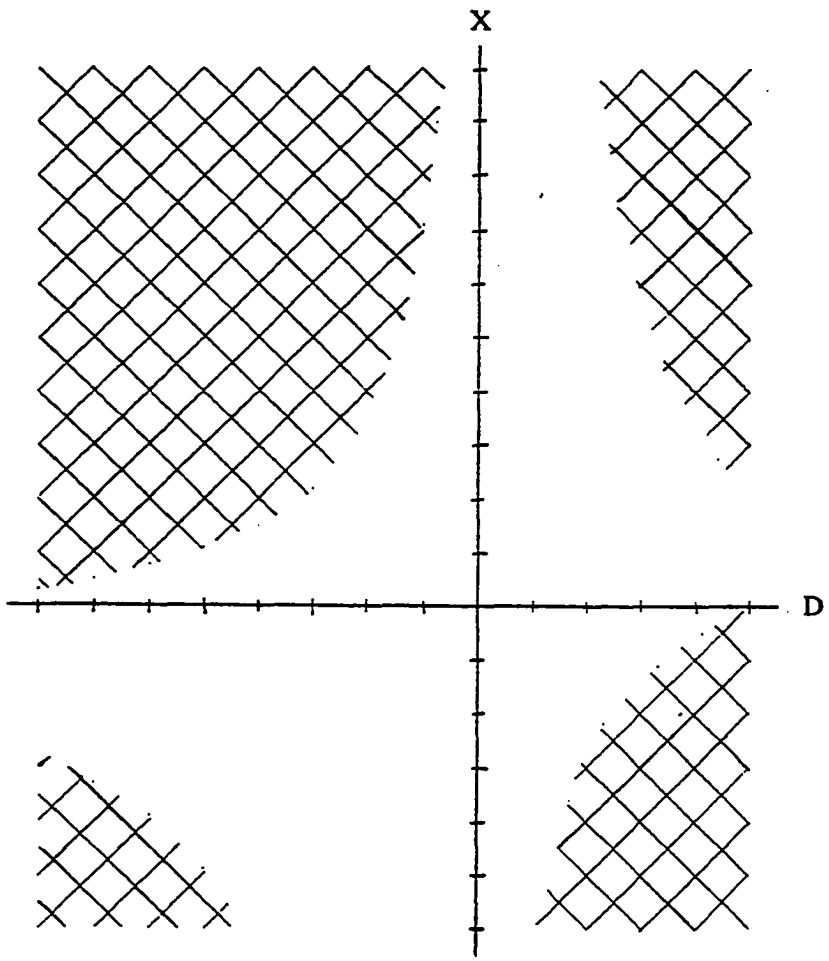

Fig. 14. Map of the Landscape Lens Parameter Space Showing the Optically Unrealizeable Configurations

The cross hatched area indicates the excluded configuration space. The ordinate represents the pupil location and the abscissa represents the bending parameter.

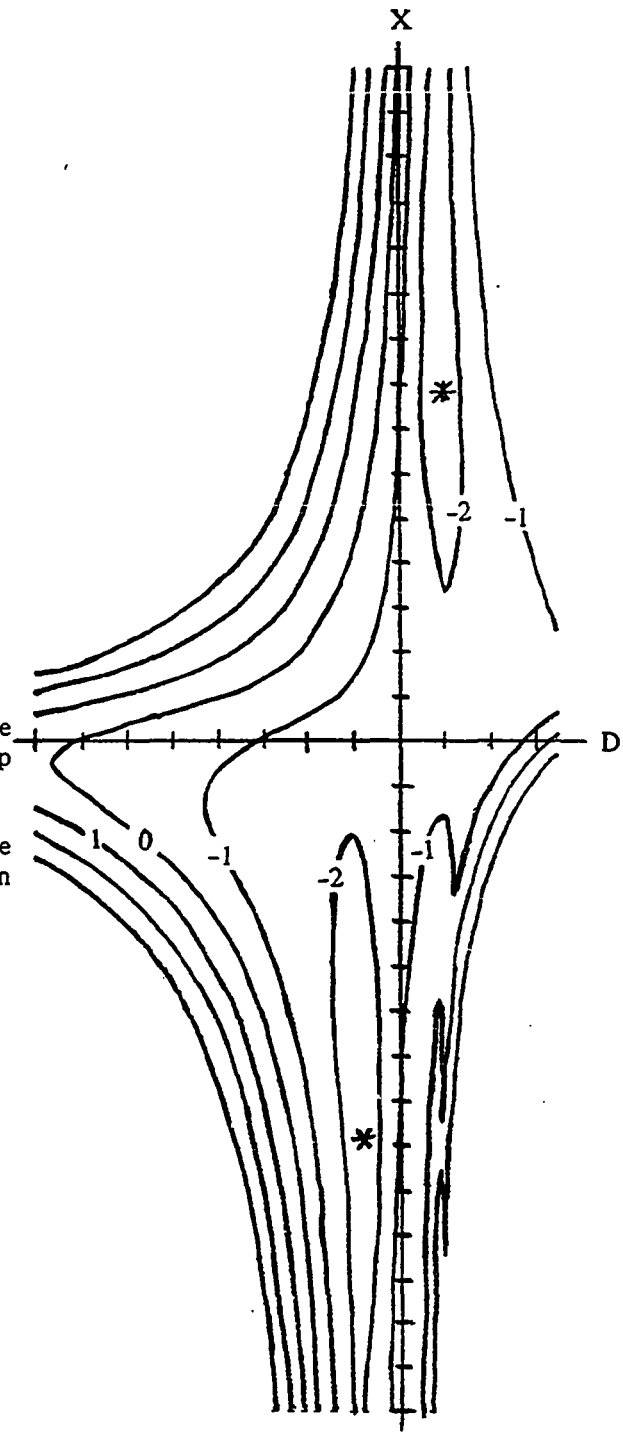

Fig. 15. Second Degree Merit Subfunction Map of the Landscape Lens

The asterisks denote the location of function minima.

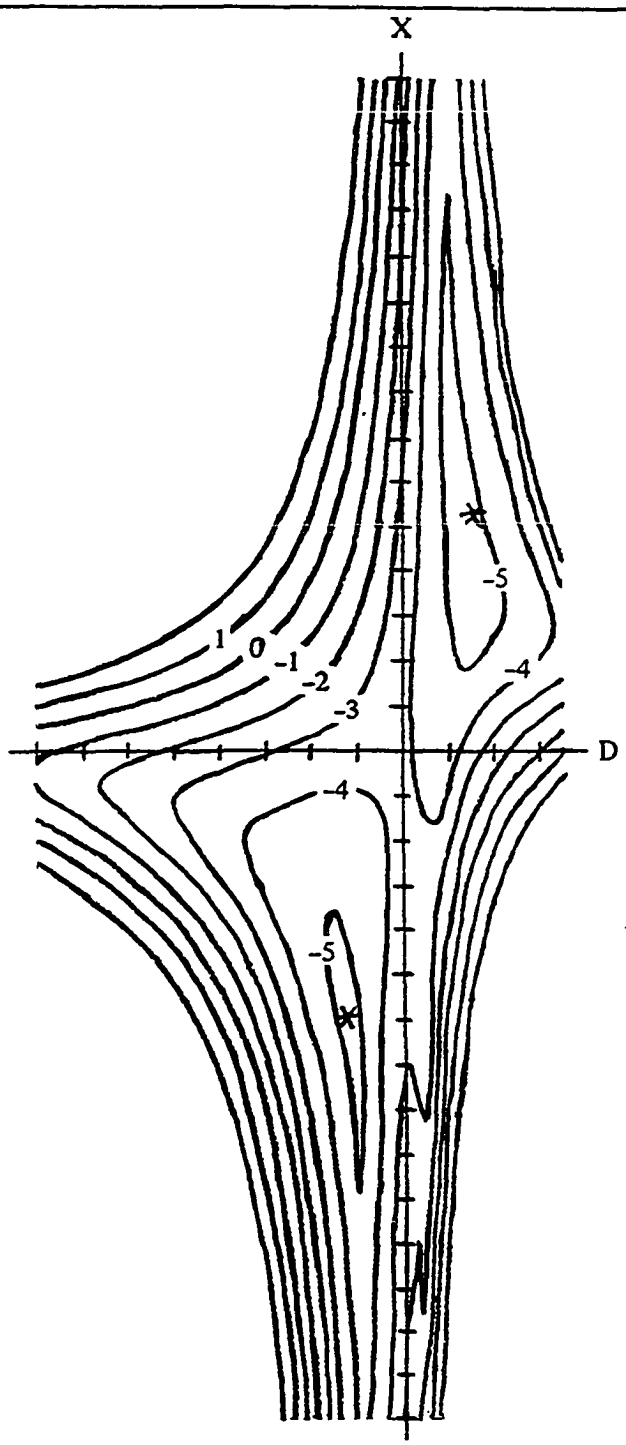

Fig. 16. Third Degree Merit Subfunction Map of the Landscape Lens

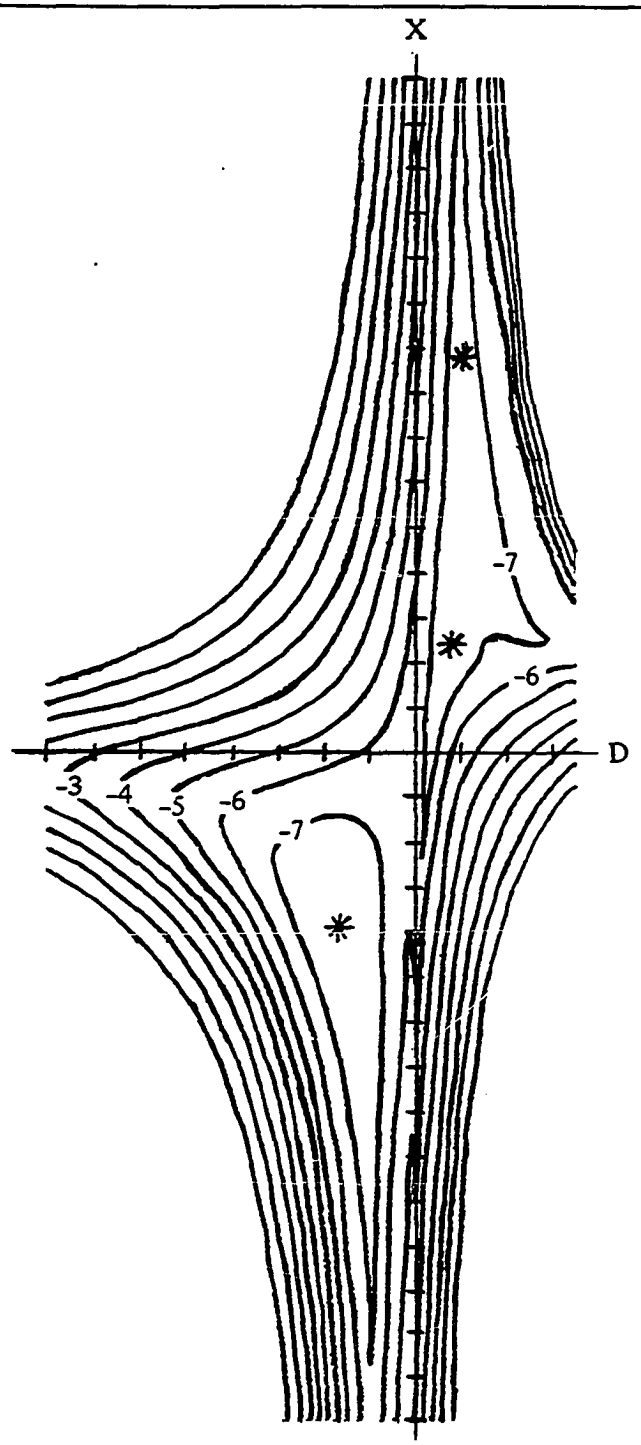

Fig. 17. Fourth Degree Merit Subfunction Map of the Landscape Lens

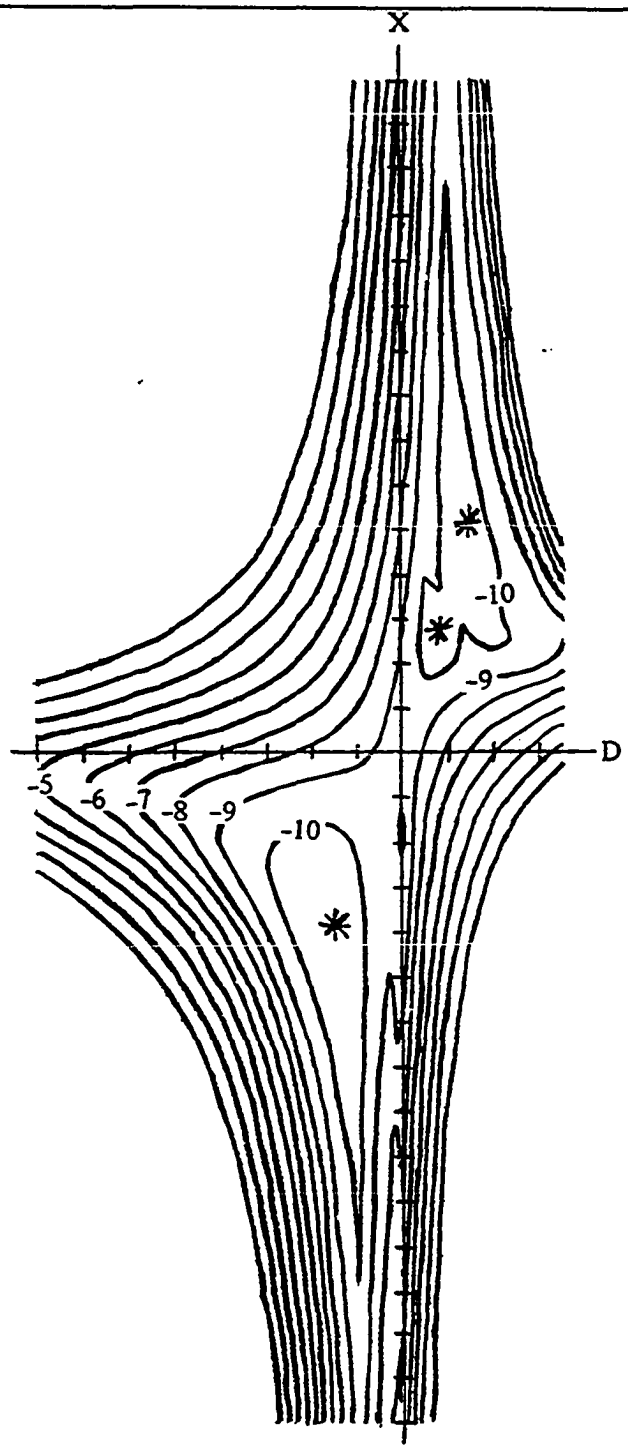

Fig. 18. Fifth Degree Merit Subfunction Map of the Landscape Lens

subfunctions. The maps also show that any particular merit subfunction minimum tends to be located in the same general region of parameter space regardless of degree. However, the lower minimum tends to migrate upward in the higher degree maps, while the behavior of the upper minimum appears to be more complex. It tends to have a small erratic migration with degree while developing a shallow secondary minimum in the same region.

However, the general features of the merit subfunctions are the same regardless of degree. This feature of the subfunctions will be seen to be a general one that applies to other systems as well. A possible explanation for this observed behavior will be presented in the next chapter.

By comparing the values of the subfunctions at any particular point in parameter space not near a boundary, one can see that the values differ by orders of magnitude per degree. This subfunction behavior will also be seen to occur in the examples to follow.

As a final observation concerning the functional behavior of the landscape lens, the lowest degree merit function displays two minima as expected. These are the familiar stop-in-front and the stop-in-back solutions shown in Figure 19.

The Gaussian Ideal

Figures 20 through 23 illustrate the behavior of the wavefront variance subfunctions (for the same landscape lens as above) in which the wavefront aberration is defined with respect to a reference sphere centered on the Gaussian image point. No first degree adjustments to the merit function have been made in this case.

One sees that the second degree subfunction of Figure 20 has a quite different appearance than that of Figure 15. This is the result of the difference in the

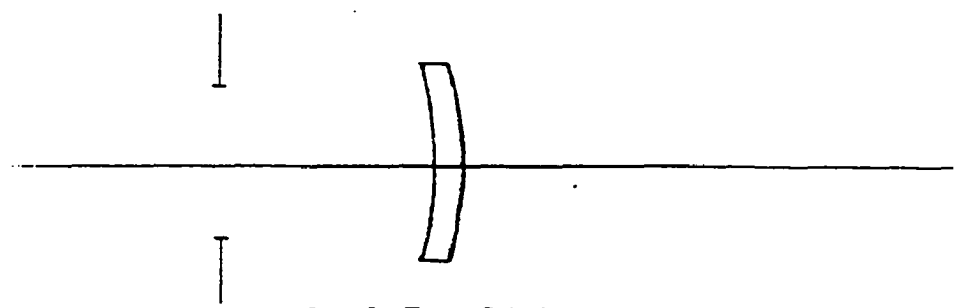

Stop-In-Front Solution

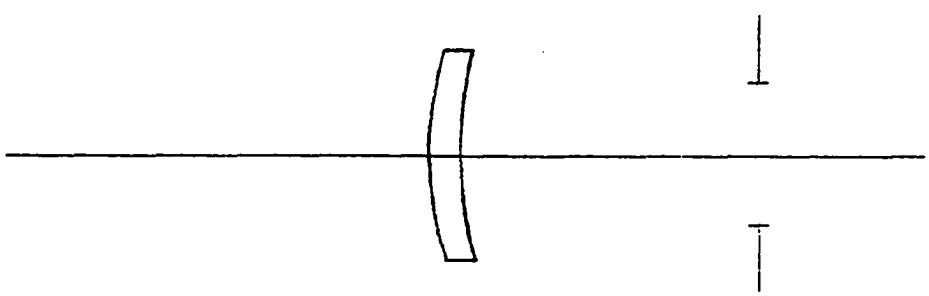

Stop-In-Back Solution

Fig. 19. The Two Solutions for the Landscape Lens

definition of the reference sphere (differences in the exact meaning of the merit function), not any change in the intrinsic behavior of the landscape lens. The aberration coefficients have not changed, but the transformation matrix is different from the transformation matrix for the first degree adjusted matrix in the example above. The figures clearly demonstrate that the exact definition of the merit function can have a profound impact on the perceived behavior of the optical system.

But what is the cause of the change in the merit function behavior? Or more precisely, why is there a minimum in Figure 15 at the point $D = -1$, $X = -9$ when there is no minimum at the corresponding point in Figure 20? The answer to this question lies in the table of aberration coefficients listed in Appendix B, where the values of the wavefront aberration coefficients that appear there were computed for the landscape lens. One immediately notes that the monochromatic distortion coefficient W_{210} (the coefficient of the second degree distortion term $h^3 \text{Cos}(\theta)\ \rho$) is about two orders of magnitude larger than any of the other second degree coefficients. In the first example. the distortion terms were balanced out by first degree adjustments to the merit function, which allowed both minima to appear in the lowest degree subfunction map. But in the second example, no such balancing was carried out, so the full effect of distortion appears in the lowest degree subfunction map and only one minimum appears.

But what about the higher degree subfunctions? If one compares the topography of the higher degree subfunctions illustrated in Figures 21 through 23 to the topography illustrated in Figures 16 through 18 respectively, one sees that the two sets of figures tend to resemble each other. Specifically, compare the fifth degree merit subfunctions of Figures 23 and 15. Note that the minima are located in approximately the same location in either figure. This might be an indication that the higher degree

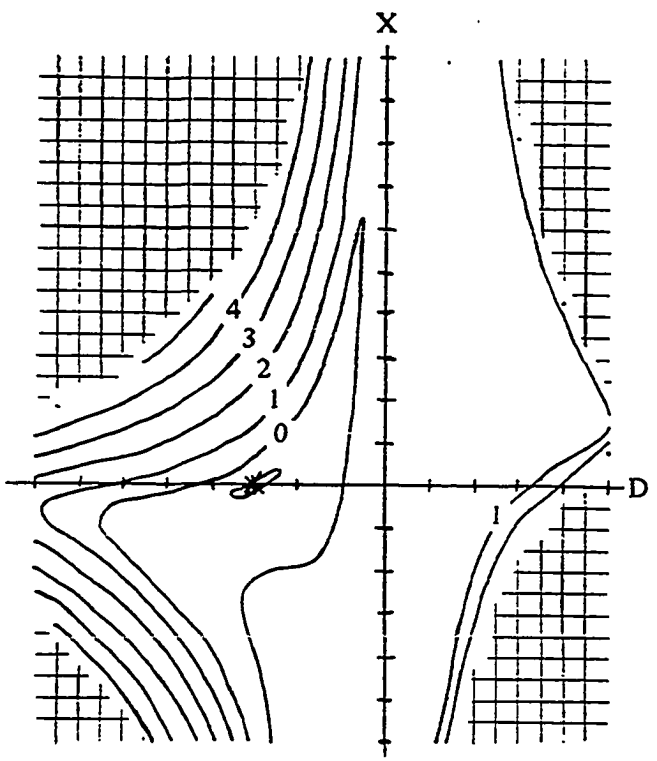

Fig. 20. Second Degree Gaussian Merit Subfunction Map of the Landscape Lens

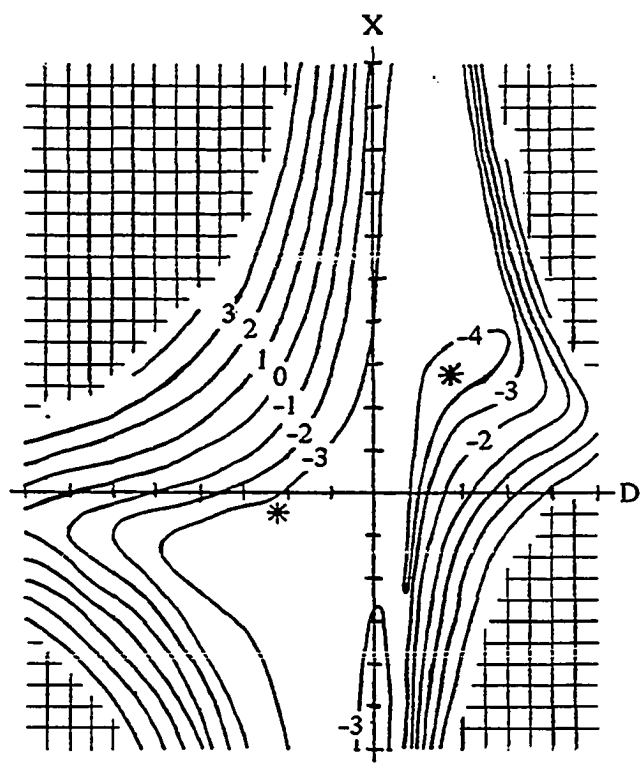

Fig. 21. Third Degree Gaussian Merit Subfunction Map of the Landscape Lens

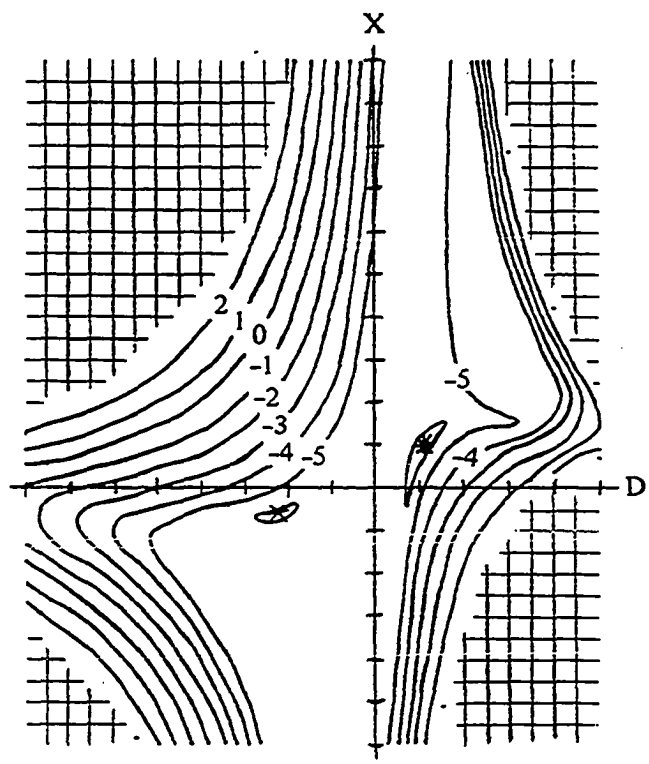

Fig. 22. Fourth Degree Gaussian Merit Subfunction Map of the Landscape Lens

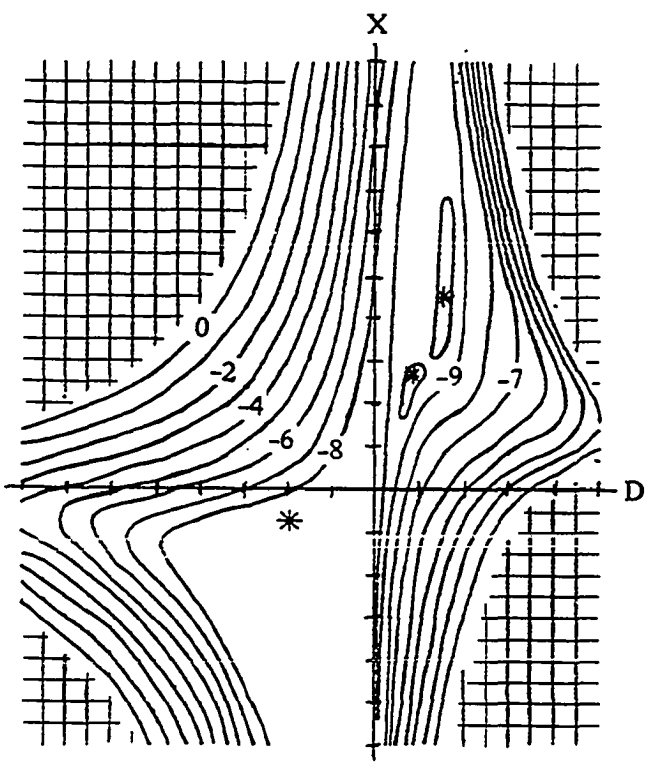

Fig. 23. Fifth Degree Gaussian Merit Subfunction Map of the Landscape Lens

subfunctions are more fundamental indicators of the imaging quality of an optical system than the low order subfunctions (since it appears that the low order subfunctions tend to be sensitive to the exact definition of the imaging ideal while high order subfunctions do not). Thus in the context of optical design, the use of higher order subfunctions as the design criterion might be useful as a guide to a solution region not readily apparent with the use of the usual low order subfunctions.

The Telescopic Doublet

The doublet of Figure 24 is a well known system with four effective design parameters. These are: the bending parameter of each lens, the relative power of the two lenses, and the air space between the lenses. In order to reduce the number of parameters, the air space will be held constant because its contribution to the behavior of the doublet is known to be relatively small. The relative power of the two lenses will also be fixed because its primary effect is to control the color correction. The remaining variables are the two lens bendings.

Figures 25 through 28 show the contour maps of the wavefront variance subfunctions where the x-axis represents the crown bending parameter X_a and the y-axis represents the flint bending parameter X_b. From an examination of the maps, the increasing nonlinearity of the subfunctions with increasing degree is obvious (as is the case with the landscape lens). Also, the global topography of the subfunctions tends to be the same regardless of degree. However there is a noticeable difference between the topographies of the second and third degree subfunctions.

With regard to minima, there are two definite minima present in the lowest degree map. In contrast to the landscape lens maps however, the lower minimum disappears in the higher degree maps, while the upper minimum remains relatively

	SYSTEM	CROWN	FLINT
Focal Length:	9.38915 mm	3.90208	-6.57276
Thickness:	0.16000 mm	0.10000	0.05000
Bending Factor:	---	0.00000	0.03529
Glass:	---	BK7	F8
F/number:	6.259		
Half Field of View:	4 degrees		
Wavelength Range:	0.4 to 0.7 microns		
Primary Wavelength:	0.58756 microns		

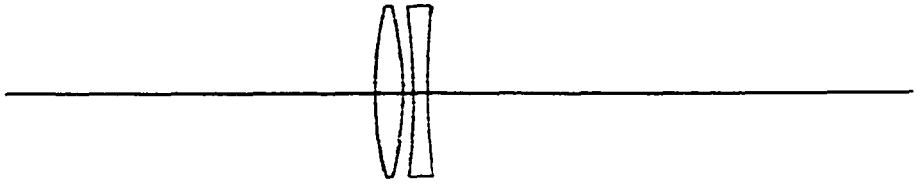

Fig. 24. Sketch of the Telescopic Doublet

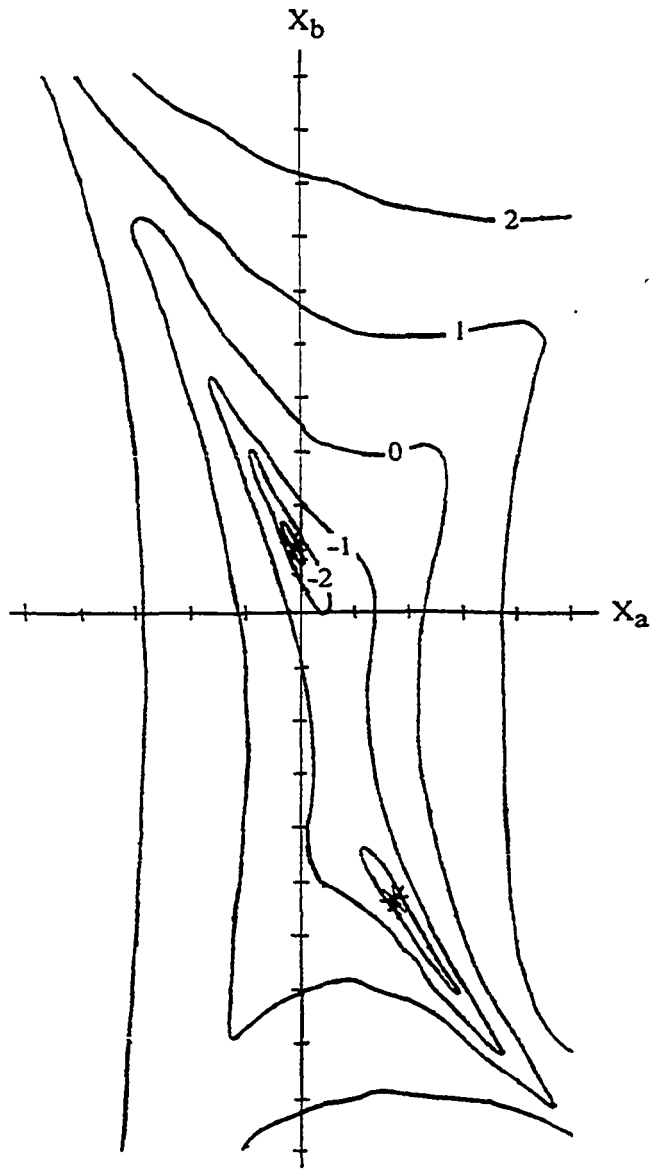

Fig. 25. Second Degree Merit Subfunction Map of the Telescopic Doublet

The ordinate is the crown bending parameter X_a , and the abscissa is the flint bending parameter X_b . The asterisks approximately locate the function minima.

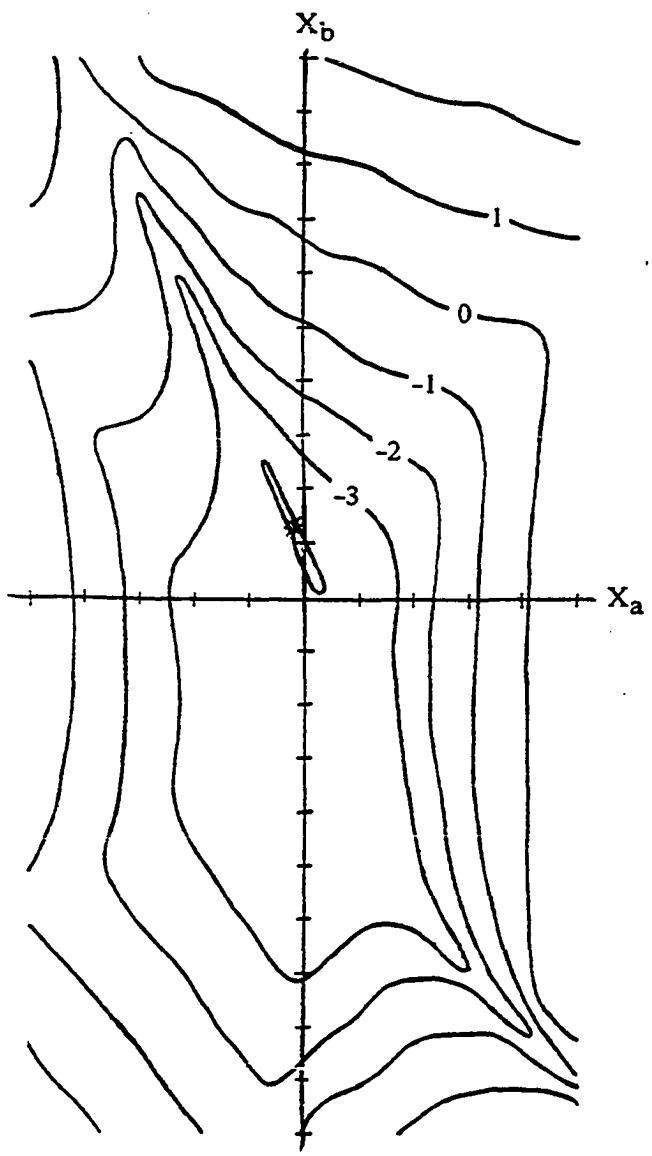

Fig. 26. Third Degree Merit Subfunction Map of the Telescopic Doublet

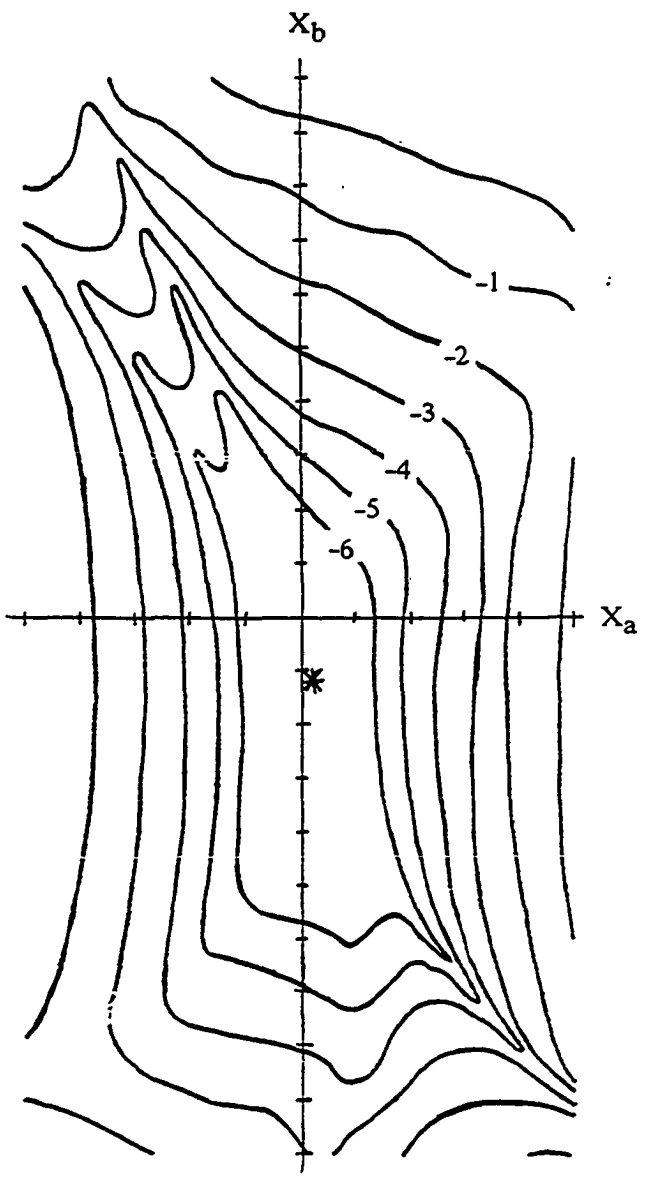

Fig. 27. Fourth Degree Merit Subfunction Map of the Telescopic Doublet

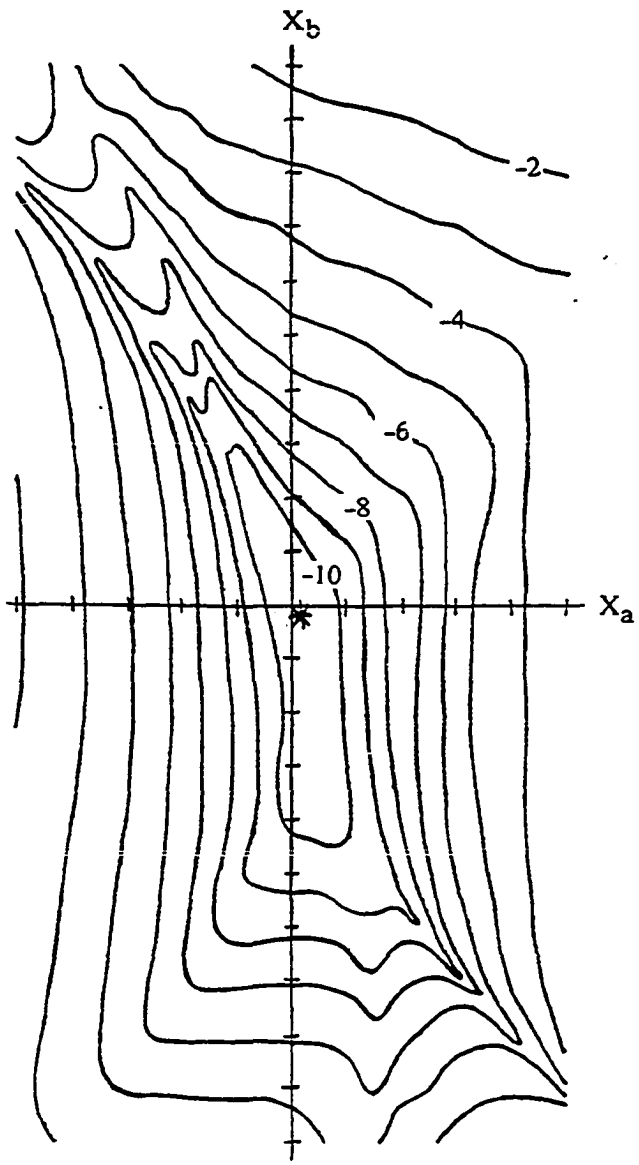

Fig. 28. Fifth Degree Merit Subfunction Map of the Telescopic Doublet

stable in location. To help illustrate the transition from two minima to a single minimum, Figure 29 shows a cross section of all the subfunctions along the parameterized line

$$X_a = 0.27\ X + 0.25 \text{ , and}$$
$$X_b = -0.96\ X + 0.07 \qquad (5.5)$$

in variable space. The line passes through the two minima of the lowest degree map.

One might wonder why subfunction maps using the Gaussian image ideal are not included for the doublet. The answer lies in the fact that thin doublets inherently do not possess distortion. Since the doublet considered here is both relatively thin and has a small field, distortion and field curvature do not play a significant role in its aberrational behavior. Since first degree adjustments of the merit function involve distortion balancing to locate the image centroid, and field curvature balancing to locate the best image plane, first degree adjustment of the merit function is unproductive.

Before investigating the last optical system, a quick re-examination of the lowest degree subfunction of Figure 25 is appropriate. A vast amount of prior experience with telescopic doublets has shown that there can exist two minima in the merit function: the Fraunhofer (upper minimum in the figure) and Gauss (lower minimum) solutions. Both are evident in the map, and Figure 30 illustrates the physical form of the two solutions.

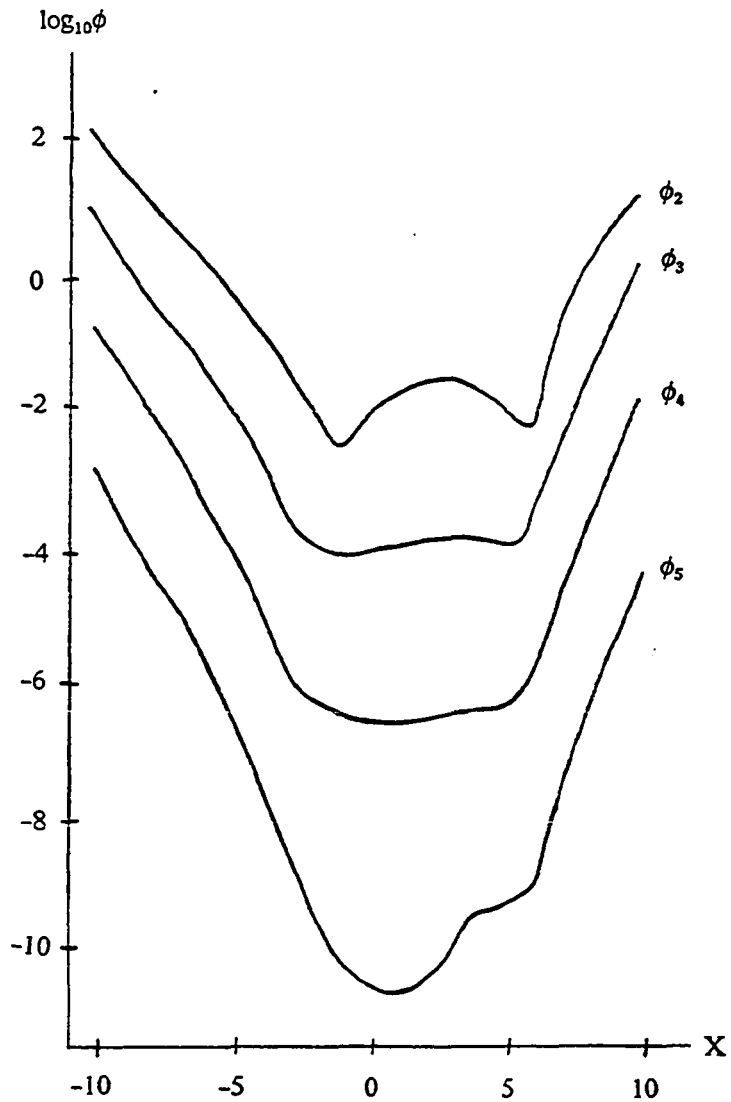

Fig. 29. Cross Sectional View of the Merit Subfunctions of the Telescopic Doublet

The cross section is taken through the two minima of the second degree subfunction (see Equation 5.5).

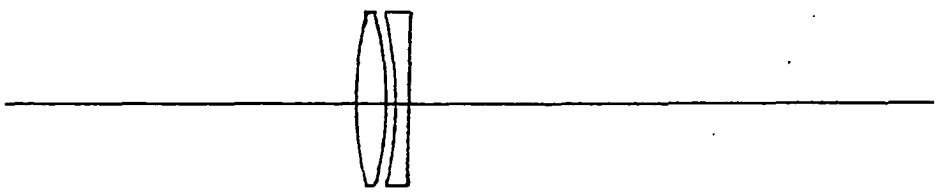

Fraunhofer Solution

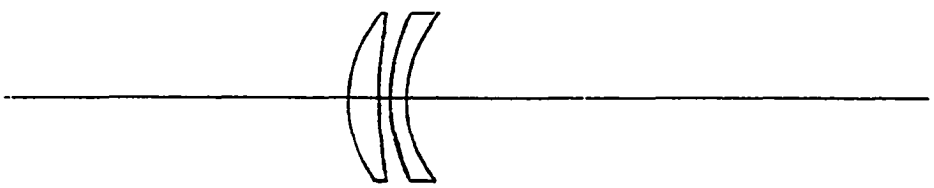

Gauss Solution

Fig. 30. The Two Solutions for the Telescopic Doublet

The Symmetric Dual Dialyte

The symmetric dual dialyte of Figure 31 is composed of two dialyte objectives placed symmetrically about a central stop. For the purposes of this dissertation, complete symmetry of the optical system about the stop is preserved in order to restrict the system to two effective parameters. They are the crown and flint bendings, X_a and X_b respectively. As is the case with the two previous examples, surface spacings are adjusted to keep all first degree system properties constant for all bendings. In addition, first degree adjustments were made to the merit function. However, since the system is symmetric, one would expect it to have little distortion. This implies that balancing distortion should have little effect on the topographies of the subfunction maps to follow. Figure 32 illustrates the excluded regions in parameter space.

The dual dialyte is not as simple as the telescopic doublet, so not as much is known about its behavior. From the lowest degree subfunction map of Figure 33, two solutions are seen. And as in the two previous optical systems, the global topography of the subfunction maps does not change dramatically as the higher degree maps of Figures 34 through 36 illustrate. With regard to minima, the upper minimum is almost perfectly stationary, while the lower minimum migrates slowly toward the upper minimum. Note that the subfunction values of the migrating minimum are smaller than the values of the upper minimum. This is the opposite of the telescopic doublet case where the minimum with larger values disappeared.

The final observation concerns the upward sloping walls of the subfunction maps near the boundaries of the physically possible system configurations. The upward slope seems to follow a roughly logarithmic rise as evidenced by the roughly equal

	SYSTEM	CROWN	FLINT
Focal Length:	9.99966 mm	3.31419	-3.69290
Thickness:	1.89290 mm	0.36642	0.10992
		0.25026	
Bending Factor:	---	0.45744	0.13082
Glass:	---	SK1	BaF4
F/number:	6.000		
Half Field of View:	22 degrees		
Wavelength Range:	0.4 to 0.7 microns		
Primary Wavelength:	0.58756 microns		

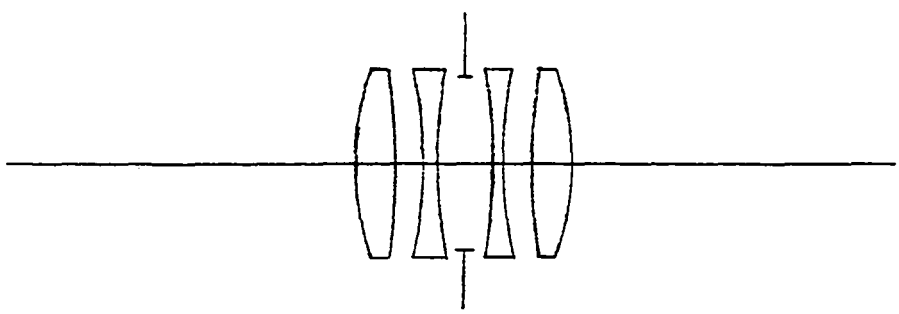

Fig. 31. Sketch of the Symmetric Dual Dialyte

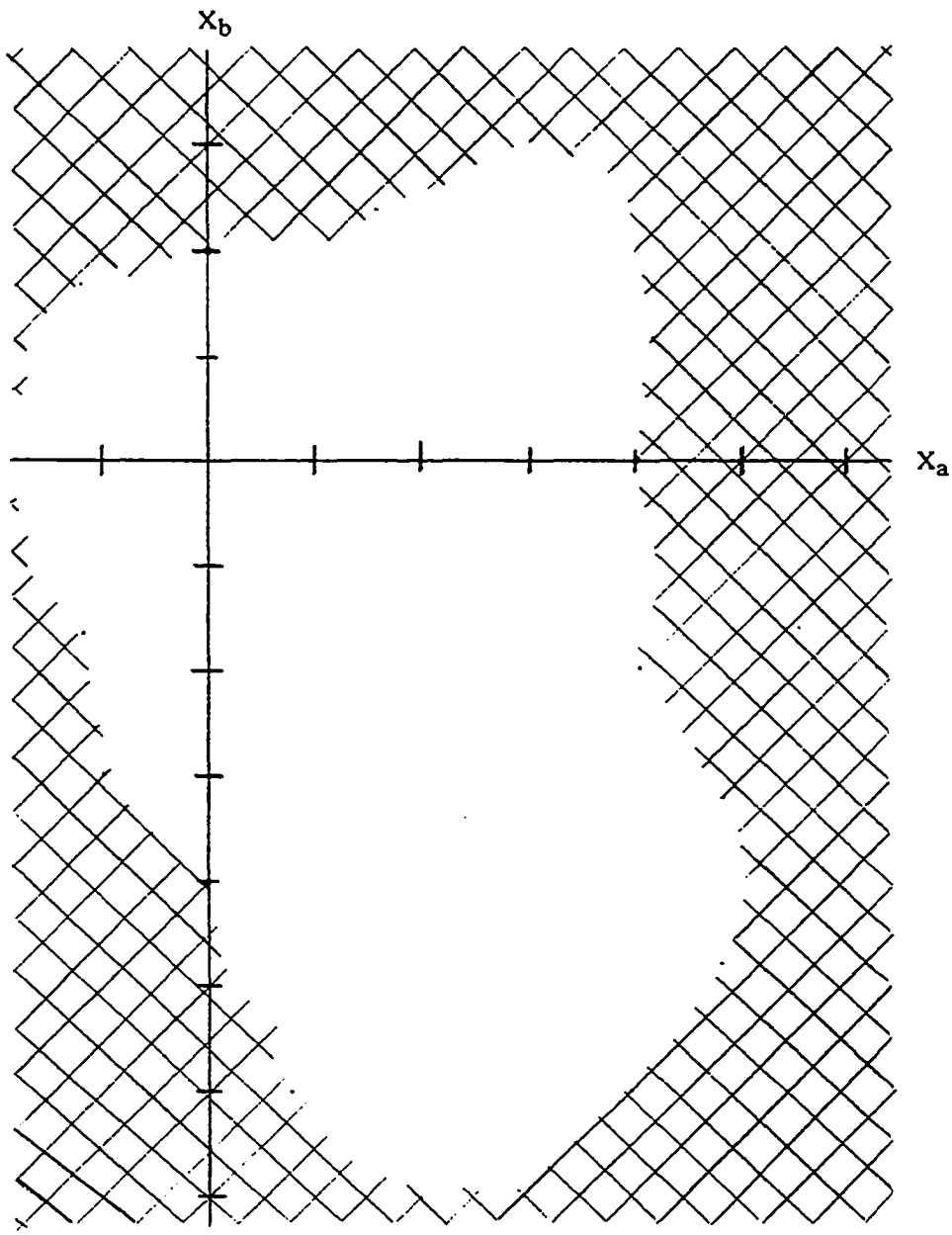

Fig. 32. Map of the Symmetric Dual Dialyte s Parameter Space Showing the Optically Unrealizeable Configurations.

The cross hatched region denotes the excluded regions. The ordinate represents the crown bending parameter, the abscissa represents the flint bending parameter.

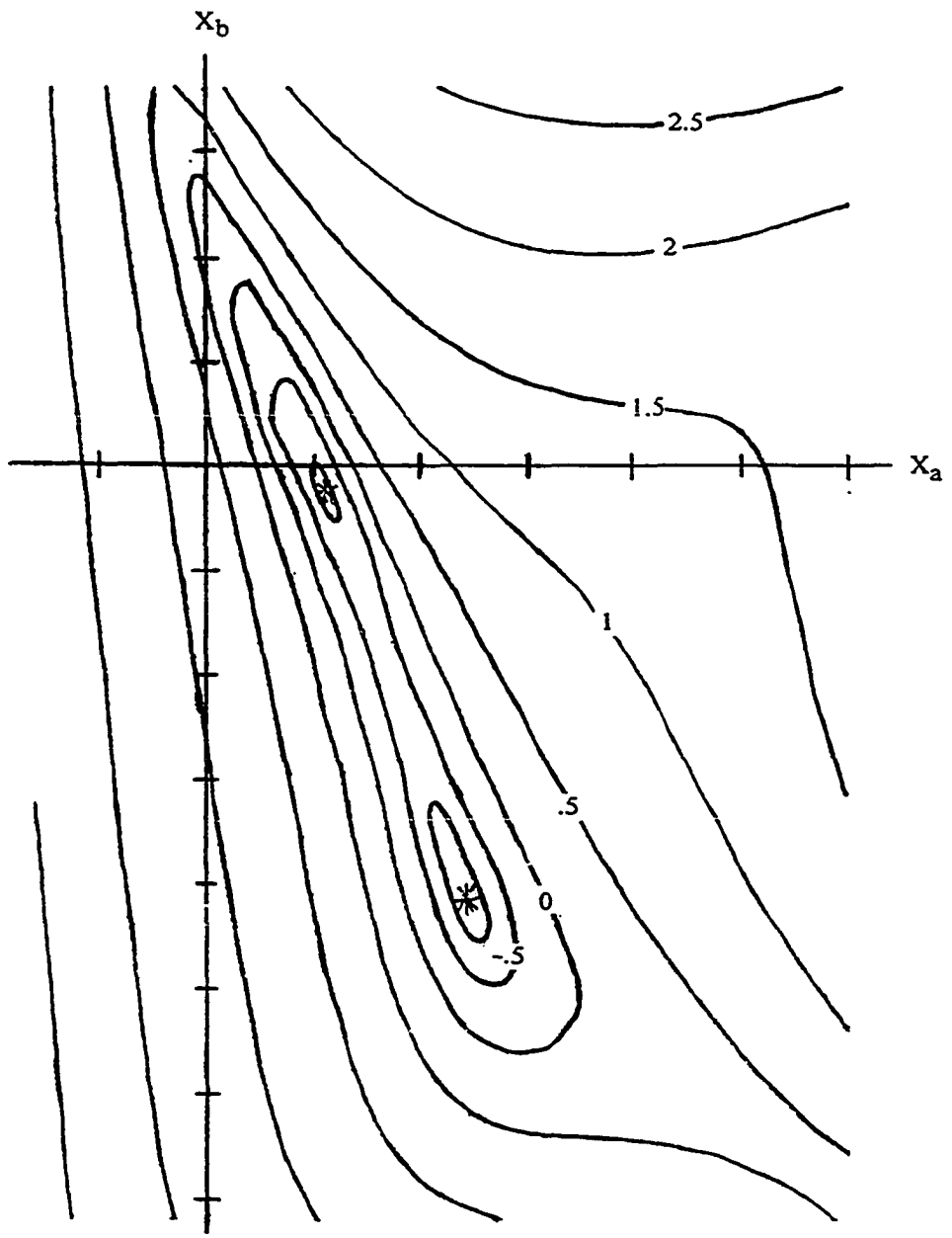

Fig. 33. Second Degree Merit Subfunction Map of the Symmetric Dual Dialyte

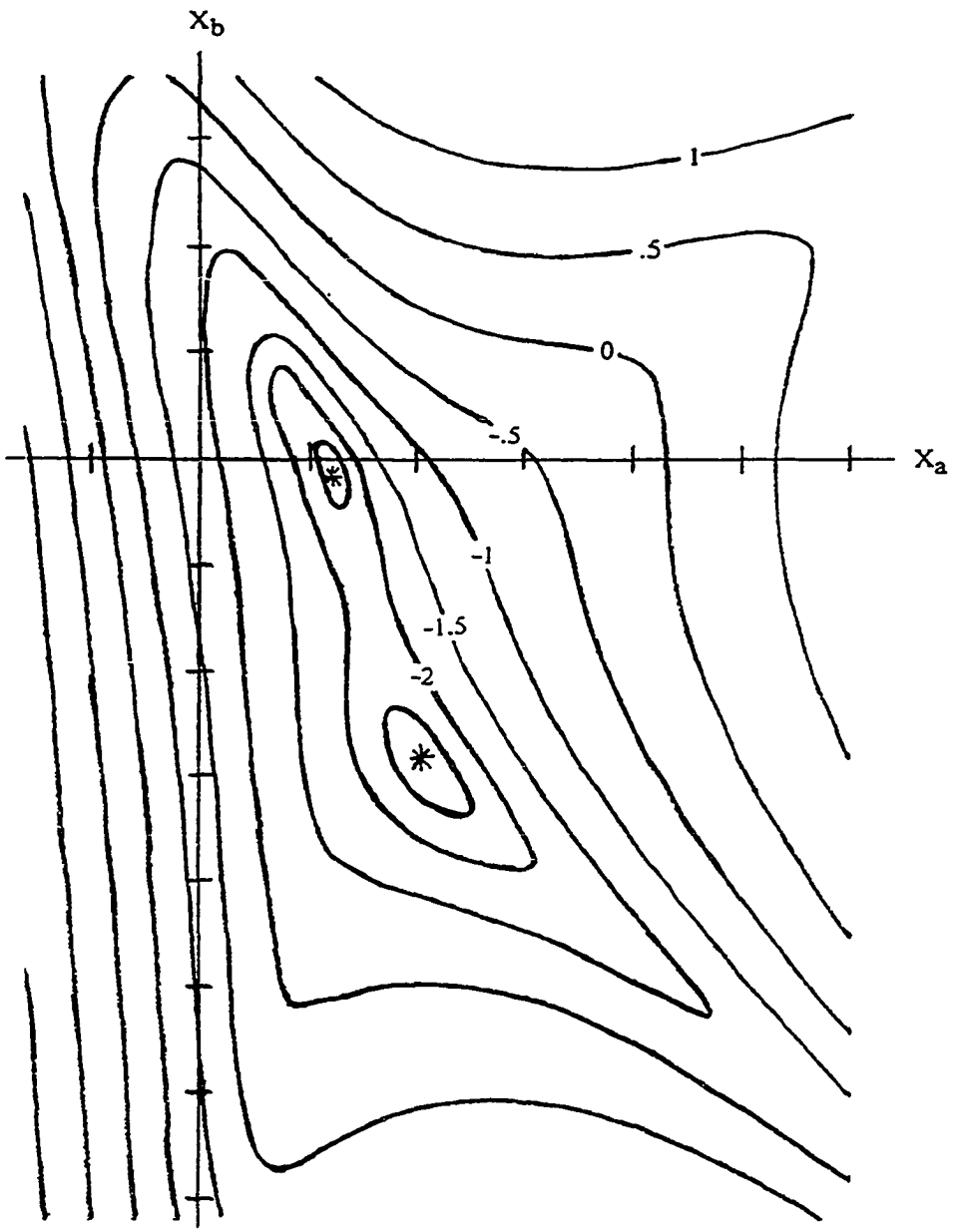

Fig. 34. Third Degree Merit Subfunction Map of the Symmetric Dual Dialyte

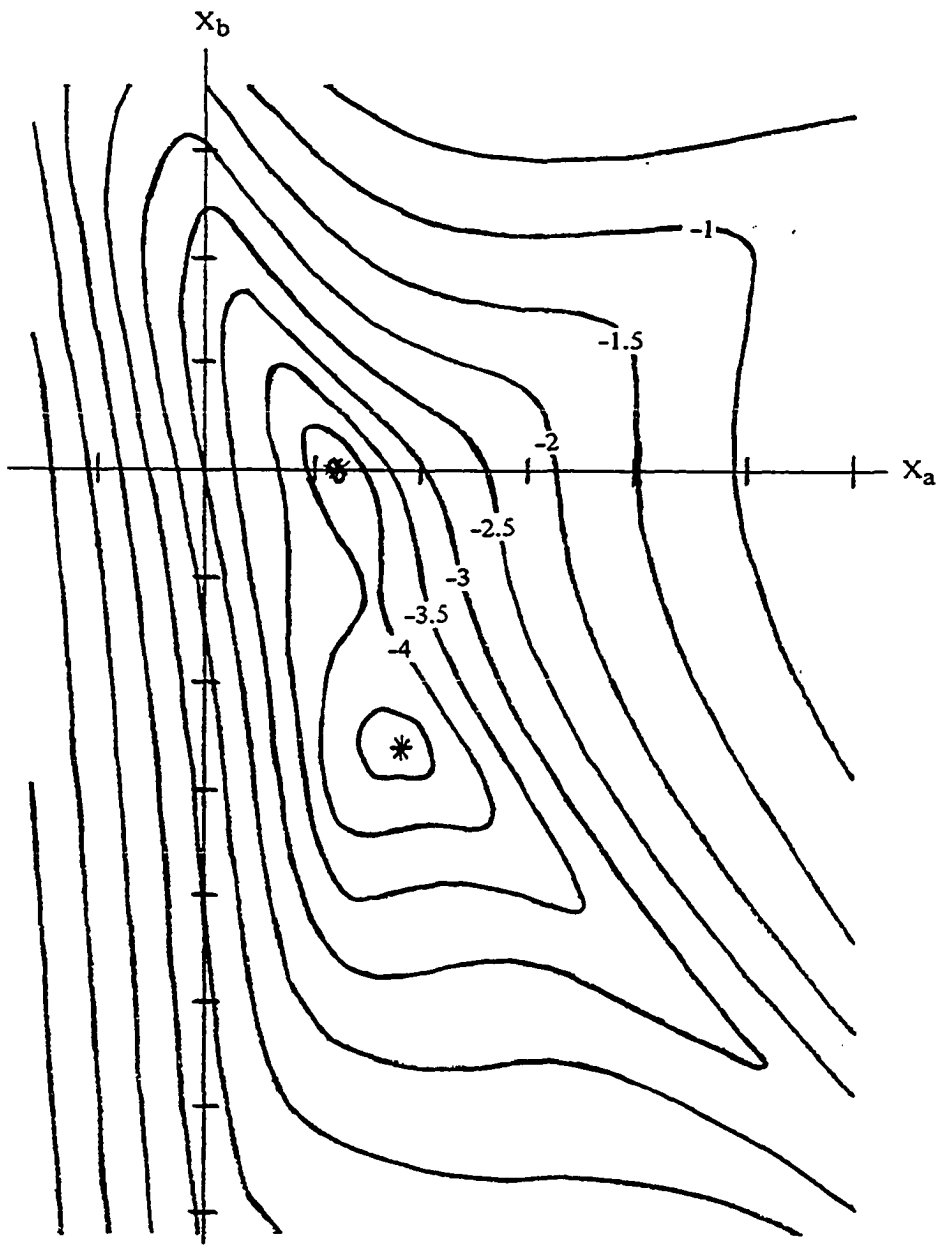

Fig. 35. Fourth Degree Merit Subfunction Map of the Symmetric Dual Dialyte

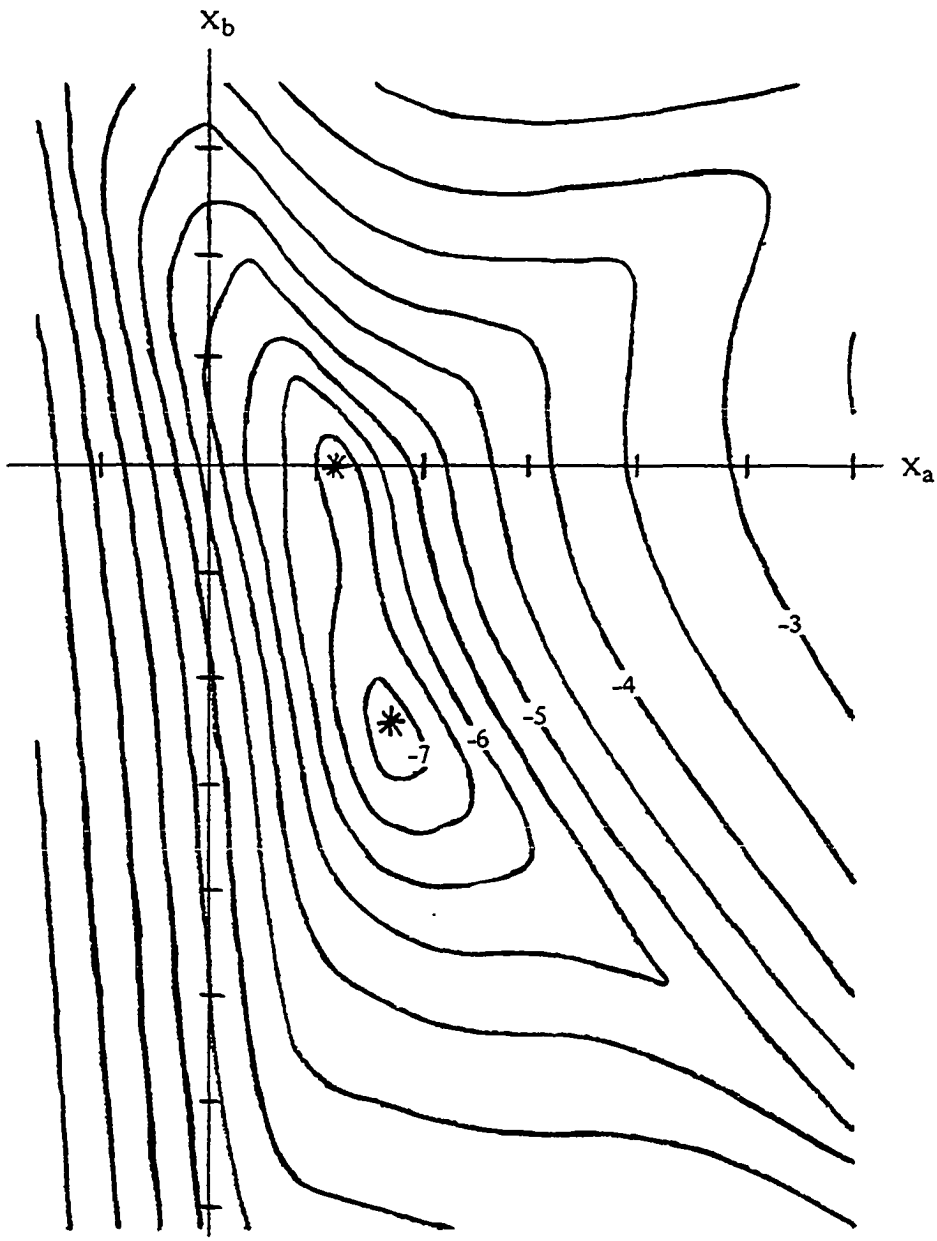

Fig. 36. Fifth Degree Merit Subfunction Map of the Symmetric Dual Dialyte

spacing of the contour lines. This seems to be a general feature of all three systems investigated, and may be more an indication of divergent aberration series truncation error than a true indication of topographical behavior.

The physical forms of the two solutions of the lowest degree map are pictured in Figure 37. The upper solution has gentle surface slopes while the lower solution has steeper slopes and is related to the Double Gauss lens. It seems from a consideration of the physical forms of the two solutions that they are influenced by the two solutions of the doublet that makes up each half of the system.

As an interesting aside, the starting point for the symmetric dual dialyte design was taken from Kingslake's book[14] at the point in the design process in which he departs from symmetry. The point to be made is that his final solution corresponds to the upper solution of Figure 33 while the better solution (according to the mean wavefront variance criterion) is the Double Gauss solution.

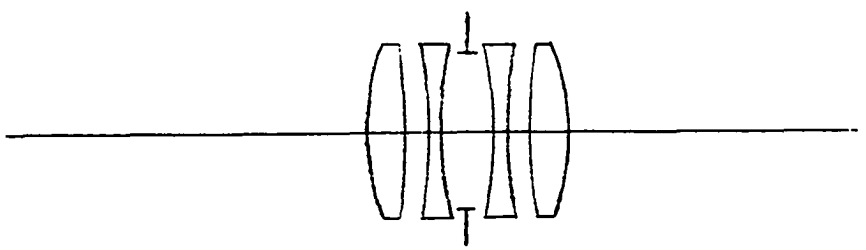

Upper Solution

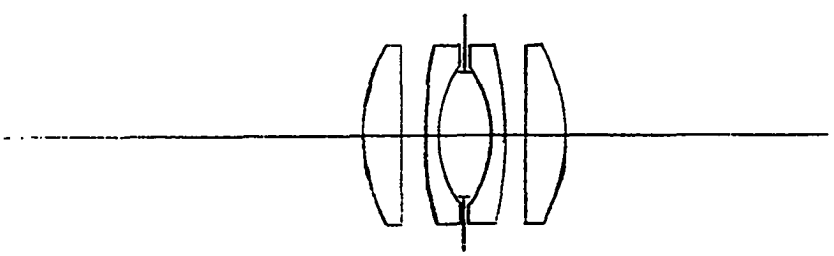

Lower Solution

Fig. 37. The Two Solutions for the Symmetric Dual Dialyte

CHAPTER 6

SUMMARY AND CONCLUSIONS

In the introductory chapter it was stated that the motivation for this investigation was to find a solution to the global minimum problem in optical design. Unfortunately, the results of Chapter Five show that the approach taken does not directly indicate a solution to the problem. However, much has been achieved on the road to the results of Chapter Five. The remainder of this chapter will summarize (following roughly the order of original development) and draw conclusions from these achievements.

The Merit Functions

We begin with the developments of Chapter Two in which two merit functions that are compatible with the isolation of aberration degrees are developed. They are: the mean square ray aberration and the wavefront variance. Because either merit function describes a useful physical property of optical systems, it can be applied advantageously to a great many systems -- not merely a few specialized systems. This implies that many of the results of this research may apply to a broad class of optical systems.

In the beginning of the chapter we saw how the wavefront aberration function was defined and then expanded as a power series. The inclusion of the chromatic variable into the series (Equation 2.2) marked its first appearance (to the

author's knowledge) in an aberration series which is used to construct a merit function. This variable expresses in a full and natural way the chromatic behavior of the aberration function on the same level as the pupil and field variables (Equation 2.5).

The wavefront variance merit function is developed from the power series expansion of the wavefront aberration by analytically carrying out the integrations over each aberration term. The inclusion of weighting functions in the averaging integrals proves advantageous because the resulting wavefront variance can be tailored somewhat to reflect the imaging requirements of the optical system. For example, the wavelength weighting can be made to match the response of a detector, image contrast can be emphasised, or the image quality at the center of the field can be emphasized.

The main weakness of the merit function construction technique is that it does not manifest any vignetting effects. A circular pupil is assumed regardless of the field point. This slightly limits its potential use as an optical design tool, but not as much as might at first be thought. For example, excluding vignetting effects in the design process may naturally guide the design to a solution region in which vignetting is not advantageous, which could produce an intrinsically better design. Since the merit functions are only approximations to the true merit function (because in practice the aberration series must be truncated), concluding the design process using a merit function constructed with real ray data would be wise. However, the important point is that a design could be guided to a superior solution region, though not necessarily to a final design.

At this point attention was shifted to the development of the mean square ray aberration merit function. The development begins with the polychromatic power series expansion of the squared ray aberration function. This aberration series has the same mathematical form as the wavefront aberration series, but the reader should note

that its coefficients are not assumed to have been derived from the coefficients of the wavefront aberration series. The mathematical development of the mean square ray aberration merit function then proceeds similarly to the development of the wavefront variance merit function.

It was then shown that the mathematical forms of the two merit functions are formally indentical. Each merit function is a quadratic form in the polychromatic aberration coefficients and can be written in a quadratic matrix form (Equation 2.53). For this reason all unnecessary distinctions between the two merit functions are dropped in what follows.

The matrix of constants in the quadratic form is termed the coupling matrix because it couples elements of the aberration coefficient vector. Many of its properties are detailed, the most important of which is the positive semidefinite property which allows the matrix to be diagonalized (implemented through the Cholesky factorization). The diagonalization defines a triangular transformation matrix which transforms the aberration coefficient vector to what is termed the orthogonal aberration vector. The term orthogonal is used because no cross terms appear when the orthogonal vectors are used to form the merit function.

The utilization of orthogonal aberrations in the formation of the merit function is extremely important because it allows two developments which are fundamental to the present research. These developments are: first degree adjustments to the merit function and the isolation of degrees of aberrations in the merit function.

Each orthogonal aberration is a linear combination of classical aberration coefficients because the orthogonal aberration vector is obtained from the classical aberration coefficient vector through simple matrix multiplication with the transformation matrix. They define define a natural balance among the aberration

coefficients that can be used to reduce the merit function. In particular, the two first degree coefficients which are the wavelength independent defocus and tilt can be used to locate the image centroid and the plane of best average imaging. These two first degree adjustments are useful because the aberration function can then represent departures from the Gaussian ideal, which, in the presence of aberrations, is not necessarily the desired physically significant property of interest. The important point is that the aberration function can be adjusted so as to be defined relative to the image centroid or a defocussed image plane.

The ability to isolate degrees of aberrations in the merit function leads to the concept of the merit subfunctions. They are the primary tools used in this research to investigate the behavior of optical systems.

The Merit Subfunctions

A few paragraphs above it was stated that each orthogonal aberration is a linear combination of classical aberration coefficients, but it was not stated which coefficients appear in any particular orthogonal aberration. This is were the form of the power series summation plays a crucial role. The particular form used in this research segregates aberration terms according to ascending degree -- which is also the form that automatically segragates the coefficients within an orthogonal aberration by degree. Since the transformation matrix is upper triangular, each orthogonal aberration contains classical coefficients of a particular and all higher degrees. The orthogonal aberration can then be associated with that degree.

The construction of subfunctions that can be associated with degree becames almost trivial at this point. Since the complete merit function is the sum of the squares of the orthogonal aberrations, one can collect all terms of a particular and

higher degree. The resulting sum is the merit subfunction of that degree since only aberration coefficients of that degree and higher occur in the subfunction (Equation 2.87). It is seen that the complete merit function is then identical with the first degree subfunction since it contains all aberrations of first degree and higher.

However, the association between a particular subfunction and its degree is not perfect because the subfunction associated with a particular degree contains classical aberration coefficients of not only that degree, but all higher degrees as well. For this reason there is some mixing of degrees in any particular subfunction, but the examples in Chapter Five demonstrate that the effects of the higher degree terms do not significantly impact the magnitude of the subfunction.

Proximate Ray Tracing and the Computation of Polychromatic Aberration coefficients

Since the merit subfunctions are composed of polychromatic aberration coefficients, it becomes necessary to actually compute the coefficients if a practical investigation into subfunction behavior is to be implemented. The algorithmic approach to proximate ray tracing developed for this purpose is the subject of Chapters Three and Four.

The advantages of this approach are several: the relevant mathematical algorithms are relatively simple, easy to program, invariant with respect to the number of series variables, and trivially extendable to any degree. There is only one disadvantage, though it is relatively severe: the choice of a suitable ray set that can be used to compute high degree aberration coefficients is difficult because the solution matrices tend to be ill conditioned. This makes automation of the selection of a ray set difficult.

The whole of Chapter Three is devoted to the relatively straightforward but tedious development of ray trace equations consistent with quantities that can be represented as power series of the same type as that used to represent the aberration functions. It is shown that those quantities are related to the rotation invariants of a cylindrical coordinate system.

Since the proximate representation of any quantity is in reality a partially summed power series, the equations developed to begin the ray trace reflect this fact. Also developed is a set of closing equations that are used to calculate the proximate values for the aberration used to form the merit function: the wavefront aberration for the wavefront variance or the squared ray error for the mean square ray error. This completes the developments of Chapter Three.

The developments of Chapter Four reveal the relationship between the proximate and power series representations of a quantity. It is shown that the proximate representation is simply a partially summed version of the same type of power series used to represent the aberration functions. Thus proximate ray tracing involves mathematical operations on partially summed power series. The proximte operations necessary to carry out the proximate ray trace correspond to addition, multiplication, division, and square root. The algorithms which implement these operations are developed and presented.

By carrying out a proximate ray trace, the proximate value for the aberration is obtained. However, this does not directly yield the aberration coefficients themselves because proximate quantities are linear combinations of the coefficients. The remainder of Chapter Four demonstrates how the coefficients are computed by tracing a set of proximate rays and then equating the set of proximate values at a particular degree to the power series terms at that degree.

The summary of proximate ray tracing is concluded here with a few remarks of a general nature. Proximate ray tracing is the ideal vehicle for computing the degrees of any ray trace quantity. For example, if one wishes to compute the total third degree component (not just a single third degree aberration) of the optical path length of a particular ray at the exit pupil, one simply traces the corresponding proximate ray to the exit pupil. The desired information is then simply the third degree component of the proximate optical path length. No secondary computation is necessary. The alternative is to determine the full power series representation of the optical path length, and then sum the series over all third degree terms. The determination of the full series involves a much larger computational load than simply tracing a single proximate ray. In addition, summing the series to obtain the desired value is required, adding further to the computational burden.

Thus, armed with the developments of the first four chapters, values for the subfunctions can actually be computed and their behavior investigated.

Subfunction Topographies

The vehicle for the investigation into consequences of isolating degrees of aberration in the merit function is the topographical map of the merit subfunctions. Chapter Five presents the subfunction topographies of three optical systems: the landscape lens, the telescopic doublet, and the symmetric dual dialyte. The maps are created by generating contour maps of the subfunctions as a function of the variable parameters, which are varied in such a way as to preserve all of the first order properties of the system. This ensures that the topography is not influenced by first degree variations in the system.

Since Chapter Five contains detailed observations of the topographies of the

merit subfunctions of the three optical systems, only observations and conclusions of a general nature within the investigated set of optical systems will be presented here.

As a general observation regarding the global features of the lowest degree maps of the landscape lens and doublet, the landscape lens map (Figure 15) correctly shows the stop-in-front and stop-in-back solutions, and the doublet map (Figure 25) correctly shows the Fraunhofer and Gauss solutions. Thus it appears that the merit subfunction maps accurately indicate the topography of the optical systems studied. However, the most striking observation is that the global topography generally does not change dramatically with increasing degree. In all three systems, the higher degree maps tend to resemble the lower degree maps.

However, an exception to global topographical invariance can be induced by first degree adjustments of the merit function. For example, it was shown in Chapter Five that defining the wavefront aberration of the landscape lens relative to a reference sphere centered on the image centroid (rather than the Gaussian image point) has a large effect on the topography of the low degree subfunctions (compare Figure 15 to Figure 20). In fact, the topography of the second degree subfunction changed from possessing two minima to a single minimum . It was demonstrated that this is a consequence of the significant amount of distortion inherent in the landscape lens where the stop is not at the lens.

Another observation is that minima tend to remain relatively stationary in position regardless of degree, although they can migrate in the same general vicinity. For example, the upper minimum for the symmetric dual dialyte is quite stationary, while the lower minimum migrates toward the upper minimum in the higher degree maps. The largest departure from this general observation occurs for the doublet, for which the details of the higher degree maps vary enough so that the two low degree

minima become a single minimum. Indeed, it may be that the two other systems simply were not investigated to a high enough degree. They may also exhibit a single minimum at higher degrees than those examined for this dissertation. The dialyte maps suggest that at approximately the eleventh degree, the migrating minimum might move far enough to merge with the stationary minimum.

One will note that the sequence of magnitudes of the subfunctions converges toward zero fairly rapidly within the region of convergence of the aberration series. The subfunction maps indicate that the convergence tends to be exponential with degree. For example, at the $D = X = 0$ configuration of the landscape lens, the magnitude of the sufunctions decreases by approximately a factor of ten thousand per subfunction.

The rapid convergence of the sequence emphasizes a puzzling aspect of the global topographical invariance phenomenon observed (but not expected at the beginning of the research) in all of the optical examples studied. This is somewhat surprising since the value of a particular degree subfunction can be four orders of magnitude different from the values of its neighboring subfunctions. If the values of neighboring subfunctions can be so vastly different, why are their topographies so similar?

A possible explanation lies in the fact that aberration coefficients are the sum of an intrinsic term, and a term induced by lower order coefficients. The behavior of the induced term may explain the observed behavior. If true, then the topography of any subfunction map is induced by the topography of its neighboring lower degree map. Thus all maps, regardless of degree, could be expected to possess the same general topography -- or a topography which changes only slowly with degree.

It can be demonstrated how the induced portion of an aberration occurs by way of an analogy with the proximate mathematical algorithms presented in Chapter

Four -- an appropriate analogy since the aberration coefficients are computed using proximate algorithms. An examination of the algorithms for proximate multiplication, division and the square root reveal that the resultant term of any particular degree is computed from lower degree terms. That is, higher degree terms are induced from lower degree terms just as occurs with aberration coefficients.

Future Investigation

The unexpected observation of global topography invariance with respect to degree of the subfunction suggests a line of future investigation. If the invariance is indeed a consequence of the induced aberration behavior dominating the intrinsic aberration behavior, then an obvious line of research is to investigate the consequences of isolating the intrinsic and induced portion of each subfunction. The intrinsic subfunction topography may then be examined and may reveal a topography of a more fundamental nature than that exhibited by the full aberration.

The isolation of the intrinsic from the induced portion of the subfunction is straightforward and proceeds as follows: each aberration coefficient is written as the sum of induced and intrinsic parts,

$$W_{mnpq} = W'_{mnpq} + W^{*}_{mnpq} , \tag{6.1}$$

where W'_{mnpq} and W^{*}_{mnpq} are the induced and intrinsic parts respectively. Next, form the aberration coefficient vectors $\vec{W}'$ and $\vec{W}^{*}$. The orthogonal aberration vector is then easily separated into induced and intrinsic parts as shown:

$$\vec{f} = A \vec{W}$$

$$= A (\vec{W}' + \vec{W}^*)$$
$$= A \vec{W}' + A \vec{W}^*$$
$$= \vec{f}' + \vec{f}^* . \qquad (6.2)$$

The merit function is then written

$$\Phi = \vec{f}^t \vec{f}$$
$$= \vec{f}'^t \vec{f}' + 2 \vec{f}'^t \vec{f}^* + \vec{f}^{*t} \vec{f}^*$$
$$= \Phi' + 2 \vec{f}'^t \vec{f}^* + \Phi^* . \qquad (6.3)$$

The pure intrinsic part, Φ', of the merit function can be written as the limit of a sequence of subfunctions in the same manner as for the full merit function. Because the influence of the induced part of the aberrations has been removed, the topography of the intrinsic subfunction sequence formed from Φ' may be vastly different and independent of degree. This has the potential to yield new insight into the behavior of optical systems and seems a logical line of future investigation.

And finally, another suggested line of future investigation stems from the fact that the three simple systems studied are inherently limited in performance by second degree aberrations, and the higher degrees are not significant. One could possibly observe different results during the study of more complex systems for which a solution region of second degree exits.

APPENDIX A

A RAY SET FOR THE COMPUTATION OF POLYCHROMATIC ABERRATION COEFFICIENTS TO DEGREE FIVE

The following ray set has been determined by the author to yield well conditioned matrices to be used for the computation of polychromatic aberration coefficients up to degree five.

The ray set was determined empirically to yield well conditioned solution matrices. An *X* in a particular column means that the ray specified by the ray coordinates in that row is to be included in the determination of that degree coefficient.

RAY COORDINATES				DEGREE					
ν	h	ρ_x	ρ_y	5	4	3	2	1	0
1.0	1.0	1.0	0.0	X	X	X		X	X
1.0	0.8	0.5	0.5	X	X				
1.0	1.0	0.2	0.85	X	X		X		
1.0	0.6	-0.4	0.2	X		X			
1.0	0.75	-0.6	0.8	X	X				
1.0	0.8	-0.9	0.2	X		X			
1.0	0.3	0.8	0.2	X	X				
1.0	0.1	0.7	0.7	X					
1.0	0.3	0.2	0.2	X	X	X	X	X	
1.0	0.3	-0.1	0.95	X	X				
1.0	0.3	-0.3	0.7	X	X				
1.0	0.4	-0.8	0.3	X	X				
1.0	-1.0	0.95	0.15	X	X				
1.0	-0.9	0.7	0.3	X			X		
1.0	-0.7	0.3	0.8	X	X	X			
1.0	-0.9	-0.2	0.1	X					

ν	h	ρ_x	ρ_y	5	4	3	2	1	0
1.0	-0.8	-0.5	0.6	X	X				
1.0	-1.0	-0.6	0.8	X	X	X			
-1.0	0.9	0.8	0.5	X	X	X	X		
-1.0	1.0	0.6	0.2	X					
-1.0	0.8	0.4	0.5	X	X				
-1.0	0.6	-0.05	0.5	X	X				
-1.0	1.0	-0.2	0.3	X		X			
-1.0	0.9	-0.7	0.3	X	X	X		X	
-1.0	-0.1	0.6	0.7	X	X		X		
-1.0	-0.3	0.5	0.2	X					
-1.0	-0.4	0.1	0.5	X	X	X			
-1.0	-0.3	-0.1	0.1	X	X				
-1.0	-0.2	-0.5	0.6	X					
-1.0	-0.5	-0.9	0.2	X	X	X			
-1.0	-0.9	0.7	0.05	X					
-1.0	-1.0	0.45	0.7	X	X		X		
-1.0	-0.7	0.2	0.5	X	X	X			
-1.0	-0.9	-0.05	0.95	X	X				
-1.0	-1.0	-0.5	0.6	X		X			
-1.0	-0.8	-0.95	0.05	X	X				
0.1	1.0	0.8	0.3	X	X	X	X		
0.1	0.7	0.5	0.5	X					
0.1	0.9	0.1	0.8	X	X				
0.1	0.5	-0.1	0.2	X	X	X			
0.1	0.9	-0.4	0.6	X	X				
0.1	1.0	-0.8	0.6	X		X			
0.1	-0.4	0.85	0.5	X	X				
0.1	0.3	0.6	0.65	X					
-0.4	0.5	0.8	0.2	X					
-0.4	0.6	-0.35	0.4	X	X				
-0.4	1.0	-0.75	0.1	X	X				
-0.4	0.91	-0.85	0.3	X		X			
-0.4	-1.0	0.9	0.15	X	X		X		
-0.4	-0.9	0.35	0.1	X	X				
-0.4	-0.9	0.1	0.5	X	X	X			
-0.4	-0.8	-0.3	0.9	X			X	X	
-0.4	-1.0	-0.7	0.7	X			X		
-0.4	-1.0	-0.9	0.2	X		X			
-0.4	0.4	0.6	0.2	X					
-0.4	0.3	-0.4	0.6	X		X			

APPENDIX B

POLYCHROMATIC ABERRATION FORMS AND COEFFICIENTS TO DEGREE FIVE

A list of the aberration functional forms and aberration coefficients of degree up to five are presented in this appendix. Note that the notation for the aberration coefficients does not conform to the norm.

The values given for the wavefront aberration coefficients are for the landscape lens of Chapter 5 (bending factor zero and stop location zero). The unit of measurement for the coefficients is waves at .58756 microns.

Polychromatic Wavefront Aberration Coefficients

Coefficient	Functional Form
Coefficients of Degree 0	
W_{0000} = -9.0665719314E-01	$\nu^0\ h^0\ COS(\phi)^0\ \rho^0$
Coefficients of Degree 1	
W_{1000} = 1.5133026774E+00	$\nu^1\ h^0\ COS(\phi)^0\ \rho^0$
W_{1100} = -3.4720584427E-02	$\nu^0\ h^2\ COS(\phi)^0\ \rho^0$
W_{1110} = 8.4165343001E-03	$\nu^0\ h^1\ COS(\phi)^1\ \rho^1$
W_{1111} = 5.6442222781E-02	$\nu^0\ h^0\ COS(\phi)^0\ \rho^2$
Coefficients of Degree 2	
W_{2000} = 2.7056719221E-02	$\nu^2\ h^0\ COS(\phi)^0\ \rho^0$
W_{2100} = 5.7752052664E-02	$\nu^1\ h^2\ COS(\phi)^0\ \rho^0$
W_{2110} = -1.3999544604E-02	$\nu^1\ h^1\ COS(\phi)^1\ \rho^1$
W_{2111} = -9.4210771439E-02	$\nu^1\ h^0\ COS(\phi)^0\ \rho^2$
W_{2200} = -2.4230507962E-01	$\nu^0\ h^4\ COS(\phi)^0\ \rho^0$
W_{2210} = -1.5829458928E+01	$\nu^0\ h^3\ COS(\phi)^1\ \rho^1$
W_{2211} = 8.0710307021E-01	$\nu^0\ h^2\ COS(\phi)^0\ \rho^2$
W_{2220} = 9.8260632712E-01	$\nu^0\ h^2\ COS(\phi)^2\ \rho^2$

Coefficient	Functional Form
W_{2221} = -7.8088907800E-02	$v^0\ h^1\ COS(\phi)^1\ \rho^3$
W_{2222} = 2.9604360320E-03	$v^0\ h^0\ COS(\phi)^0\ \rho^4$
Coefficients of Degree 3	
W_{3000} = -4.9042975133E-05	$v^3\ h^0\ COS(\phi)^0\ \rho^0$
W_{3100} = 1.3654292801E-03	$v^2\ h^2\ COS(\phi)^0\ \rho^0$
W_{3110} = -3.3097348233E-04	$v^2\ h^1\ COS(\phi)^1\ \rho^1$
W_{3111} = -1.6794142218E-03	$v^2\ h^0\ COS(\phi)^0\ \rho^2$
W_{3200} = -6.8612649175E-03	$v^1\ h^4\ COS(\phi)^0\ \rho^0$
W_{3210} = -3.8984317905E-04	$v^1\ h^3\ COS(\phi)^1\ \rho^1$
W_{3211} = -3.7697483558E-03	$v^1\ h^2\ COS(\phi)^0\ \rho^2$
W_{3220} = -3.3801449648E-02	$v^1\ h^2\ COS(\phi)^2\ \rho^2$
W_{3221} = -1.2490964029E-04	$v^1\ h^1\ COS(\phi)^1\ \rho^3$
W_{3222} = -3.8146293339E-05	$v^1\ h^0\ COS(\phi)^0\ \rho^4$
W_{3300} = 5.5671711581E-02	$v^0\ h^6\ COS(\phi)^0\ \rho^0$
W_{3310} = -7.3570757478E-01	$v^0\ h^5\ COS(\phi)^1\ \rho^1$
W_{3311} = -9.0811168906E-02	$v^0\ h^4\ COS(\phi)^0\ \rho^2$
W_{3320} = 3.8098996607E-01	$v^0\ h^4\ COS(\phi)^2\ \rho^2$
W_{3321} = 1.1600138601E-02	$v^0\ h^3\ COS(\phi)^1\ \rho^3$
W_{3322} = -2.9409340306E-04	$v^0\ h^2\ COS(\phi)^0\ \rho^4$
W_{3330} = -1.7328251408E-02	$v^0\ h^3\ COS(\phi)^3\ \rho^3$
W_{3331} = 1.1006993795E-03	$v^0\ h^2\ COS(\phi)^2\ \rho^4$
W_{3332} = 2.7001647429E-05	$v^0\ h^1\ COS(\phi)^1\ \rho^5$
W_{3333} = 1.0670197512E-06	$v^0\ h^0\ COS(\phi)^0\ \rho^6$
Coefficients of degree 4	
W_{4000} = 1.1264481186E-06	$v^4\ h^0\ COS(\phi)^0\ \rho^0$
W_{4100} = 1.1949350063E-05	$v^3\ h^2\ COS(\phi)^0\ \rho^0$
W_{4110} = -2.9053741194E-06	$v^3\ h^1\ COS(\phi)^1\ \rho^1$
W_{4111} = 3.1973316198E-04	$v^3\ h^0\ COS(\phi)^0\ \rho^2$
W_{4200} = -1.4366961999E-04	$v^2\ h^4\ COS(\phi)^0\ \rho^0$
W_{4210} = -2.8737476054E-05	$v^2\ h^3\ COS(\phi)^1\ \rho^1$
W_{4211} = -8.6672388308E-05	$v^2\ h^2\ COS(\phi)^0\ \rho^2$
W_{4220} = -5.9730221028E-04	$v^2\ h^2\ COS(\phi)^2\ \rho^2$
W_{4221} = 1.9644893142E-05	$v^2\ h^1\ COS(\phi)^1\ \rho^3$
W_{4222} = -1.3287889008E-06	$v^2\ h^0\ COS(\phi)^0\ \rho^4$
W_{4300} = 4.1003471978E-04	$v^1\ h^6\ COS(\phi)^0\ \rho^0$
W_{4310} = 2.9560335457E-04	$v^1\ h^5\ COS(\phi)^1\ \rho^1$
W_{4311} = 3.9259885798E-04	$v^1\ h^4\ COS(\phi)^0\ \rho^2$
W_{4320} = -7.6098657884E-03	$v^1\ h^4\ COS(\phi)^2\ \rho^2$
W_{4321} = -6.2466611195E-04	$v^1\ h^3\ COS(\phi)^1\ \rho^3$
W_{4322} = 1.2315886731E-05	$v^1\ h^2\ COS(\phi)^0\ \rho^4$
W_{4330} = -3.9637723606E-04	$v^1\ h^3\ COS(\phi)^3\ \rho^3$
W_{4331} = 3.0572431329E-05	$v^1\ h^2\ COS(\phi)^2\ \rho^4$
W_{4332} = -4.8863126215E-06	$v^1\ h^1\ COS(\phi)^1\ \rho^5$
W_{4333} = 7.5310179075E-08	$v^1\ h^0\ COS(\phi)^0\ \rho^6$
W_{4400} = 1.0447868968E-03	$v^0\ h^8\ COS(\phi)^0\ \rho^0$
W_{4410} = -3.2283948896E-01	$v^0\ h^7\ COS(\phi)^1\ \rho^1$

Coefficient	Functional Form
W_{4411} = 6.1957239181E-03	$\nu^0\ h^6\ COS(\phi)^0\ \rho^2$
W_{4420} = 4.9482906422E-02	$\nu^0\ h^6\ COS(\phi)^2\ \rho^2$
W_{4421} = 2.6500510935E-03	$\nu^0\ h^5\ COS(\phi)^1\ \rho^3$
W_{4422} = -2.4856238448E-05	$\nu^0\ h^4\ COS(\phi)^0\ \rho^4$
W_{4430} = 4.9335157468E-03	$\nu^0\ h^5\ COS(\phi)^3\ \rho^3$
W_{4431} = -4.0595885287E-04	$\nu^0\ h^4\ COS(\phi)^2\ \rho^4$
W_{4432} = 4.5720804730E-05	$\nu^0\ h^3\ COS(\phi)^1\ \rho^5$
W_{4433} = -7.3579690176E-07	$\nu^0\ h^2\ COS(\phi)^0\ \rho^6$
W_{4440} = -1.3931385032E-04	$\nu^0\ h^4\ COS(\phi)^4\ \rho^4$
W_{4441} = 5.9113215501E-05	$\nu^0\ h^3\ COS(\phi)^3\ \rho^5$
W_{4442} = -3.0293013753E-06	$\nu^0\ h^2\ COS(\phi)^2\ \rho^6$
W_{4443} = 2.1280994709E-07	$\nu^0\ h^1\ COS(\phi)^1\ \rho^7$
W_{4444} = -2.5195631157E-09	$\nu^0\ h^0\ COS(\phi)^0\ \rho^8$
Coefficients of Degree 5	
W_{5000} = 1.4580573815E-09	$\nu^5\ h^0\ COS(\phi)^0\ \rho^0$
W_{5100} = 2.4176108647E-07	$\nu^4\ h^2\ COS(\phi)^0\ \rho^0$
W_{5110} = -5.9211886804E-08	$\nu^4\ h^1\ COS(\phi)^1\ \rho^1$
W_{5111} = -7.0921310803E-08	$\nu^4\ h^0\ COS(\phi)^0\ \rho^2$
W_{5200} = -5.0794332854E-07	$\nu^3\ h^4\ COS(\phi)^0\ \rho^0$
W_{5210} = -9.6350741108E-07	$\nu^3\ h^3\ COS(\phi)^1\ \rho^1$
W_{5211} = -6.7583150584E-07	$\nu^3\ h^2\ COS(\phi)^0\ \rho^2$
W_{5220} = 1.3534386722E-06	$\nu^3\ h^2\ COS(\phi)^2\ \rho^2$
W_{5221} = 8.1805136096E-07	$\nu^3\ h^1\ COS(\phi)^1\ \rho^3$
W_{5222} = -2.0079713145E-08	$\nu^3\ h^0\ COS(\phi)^0\ \rho^4$
W_{5300} = 5.3908200385E-06	$\nu^2\ h^6\ COS(\phi)^0\ \rho^0$
W_{5310} = 3.5600932427E-06	$\nu^2\ h^5\ COS(\phi)^1\ \rho^1$
W_{5311} = 8.3599950898E-06	$\nu^2\ h^4\ COS(\phi)^0\ \rho^2$
W_{5320} = -1.4004969519E-04	$\nu^2\ h^4\ COS(\phi)^2\ \rho^2$
W_{5321} = -7.4221606549E-06	$\nu^2\ h^3\ COS(\phi)^1\ \rho^3$
W_{5322} = 2.3004753231E-07	$\nu^2\ h^2\ COS(\phi)^0\ \rho^4$
W_{5330} = 3.6529464493E-06	$\nu^2\ h^3\ COS(\phi)^3\ \rho^3$
W_{5331} = -7.1317883326E-07	$\nu^2\ h^2\ COS(\phi)^2\ \rho^4$
W_{5332} = 8.9609399818E-09	$\nu^2\ h^1\ COS(\phi)^1\ \rho^5$
W_{5333} = -1.7069243966E-09	$\nu^2\ h^0\ COS(\phi)^0\ \rho^6$
W_{5400} = -6.1609772806E-05	$\nu^1\ h^0\ COS(\phi)^0\ \rho^0$
W_{5410} = 1.0461728714E-04	$\nu^1\ h^7\ COS(\phi)^1\ \rho^1$
W_{5411} = -2.9797035557E-05	$\nu^1\ h^6\ COS(\phi)^0\ \rho^2$
W_{5420} = -1.4325508100E-03	$\nu^1\ h^6\ COS(\phi)^2\ \rho^2$
W_{5421} = -1.1384746306E-04	$\nu^1\ h^5\ COS(\phi)^1\ \rho^3$
W_{5422} = -2.2686629855E-07	$\nu^1\ h^4\ COS(\phi)^0\ \rho^4$
W_{5430} = -4.8521075098E-04	$\nu^1\ h^5\ COS(\phi)^3\ \rho^3$
W_{5431} = 3.3339435418E-05	$\nu^1\ h^4\ COS(\phi)^2\ \rho^4$
W_{5432} = -2.3271712626E-06	$\nu^1\ h^3\ COS(\phi)^1\ \rho^5$
W_{5433} = 3.5740862292E-08	$\nu^1\ h^2\ COS(\phi)^0\ \rho^6$
W_{5440} = 2.2751855736E-05	$\nu^1\ h^4\ COS(\phi)^4\ \rho^4$
W_{5441} = -5.8071517506E-06	$\nu^1\ h^3\ COS(\phi)^3\ \rho^5$
W_{5442} = 3.4887373878E-07	$\nu^1\ h^2\ COS(\phi)^2\ \rho^6$

Coefficient	Functional Form
W_{5443} = -1.6844041715E-08	$\nu^1\ h^1\ COS(\phi)^1\ \rho^7$
W_{5444} = 3.4468652964E-10	$\nu^1\ h^0\ COS(\phi)^0\ \rho^8$
W_{5500} = 1.0621792589E-03	$\nu^0\ h^{10}\ COS(\phi)^0\ \rho^0$
W_{5510} = -3.2184907004E-02	$\nu^0\ h^9\ COS(\phi)^1\ \rho^1$
W_{5511} = -1.3743324362E-03	$\nu^0\ h^8\ COS(\phi)^0\ \rho^2$
W_{5520} = 7.4003196605E-03	$\nu^0\ h^8\ COS(\phi)^2\ \rho^2$
W_{5521} = 8.2727496279E-04	$\nu^0\ h^7\ COS(\phi)^1\ \rho^3$
W_{5522} = -6.3115928870E-06	$\nu^0\ h^6\ COS(\phi)^0\ \rho^4$
W_{5530} = 4.1673668078E-03	$\nu^0\ h^7\ COS(\phi)^3\ \rho^3$
W_{5531} = -2.6127601895E-04	$\nu^0\ h^6\ COS(\phi)^2\ \rho^4$
W_{5532} = 1.5131877014E-05	$\nu^0\ h^5\ COS(\phi)^1\ \rho^5$
W_{5533} = -1.3553669813E-07	$\nu^0\ h^4\ COS(\phi)^0\ \rho^6$
W_{5540} = -3.8960566258E-04	$\nu^0\ h^6\ COS(\phi)^4\ \rho^4$
W_{5541} = 8.1558893046E-05	$\nu^0\ h^5\ COS(\phi)^3\ \rho^5$
W_{5542} = -4.0398220225E-06	$\nu^0\ h^4\ COS(\phi)^2\ \rho^6$
W_{5543} = 1.5545685384E-07	$\nu^0\ h^3\ COS(\phi)^1\ \rho^7$
W_{5544} = -2.1524304759E-09	$\nu^0\ h^2\ COS(\phi)^0\ \rho^8$
W_{5550} = 2.2193851441E-05	$\nu^0\ h^5\ COS(\phi)^5\ \rho^5$
W_{5551} = -4.0511394572E-06	$\nu^0\ h^4\ COS(\phi)^4\ \rho^6$
W_{5552} = 4.2707736572E-07	$\nu^0\ h^3\ COS(\phi)^3\ \rho^7$
W_{5553} = -1.8260522371E-08	$\nu^0\ h^2\ COS(\phi)^2\ \rho^8$
W_{5554} = 6.3532624736E-10	$\nu^0\ h^1\ COS(\phi)^1\ \rho^9$
W_{5555} = -9.6483553210E-12	$\nu^0\ h^0\ COS(\phi)^0\ \rho^{10}$

Monochromatic Wavefront Aberration coefficients

The monochromatic wavefront aberration coefficients were computed from the above polychromatic coefficients using the following equation:

$$W_{npq} = \sum_{m=0}^{5} \left[W_{mnpq}\ \nu^{(m-n)} \right] \qquad \text{where } \nu = .58756\ .$$

Ideally the summation should be from m = 0 to ∞ . But Since the polychromatic coefficients were only computed to degree five, the monochromatic coefficients are accurate to the fifth degree in the chromatic variable.

Coefficient	Functional Form
Coefficients of Degree 0	
W_{000} = 1.7500134594E-11	$h^0\ COS(\phi)^0\ \rho^0$
Coefficients of Degree 1	
W_{100} = -1.9672906063E-10	$h^2\ COS(\phi)^0\ \rho^0$
W_{110} = 4.8690824026E-12	$h^1\ COS(\phi)^1\ \rho^1$
W_{111} = 8.9577456554E-12	$h^0\ COS(\phi)^0\ \rho^2$
Coefficients of Degree 2	
W_{200} = -2.4642336445E-01	$h^4\ COS(\phi)^0\ \rho^0$
W_{210} = -1.5829700347E+01	$h^3\ COS(\phi)^1\ \rho^1$
W_{211} = 8.0483758094E-01	$h^2\ COS(\phi)^0\ \rho^2$
W_{220} = 9.6235757176E-01	$h^2\ COS(\phi)^2\ \rho^2$
W_{221} = -7.8155885158E-02	$h^1\ COS(\phi)^1\ \rho^3$
W_{222} = 2.9373498867E-03	$h^0\ COS(\phi)^0\ \rho^4$
Coefficients of Degree 3	
W_{300} = 5.5916694338E-02	$h^6\ COS(\phi)^0\ \rho^0$
W_{310} = -7.3553107581E-01	$h^5\ COS(\phi)^1\ \rho^1$
W_{311} = -9.0575479386E-02	$h^4\ COS(\phi)^0\ \rho^2$
W_{320} = 3.7642925321E-01	$h^4\ COS(\phi)^2\ \rho^2$
W_{321} = 1.1227198210E-02	$h^3\ COS(\phi)^1\ \rho^3$
W_{322} = -2.8671110612E-04	$h^2\ COS(\phi)^0\ \rho^4$
W_{330} = -1.7561958764E-02	$h^3\ COS(\phi)^3\ \rho^3$
W_{331} = 1.1185735092E-03	$h^2\ COS(\phi)^2\ \rho^4$
W_{332} = 2.4107958729E-05	$h^1\ COS(\phi)^1\ \rho^5$
W_{333} = 1.1110672724E-06	$h^0\ COS(\phi)^0\ \rho^6$
Coefficients of Degree 4	
W_{400} = 1.0082616975E-01	$h^8\ COS(\phi)^0\ \rho^0$
W_{410} = -3.2277746687E-01	$h^7\ COS(\phi)^1\ \rho^1$
W_{411} = 6.1780588203E-03	$h^6\ COS(\phi)^0\ \rho^2$
W_{420} = 4.8633622266E-02	$h^6\ COS(\phi)^2\ \rho^2$
W_{421} = 2.5825569105E-03	$h^5\ COS(\phi)^1\ \rho^3$
W_{422} = -2.4990735564E-05	$h^4\ COS(\phi)^0\ \rho^4$
W_{430} = 4.6458597697E-03	$h^5\ COS(\phi)^3\ \rho^3$
W_{431} = -3.8619365218E-04	$h^4\ COS(\phi)^2\ \rho^4$
W_{432} = 4.4341147082E-05	$h^3\ COS(\phi)^1\ \rho^5$
W_{433} = -7.1460802116E-07	$h^2\ COS(\phi)^0\ \rho^6$
W_{440} = -1.2582546969E-04	$h^4\ COS(\phi)^4\ \rho^4$
W_{441} = 5.5670460147E-05	$h^3\ COS(\phi)^3\ \rho^5$
W_{442} = -2.8224724541E-06	$h^2\ COS(\phi)^2\ \rho^6$
W_{443} = 2.0282399919E-07	$h^1\ COS(\phi)^1\ \rho^7$
W_{444} = -2.3152165709E-09	$h^0\ COS(\phi)^0\ \rho^8$

Coefficent	Functional Form
Coefficients of Degree 5	
W_{500} = 1.0621792589E-03	h^{10} $COS(\phi)^0$ ρ^0
W_{510} = -3.2184907004E-02	h^9 $COS(\phi)^1$ ρ^1
W_{511} = -1.3743324362E-03	h^8 $COS(\phi)^0$ ρ^2
W_{520} = 7.4003196605E-03	h^8 $COS(\phi)^2$ ρ^2
W_{521} = 8.2727496279E-04	h^7 $COS(\phi)^1$ ρ^3
W_{522} = -6.3115928870E-06	h^6 $COS(\phi)^0$ ρ^4
W_{530} = 4.1673668078E-03	h^7 $COS(\phi)^3$ ρ^3
W_{531} = -2.6127610895E-04	h^6 $COS(\phi)^2$ ρ^4
W_{532} = 1.5131877014E-05	h^5 $COS(\phi)^1$ ρ^5
W_{533} = -1.3553669813E-07	h^4 $COS(\phi)^0$ ρ^6
W_{540} = -3.8960566258E-04	h^6 $COS(\phi)^4$ ρ^4
W_{541} = 8.1558893046E-05	h^5 $COS(\phi)^3$ ρ^5
W_{542} = -4.0398220225E-06	h^4 $COS(\phi)^2$ ρ^6
W_{543} = 1.5545685384E-07	h^3 $COS(\phi)^1$ ρ^7
W_{544} = -2.1524304759E-09	h^2 $COS(\phi)^0$ ρ^8
W_{550} = 2.2193851441E-05	h^5 $COS(\phi)^5$ ρ^5
W_{551} = -4.0511394572E-06	h^4 $COS(\phi)^4$ ρ^6
W_{552} = 4.2707736572E-07	h^3 $COS(\phi)^3$ ρ^7
W_{553} = -1.8260522371E-08	h^2 $COS(\phi)^2$ ρ^8
W_{554} = 6.3532624736E-10	h^1 $COS(\phi)^1$ ρ^9
W_{555} = -9.6483553210E-12	h^0 $COS(\phi)^0$ ρ^{10}

REFERENCES

1. The information in this and the next paragraph was gleaned from E. Hecht and A. Zajac, "Optics", 4th printing, Addision-Wessley, pp. 2-3 (1979)

2. Dr. O. Stavroudis, private communication (June 1987)

3. F. Wachendorf, Optik 5, p. 80 (1949)

4. G. Hopkins, "Aberrational Analysis of Optical Systems: A Proximate Ray Trace Approach", Ph.D. Dissertation, University of Arizona (1976)

5. T. Andersen, "Automatic Computation of Optical Aberration Coefficients", A.O. **19**, p. 3800 (1980)

6. G. Forbes, "Automation of the Computation of Chromatic Aberration Coefficients", JOSA A **1**, p. 1298 (1984)

7. G. Forbes, "Weighted Truncation of Power Series and the Computation of Chromatic Aberration Coefficients", JOSA A **1**, p. 350 (1984)

8. H. Unvala, "The Orthonormalization of Aberrations", Proceedings of the Conference on Lens Design with Large Computers, University of Rochester, New York (1967)

9. G. Weise, "Use of Physically Significant Merit Functions in Automatic Design", Masters Thesis, University of Arizona (1974)

10. G. Forbes, "Chromatic Coordinates in Aberration Theory", JOSA A **1**, p. 344 (1984)

11. See reference 10, Equation 4.3

12. See reference 10, Equation 4.4

13. The need and general method for first degree adjustments was pointed out to the author during a discussion with Dr. R. Shack (May 1987) after his review of some surprising results obtained from an investigation of the landscape lens. When asked why he suspected first degree behavior explained the observed results, his response was "It's obvious". Thus are we humbled.

REFERENCES--Continued

14. R. Kingslake, "Lens Design Fundamentals", Academic Press, p. 240

15. I. Bohachevsky, V. Viswanathan, and G. Woodfin, "An Intelligent Optical Design Program", SPIE Proc. 485, p. 104